# MODEL DEVELOPMENT AND PERFORMANCE ANALYSIS OF INTEGRATED GASIFICATION PROCESS AND PROTON EXCHANGE MEMBRANE FUEL CELL

MUHAMMAD BILAL BIN MUSLIM

MASTER OF SCIENCE

UNIVERSITI MALAYSIA PAHANG

# UNIVERSITI MALAYSIA PAHANG

## DECLARATION OF THESIS AND COPYRIGHT

Author's Full Name : MUHAMMAD BILAL BIN MUSLIM

Date of Birth : 16 DECEMBER 1991

Title : MODEL DEVELOPMENT AND PERFORMANCE ANALYSIS OF INTEGRATED GASIFICATION PROCESS AND PROTON EXCHANGE MEMBRANE FUEL CELL

Academic Session : SEMESTER 1 SESSION 2018/2019

I declare that this thesis is classified as:

| | |
|---|---|
| ☐ CONFIDENTIAL | (Contains confidential information under the Official Secret Act 1997)* |
| ☐ RESTRICTED | (Contains restricted information as specified by the organization where research was done)* |
| ☑ OPEN ACCESS | I agree that my thesis to be published as online open access (Full Text) |

I acknowledge that Universiti Malaysia Pahang reserves the following rights:

1. The Thesis is the Property of Universiti Malaysia Pahang
2. The Library of Universiti Malaysia Pahang has the right to make copies of the thesis for the purpose of research only.
3. The Library has the right to make copies of the thesis for academic exchange.

Certified by:

| | |
|---|---|
| _______________________ | _______________________ |
| (Student's Signature) | (Supervisor's Signature) |
| 911216-01-5015 | Dr Noor Asma Fazli Abdul Samad |
| New IC/Passport Number | Name of Supervisor |
| Date: 21 January 2019 | Date: 21 January 2019 |

NOTE : * If the thesis is CONFIDENTIAL or RESTRICTED, please attach a thesis declaration letter.

# SUPERVISOR'S DECLARATION

We hereby declare that We have checked this thesis and in our opinion, this thesis is adequate in terms of scope and quality for the award of the degree of Master of Science

(Supervisor's Signature)

Full Name : DR NOOR ASMA FAZLI BIN ABDUL SAMAD
Position : SENIOR LECTURER
Date : 21 JANUARY 2019

(Co-supervisor's Signature)

Full Name : DR SURIYATI BINTI SALEH
Position : SENIOR LECTURER
Date : 21 JANUARY 2019

Universiti
Malaysia
PAHANG
Engineering • Technology • Creativity

# STUDENT’S DECLARATION

I hereby declare that the work in this thesis is based on my original work except for quotations and citations which have been duly acknowledged. I also declare that it has not been previously or concurrently submitted for any other degree at Universiti Malaysia Pahang or any other institutions.

(Student’s Signature)

Full Name : MUHAMMAD BILAL BIN MUSLIM
ID Number : MKC15038
Date : 21 JANUARY 2019

# MODEL DEVELOPMENT AND PERFORMANCE ANALYSIS OF INTEGRATED GASIFICATION PROCESS AND PROTON EXCHANGE MEMBRANE FUEL CELL

MUHAMMAD BILAL BIN MUSLIM

Thesis submitted in fulfillment of the requirements
for the award of the degree of
Master of Science

Faculty of Chemical & Natural Resources Engineering
UNIVERSITI MALAYSIA PAHANG

JANUARY 2019

# ACKNOWLEDGEMENTS

First and foremost, I would like to thank to ALLAH for giving me a chance to complete this thesis. Actually, I definitely did not expect that out of all chapters in this thesis, writing down this acknowledgement section is going to be the hardest of all. However, I would try my very best and for individuals that are inadvertently omitted, I would like to propose my apologies and thank you for everything. As often said, old age comes in hand not only with wisdoms but also forgetfulness.

Secondly, I would like to extend my deepest gratitude to Abah, Muslim Ahmad and Umi, Zalina Zainon. Both of you have been the backbone of my entire being, my emotional support for the past 26 years. I do honestly hope I have made both of you proud. For my siblings, Umairah, Aini Khalida and Fatihah, well what I can say, all of you have been my support of strength, someone that I know I can look up to and always be there for me during my up and down.

Well, where would I be in my studies without my two esteemed supervisors and co-supervisor, Dr Noor Asma Fazli Abdul Samad and Dr. Suriyati Saleh, Thank you foremost for giving me the opportunity of lifetime to do my Master's here and most importantly for the never-ending trust, dedications, and faith not only in my ability but also in me personally. I also want to thank to all lecturers in Faculty of Chemical & Natural Resources Engineering (FKKSA) that always giving me advice and supporting me directly or indirectly. My deepest gratitude also goes to all technical and administrative staffs that had assisted me in thousand ways I could ever possibly imagine. I am also very much indebted to Ministry of High Education (MOHE), for providing me with the scholarship (MYBRAINS) throughout my duration of study here.

Next, to my best friends, Fakhrul Razil Alawi, Zakirah and Hazirah, thank you for being there always for me. You three certainly seen the inferior of me but yet never fail to bring out the best in me. To Ameerul Hakeem, Abu and Syafiq, thank you all for the times we spend together. We certainly define the meaning of working hard and playing harder, but ultimately; no matter how terrible the world goes at times, it will be better eventually when you have friends around to cheer you up. To my best mates, well I am truly proud and honored to share this ride along with all of you. Thank you so much. For everyone, cheers, and meet all of you again in the future.

MUHAMMAD BILAL BIN MUSLIM

21 JANUARY 2019

DEDICATION TO MY FAMILY

ABAH, UMI, MERAH, IDA & TEHAH

# ABSTRAK

Ketika ini, jumlah permintaan tenaga dari seluruh dunia semakin meningkat selaras dengan pertumbuhan ekonomi. Kebanyakan sumber tenaga yang digunakan adalah berpunca daripada bahan api fosil yang merupakan sumber yang tidak boleh diperbaharui. Walaupun sumber bahan api fosil masih lagi banyak, permintaan tinggi terhadap sumber bahan api yang terhad ini tidak dapat dielakkan di mana sumber ini akan kehabisan kelak. Jadi, sumber tenaga yang boleh diperbaharui kini dilihat sebagai pilihan terbaik untuk menggantikan sumber bahan api fosil sebagai penjana utama tenaga. Sisa kelapa sawit merupakan salah satu alternatif untuk menggantikan bahan api fosil dimana sisa ini boleh digunapakai untuk penggunaan tenaga kerana jumlahnya yang banyak dan ketersediaannya di Malaysia. Sisa ini boleh digunakan untuk menghasilkan produk yang berguna seperti gas sintesis untuk penjanaan tenaga. Oleh itu, integrasi kerangka kerja bagi sistem penggegasan dan sel bahan api berasaskan membran pertukaran proton (PEMFC) telah dibuat untuk menghasilkan gas sintesis yang diperlukan dan penjanaan tenaga melalui langkah yang spesifik di dalam rangka kerja. Aplikasi rangka kerja ini diaplikasikan melalui lima kajian kes yang berbeza di mana setiap kes mempunyai objektif yang berlainan. Kesemua lima kajian kes meliputi pengesahan penggegas lapisan tetap dan penggegas lapisan terbendalir, perbandingan prestasi kedua-dua pengegas tersebut, penggegasan sisa kelapa sawit yang mentah dan telah ditorekfasi, kesan penulenan hidrogen serta penghasilan kuasa. Kedua-dua model penggegas jenis lapisan tetap dan lapisan terbendalir telah dibuat menggunakan perisian Aspen Plus dan keputusan pengesahan yang didapati adalah bertepatan dengan data kajian yang telah dijalankan. Jumlah hidrogen yang tinggi didapati dalam penggegas lapisan terbendalir berbanding lapisan tetap menunjukkan penggegas lapisan terbendalir memberi prestasi yang lebih tinggi dalam menghasilkan gas sintesis. Pelbagai jenis sisa kelapa sawit seperti pelepah kelapa sawit, tandan kelapa sawit, tempurung kelapa sawit dan gentian mesokarpa sawit telah digunakan sebagai bahan suapan untuk kedua-dua penggegas dan keputusan simulasi menunjukkan pelepah kelapa sawit menghasilkan 7.81 % dan 5.12 % gas hidrogen untuk penggegas lapisan terbendalir dan lapisan tetap. Untuk komposisi gas sintesis, pelepah kelapa sawit yang ditorefaksi pada 300 °C menghasilkan gas hidrogen tertinggi berbanding pelepah kelapa sawit yang mentah menunjukkan torefaksi merupakan cara rawatan yang dapat menambahbaik penghasilan gas sintesis. Kesan penulenan juga telah diuji dan menunjukkan lebih banyak gas hidrogen telah terhasil dan jumlah gas karbon monoksida telah dikurangkan sehingga di bawah paras 10 ppm bagi memenuhi prasyarat untuk menggunakan sel bahan api berasaskan membran pertukaran proton (PEMFC). Bagi penghasilan kuasa, pelepah kelapa sawit yang ditorefaksi pada 300 °C menghasilkan kuasa yang paling tinggi iaitu 5.74 kW dan 6.65 kW untuk penggegas lapisan tetap-PEMFC dan penggegas lapisan terbendalir-PEMFC. Dari segi kecekapan pula, untuk penggegas lapisan terbendalir-PEMFC, pelepah kelapa sawit yang ditorefaksi pada 300 °C menghasilkan 55.88 % untuk kecekapan elektrik, 74.24 % untuk kecekapan keseluruhan dan 34.98 % untuk kecekapan tindan sel bahan api. Manakala untuk penggegas lapisan tetap-PEMFC, pelepah kelapa sawit yang ditorefaksi pada 300 °C menghasilkan 48.27 % untuk kecekapan elektrik, 69.47 % untuk kecekapan keseluruhan dan 27.74 % untuk kecekapan tindan sel bahan api. Kesimpulannya, integrasi kerangka kerja untuk penggegasan dan PEMFC boleh digunakan sebagai alat untuk penjanaan tenaga dan penunjuk kecekapan manakala torefaksi sebagai cara rawatan boleh meningkatkan penghasilan gas hidrogen dan penjanaan tenaga.

# ABSTRACT

The total energy demands from the entire global are increasing every day in order to support economic growth. Most of the sources of energy used are coming from fossil fuel which is non-renewable energy sources. Although there are still large supplies of fossil fuel, it is inevitable that one day the amount of fossil fuel will be decreased and running out. Hence, the renewable energy sources are currently identified as the best choice for replacing the fossil fuels as main energy supply. Palm oil wastes as the alternative for fossil fuel substitution have the potential to be utilized for energy purpose due to its abundances and availabilities in Malaysia. This biomass can be used to produce useful product such as synthesis gas which can be utilized for power production. Thus, an integrated workflow of biomass gasification and PEMFC has been developed for producing the required synthesis gas and power production. The applications of the integrated workflow are highlighted through five different case studies which each have different objectives. All five case studies are covering the model validation of fixed and fluidized bed gasifiers, performance of the gasifiers, gasification of raw and torrefied palm oil wastes, and effects of purification on the hydrogen and power production. Both models of fixed and fluidized bed gasifiers have been developed in Aspen Plus software and the validation results obtained are in good agreement with literature data. Higher amount of hydrogen gas was obtained in fluidized bed gasifier compare to fixed bed gasifier which indicates fluidized bed provides better performance for producing synthesis gas. Palm oil wastes such as Oil Palm Frond (OPF), Palm Kernel Shell (PKS), Palm Mesocarp Fiber (PMF) and Empty Fruit Bunch (EFB) have been used as inputs for both gasifiers and the simulation results show the OPF obtained 7.81 % and 5.12 % of hydrogen gas for fluidized bed and fixed bed gasifiers respectively. For synthesis gas composition, the torrefied OPF at 300 °C provides the highest hydrogen production compare to raw OPF indicating torrefaction as pre-treatment method is able to improve synthesis gas production. The effects of purification have been tested where more hydrogen gas are produced and the amount of carbon monoxide (CO) is reduced below 10 ppm which is the allowable amounts as input for Proton Exchange Membrane Fuel Cell (PEMFC). For power production, torrefied OPF at 300 °C provides the highest power produced around 5.74 kW and 6.65 kW for integrated fixed bed-PEMFC and fluidized bed-PEMFC respectively. In terms of efficiencies, for integrated fluidized bed-PEMFC, the torrefied OPF at 300 °C produces 55.88 % for electrical efficiency, 74.24 % for overall efficiency and 34.98 % for stack efficiency. Meanwhile for integrated fixed bed-PEMFC, the torrefied OPF at 300 °C produces 48.27 % for electrical efficiency, 69.47% for overall efficiency and 27.74 % for stack efficiency. In overall, the integrated gasification and PEMFC is able to be used as tools for power production and efficiency indicator and torrefaction as pre-treatment method is a useful for upgrading the hydrogen and power production.

# TABLE OF CONTENT

## CHAPTER 3 METHODOLOGY 48

## CHAPTER 4 RESULTS AND DISCUSSIONS 68

# LIST OF TABLES

# LIST OF FIGURES

# LIST OF SYMBOLS

| | |
|---|---|
| $E_{cell}$ | Cell voltage |
| $E_R$ | Reversible cell potential |
| $\eta_a$ | Activation loss at the anode |
| $\eta_c$ | Activation loss at the cathode |
| $\eta_{ohmic}$ | Ohmic loss (V) |
| R | Ideal gas constant ($Jmol^{-1}K^{-1}$) |
| T | Operating temperature (K) |
| $\alpha$ | Charge transfer coefficient |
| F | Faraday constant (C/mol) |
| i | Quantity of current density ($Acm^{-2}$) |
| keh | Rate constant of hydrogen electro-oxidation ($Acm^{-2}$) |
| $\theta_h$ | Fractional surface coverage of hydrogen |
| $i_{oc}$ | Cathode exchange current density ($Acm^{-2}$) |
| n | Number of cells used in PEMFC |
| $R_{ohmic}$ | Ohmic resistance |
| A | Area of the active cell ($cm^2$) |
| $y_{ie}$ | Experimental values |
| $y_{ip}$ | Predicted values |
| N | Number of data points |
| $P_{actual}$ | Exact value of the data |
| $P_{measured}$ | Approximate value of the data |
| V | Cell voltage (V) |
| $\dot{m}_{PG}$ | Mass flow of product gas (kg/h) |
| $\dot{m}_{Bio}$ | Mass flow of biomass (kg/h) |
| $P_e$ | Amount of power produce from the PEMFC |
| $P_h$ | Amount of thermal energy from the PEMFC |
| $\eta_{electrical}$ | Electrical efficiency |
| $\eta_{therma}l$ | Thermal efficiency |
| $\eta_{overall}$ | Overall efficiency |
| $\eta_{stack}$ | Stack efficiency |
| E | electric energy input |
| $P_{fc}$ | Output power produced by PEMFC (W) |

# LIST OF ABBREVIATIONS

| | |
|---|---|
| AMFCs | Alkaline Membrane Fuel Cells |
| ABR | Air to Biomass Ratio |
| AFC | Alkaline Fuel Cells |
| CGE | Cold Gas Efficiency |
| CO-PROX | Catalytic Preferential Oxidation of CO |
| DMFCs | Direct Methanol Fuel Cells |
| EFB | Empty Fruit Bunch |
| FC | Fixed Carbon |
| HHV | Higher Heating Value |
| HTS | High-Temperature Water Gas Shift Reactor |
| LHV | Lower Heating Value |
| LTS | Low-Temperature Water Gas Shift Reactor |
| MC | Moisture Content |
| MCFCs | Molten Carbonate Fuel Cells |
| OPF | Oil Palm Frond |
| PAFCs | Phosphoric Acid Fuel Cells |
| PEMFC | Proton Exchange Membrane Fuel Cell |
| PKS | Palm Kernel Shell |
| PMF | Palm Modecate Fibre |
| PR-BM | Peng Robinson with Boston-Mathias |
| PROXANAL | Proximate Analysis |
| RKS-BM | Redlich-Kwong-Soave with Boston-Mathias |
| RMSE | Root Mean Square Error |
| SBR | Steam to Biomass Ratio |
| SOFCs | Solid Oxide Fuel Cells |
| ULTANAL | Ultimate Analysis |
| VM | Volatile Matter |

# CHAPTER 1

# INTRODUCTION

## 1.1 Introduction

Energy is an important factor in development since it supports and stimulates the economic growth and development. Research study from Ozturk (2010) indicates that the energy consumption tends to be more responsive to the economic growth. The contributions of energy consumption increases economic growth, raises incomes, raises education levels as well as improves health and infrastructure (Asafu-Adjaye et al., 2016). Currently, the worldwide needs energy in order to sustain the economic growth. Over 70 % of global energy demands growth is achieved by fossil fuels utilization such as oil, natural gas and coal. The demand of energy rose by 2.1 % in 2017, more than twice the previous year's rate, boosted by strong global economic growth (IEA, 2017). Until today, fossil fuels cover almost of world consumption of primary energy, in spite of our strong anxiety over their supremacy. In particular, fossil fuels employ a strong influence on the transportation sector.

Almost all countries in the world employ fossil fuels which approximately 97 % contributing to the transportation fuel (Fulton, 2004). This is because fossil fuels are easily transport, mainly due to their high energy content, easy to handle and burn, which is suitable for usage in transportation containers. The usage of transportation will give impact to the trends of economic growth. Mostly all countries in the world are using transportation in their daily routine (Ishida, 2013). However, these fossils fuels are defined as a finite resource. Although there are still large supplies of coal, oil and natural gas, however given the increasing demand and limited supply it is inevitable that one day supplies will run out (Apergis and Danuletiu, 2014). Thus, it is important to search for alternative energy sources. The world nowadays enhances the efforts which are focusing to reduce dependency on fossil fuels and achieve a sustainable and renewable energy supply (MTI, 2007). The renewable energy sources are currently identified as the best choice for substituting the fossil fuels as main energy supply. One of the renewable energy that has high potential for energy purpose is bioenergy. Nowadays, bioenergy is beginning to be considered as attractive energy resources that can be used to replace the depleting current non-renewable energy resources (Quintana et al., 2011).

Biomass is one of the examples of bioenergy sources that can be derived from organic waste materials. The exploitation of energy from biomass has played an important key role in the evolution of mankind. To date, it is one of energy form which has been utilized as the main source of energy for more than half of the world's population for domestic energy needs. There are many sources of biomass such as forest products, agriculture wastes, trees, animal residues and municipal solid wastes. However, in a country that has a significant amount of agricultural activities such as Malaysia; agriculture waste can be a very promising alternative source of renewable energy. In Malaysia, the main waste coming from agriculture activities is oil palm wastes. In year 2018, Malaysia is the second largest producer of palm oil in the world with production over 15 million tonnes per year. Up to date, Malaysia has 453 palm oil mills with operating capacity of 113 million tonnes (Malaysia Palm Oil Palm Statistics, 2018). With this large oil palm production, this will contribute high amount of oil palm waste residues (Aghamohammadi et al., 2016). This kind of wastes can be useful for derivation of energy sources since the biomass waste is renewable source for energy supply.

The chemical structure and major organic components in biomass are extremely important in the process development for producing derived fuels and chemicals. This renewable biomass can provides another source of energy which is hydrogen gas. Hydrogen gas production is one of the most promising alternative energy technologies (Milne et al., 2002). Hydrogen gas is a secondary form of energy that has to be manufactured and is considered as an energy carrier. The use of renewable biomass as a major feedstock for hydrogen gas production has received considerable attention in recent years. Hydrogen from biomass can be produced through thermochemical conversion processes such as combustion, pyrolysis and gasification (Ni et al., 2006). Among these approaches, gasification process is identified as the promising method to produce hydrogen gas since this method is applicable for a wide variety of inputs and multiple useful products such as clean synthesis gas can be produced. Besides, the clean synthesis gas can be combusted in the gasification system by using higher temperature which improves the overall efficiency of the process (Muslim et al., 2017).

Biomass gasification is a process whereas the biomass undergone chemical conversion to produce fuel gas or synthesis gas which consists of carbon dioxide ($CO_2$), carbon monoxide (CO), hydrogen ($H_2$) and traces of methane ($CH_4$). This process occurs under the presence of gasifying agents such as air, oxygen and/or steam. There are four main types of reactor for gasification process which are the fixed bed, fluidized bed, entrained flow and moving bed (Warnecke, 2000). Each of the reactors has its advantages and disadvantages. For example, moving bed reactor has lower pressure drop but it has high tar yields. While for fixed bed reactor it is cheaper and produces low tar in gasification but it has high ash content meanwhile fluidized bed reactor has the ability to reach isothermal condition in the bed, the scale up is easy, high combustion efficiency and low emission of nitric oxide ($NO_2$). The output gas particularly hydrogen gas is the main focus since this gas can be used as an input for the fuel cell to generate electricity.

Studies regarding the fuel cell are mainly focusing on transforming fossil fuel energy into electrical energy. Different types of fuel cell have been developed. For example, the low temperature fuel cells include proton exchange membrane fuel cell (PEMFC), alkaline fuel cells (AFCs), direct methanol fuel cells (DMFCs) and phosphoric acid fuel cells (PAFCs) whereas high temperature fuels cells consists of molten carbonate fuel cells (MCFCs) and solid oxide fuel cells (SOFCs) (Shaari and Kamarudin, 2015). All the fuel cells are applicable for converting the input such as hydrogen gas into electricity and heat. The main different among the fuel cells are their electrolyte and operating temperature. A typical fuel cell consists of three parts which are the anode side flow channel plate, the membrane electrode assembly and the cathode flow channel plate. The anode and cathode serve as catalyst. The middle layer of fuel cell consists of a carrier structure which absorbs the electrolyte. In different types of fuel cell different substances are used as electrolyte. Some electrolytes are liquid and some are solid with a membrane structure. From all the fuel cells, the proton exchange membrane fuel cell (PEMFC) is recognized as an efficient power generation device because of its high energy density, low emissions, long service life, good ecological balance and very low self-discharge (Kamarudin et al., 2004). The performance of the PEMFC will be determined by examining the power produced and overall efficiency.

## 1.2 Problem Statement and Motivation

The increasing of palm oil demand in Malaysia is directly increasing the amounts of oil palm wastes. In Malaysia, one hectare of palm oil plantation can produce about 50–70 tonnes of waste residues which can cause waste disposal problems. Our oil palm industry is currently producing the largest amount of oil palm wastes in Malaysia with 85.5 % out of more than 70 million tonnes (Mahat, 2012). This amount of oil palm wastes such as oil palm fronds, empty fruit bunch, palm mesocarp fibre and palm kernel shell could be exploited as renewable energy sources for generating electricity and thus overcome the waste disposal problem. Hence, this palm oil wastes will be exploited as energy contributor through biomass gasification process that will be focused in this research.

Gasification in real experimental work is complex and sensitive process. The process of gasification will involve the pyrolysis, combustion and gasification which take a lot of time and energy consuming even for one gasification process (Sikarwar et al., 2016). The experimental work will need to be repeated immediately if the results are not satisfactory. In addition, the experimental work involves trial and error approach for finding the optimal operating conditions and desired synthesis gas. In order to overcome these limitations, gasification based on simulation can be employed. Simulation based analysis provides valuable insights to supplement experimental studies which are considered to be more reliable. The use of simulation models can considerably reduce the time and investment involved in exploring the favourable process conditions for sorbent incorporated gasification process. For example, the simulator such as Aspen Plus have been chosen widely for gasification simulator because it enables to model and simulate each component of an integrated system separately, using default block settings or by modifying them to perform, in a directed way, using FORTRAN or EXCEL subroutines (Rupesh et al., 2016). Besides, through simulation approach, its present predictive performance and the potential areas for further improvement can be obtained (Chui et al., 2009). Hence, the simulation using

Aspen Plus software based study will be carry out for implementing the biomass gasification process in this research.

One of the most common problems in gasification process is low production of synthesis gas and low efficiency. This is due to the properties of raw biomass which have low carbon content (high O/C ratio) and low calorific value which lead to low amounts of synthesis gas production particularly hydrogen gas which contributing to the low cold gas energy and efficiencies (Chen et al., 2013). In order to improve properties of biomass and make it more suitable for energy applications, varieties of pre-treatment methods for improving biomass have been developed. One of the suitable methods for upgrading the biomass properties is torrefaction. Through torrefaction, biomass with higher energy density, hydrophobic property, improved grindability, and has lower oxygen-to-carbon (O/C) ratio can be obtained and therefore more appropriate for residential combustion and gasification applications (Chen et al., 2013). Although there are few papers that have highlighted on the gasification of torrefied biomass, there are still remains a lot of knowledge about the effect of torrefied biomass in gasification process for hydrogen gas and power production that is not presented in sufficient detail which focusing the effect of torrefaction on hydrogen production and effect of torrefaction on power production. Hence, this study about the performance of torrefied biomass on hydrogen and power production will be focused in this study.

Many previous simulation case studies have evaluated and focusing on biomass behaviour in gasification process especially for fluidized bed and fixed bed gasifiers. For fluidized bed example, previous study done by Fatoni et al. (2014) use Aspen Plus to study the biomass gasification in a circulating fluidized bed model. Besides, Nikoo and Mahinpey (2008) studied the development of simulation model which capable of predicting the steady-state performance of an atmospheric fluidized bed gasifier by considering the hydrodynamic and reaction rate kinetics simultaneously. For fixed bed, Shaohua et al. (2012) provides study about biomass gasification in a fixed bed using Aspen Plus simulation meanwhile Begum et al. (2013) studied about performance analysis of an integrated fixed bed gasifier model for different biomass feedstock. However, all this previous studies just focusing on one gasifier only either fluidized or fixed bed gasifier. There are limited of studies that regarding to comparison of both gasifier in terms of performances such as hydrogen production, lower heating value and cold gas efficiency. Hence, in this research, both of gasifier will be simulated and compared to study their optimum condition and performances.

The synthesis gas produced from gasification process can be used to produce energy by using fuel cells. The proton exchange membrane fuel cell (PEMFC) is known as one of the best among the fuel cells since this PEMFC provide more energy density which have low emissions and long service life (Kamarudin et al., 2004). However, the synthesis gas needs to undergo hydrogen purification process because some of the synthesis gas such as carbon monoxide (CO) is poisoning to the Proton Exchange Membrane Fuel Cell (PEMFC) and thus it needs to be lower than 10 ppm or it can cause serious damage to the PEMFC membrane layer. Hence, hydrogen purification needs to be included in order to purify the hydrogen gas and reduce the amount of CO. Preferential oxidation of CO (CO-PROX) is one of the most suitable methods of purification of $H_2$ because of high CO conversion rate at low temperature range, which is preferable for PEMFC operating conditions (Mishra and Prasad, 2011). The effect of hydrogen purification case study also will become of one contribution in this study since it is importance to have lower amount of CO as an input for PEMFC.

For integration of gasification and fuel cell, there are several previous literature that have been done. For example, in the work of Schmidt and Gunderson (2000), where the authors considers the requirements on how to apply the three types of fuel cell which are PEMFC, PAFCs and MCFCs to biomass gasification with hydrogen purification. Besides, integrated gasification and fuel cell work that have been done by Sordi et al. (2017), they focusing on simulating of synthesis gas from sugarcane bagasse gasification at the PEMFC. In addition, Balan et al. (2004) analyzes the performance and economics of power generation systems based on Solid Oxide Fuel Cell (SOFC) technology and fuelled by gasified coal. However, this previous study has lack information of thermal, electrical, overall and stacks efficiency of the fuel cell. For the station power generation like the biomass gasification and PEMFC integrated system, the process has the ability to generate both energy and power simultaneously. These kinds of efficiencies information are important to show the capabilities of the fuel cells as energy conversion device. Hence, the integration of PEMFC and gasification will be carry out in this research in order to provide the thermal, electrical and overall efficiency study.

## 1.3 Objective

There are several objectives which will be focused of this study which are:

a) To develop and study the performances of integrated gasification and proton exchange membrane fuel cell (PEMFC) using fluidized bed gasifier and fixed bed gasifier for power production.

b) To develop and evaluate the performance of fluidized bed and fixed bed gasification models using different types of oil palm waste in Aspen Plus software.

c) To study the effect of biomass torrefaction for hydrogen production using fluidized bed gasifier and fixed bed gasifier.

## 1.4 Scopes of Work

a) To develop and simulate fluidized bed and fixed bed gasifier for gasification process using Aspen Plus software.

b) To validate the developed model of fluidized bed and fixed bed using Aspen Plus software.

c) To evaluate and compare the performance of fluidized bed gasifier and fixed bed gasifier for producing hydrogen gas using oil palm fronds, empty fruit bunch, palm kernel shell and palm mesocarp fibre.

d) To study and evaluate the effects of biomass torrefaction on the hydrogen production using fluidized bed gasifier and fixed bed gasifier.

e) To examine the effects of hydrogen purification on the hydrogen production in biomass gasification process.

f) To develop and study the performances of integrated gasification and proton exchange membrane fuel cell (PEMFC) using fluidized bed gasifier and fixed bed gasifier for power production.

## 1.5 Thesis Organization

The thesis has been arranged as follows:

Chapter 2 provides brief overview of biomass properties including raw and torrefied biomass characteristics, gasification technology such as fluidized and fixed bed gasifier, overview of fuel cells for energy production, approaches for hydrogen purification and summary of previous study related to raw and torrefied biomass gasification studies and fuel cell. Chapter 3 includes the development of workflow for biomass gasification and PEMFC as a stand-alone model or integrated model for producing the synthesis gas and/or power production. For Chapter 4, the applications of the workflow are highlighted through different case studies covering the model validation for fluidized and fixed bed models, simulation of biomass gasification using raw and torrefied oil palm wastes. The effects of hydrogen purification for synthesis gas is also highlighted which subsequently be applied in the integrated biomass gasification and PEMFC for power production. Finally, some conclusions and recommendations for future work are summarized in Chapter 5.

# CHAPTER 2

# LITERATURE REVIEW

## 2.1 Biomass: The Definition

Biomass is defined as the organic matter produced by photosynthesis. Biomass is a renewable energy resource that derived from the carbonaceous waste of various human and natural activities. Biomass is derived from numerous sources including the by-products from the agricultural crops, raw materials from the forest, timber industry, major parts of household wastes and wood. With its zero emission of carbon dioxide ($CO_2$), biomass is one of the most potential rich resources of energy that is not fully tapped for energy related application.

The main advantage of biomass as renewable energy source is it does not release carbon dioxide to the atmosphere as it absorbs the same amount of carbon in growing as it releases when it has been consumed as a fuel. Biomass recycles carbon from the air and spares the use of fossil fuels which reduces the need to utilize additional fossil carbon. Based on this fact, biomass is considered a natural, clean and safe material, with unlimited availability and high potential to be used as a renewable resource for the production of energy and alternative fuels (McPhail et al., 2012).

## 2.2 Main Biomass Resources in Malaysia

Biomass energy is an energy that is derived from living matter such as field's crops and trees. Malaysia is blessed with abundant supplies of biomass resources. These biomass resources are basically contributing a lot of biomass wastes. Biomass wastes in Malaysia can be categorized into agricultural and forestry wastes and municipal solid wastes. However, the main sources of biomass in Malaysia are come from plantation and agricultural residue. Availability of biomass base can be summarized in Figure 2.1. Basically, there are five main categories of biomass in Malaysia, which are produced in the following categories of oil palm, wood, rice, sugar cane and municipal waste.

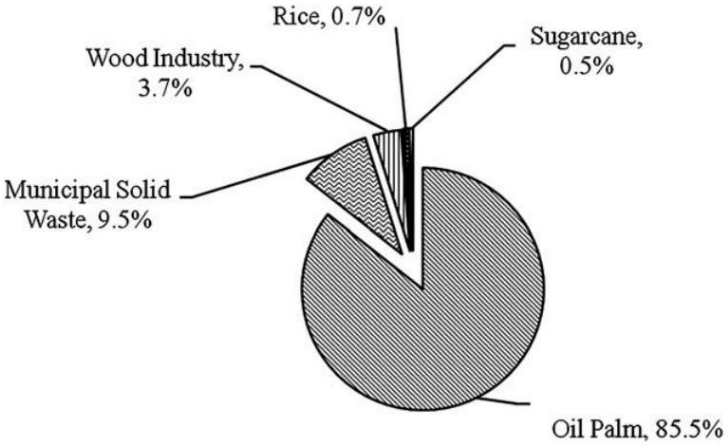

Figure 2.1 Production of wastes from different industry in Malaysia
Source: Shahbaz et al. (2016)

Based on Figure 2.1, palm oil residue has become prior potential source by providing 85 % share of total biomass in Malaysia. South East Asia main producer of palm oil especially Malaysia and Indonesia are provides 87 % of total palm oil of world (Shuit et al., 2009). Malaysia has great potential of palm oil cultivation about 3 million hectors area are used for its cultivation (Shuit et al., 2009) .The main biomass wastes produced during palm oil cultivation and its processing are palm kernel shell, trunks, fronds, empty fruit bunches and microscopic fibre. The total biomass waste production is 198 million ton/year which consist of 154.8 million ton/year of palm oil fronds (OPF), 10.1 million ton/year of trunks, 18.1 million ton/year for empty fruit bunches (EFB), 10.9 million ton/year for palm mesocarp fibre (PMF) and 4.2 million ton/year for palm kernel shells (PKS) (Khan et al., 2010). This amount of wastes is expected to increase due to the increasing demand and plantation expansion.

## 2.3 Biomass Properties

The most common analysis used for characterizing biomass is proximate analysis (moisture, ash, volatile matter, fixed carbon) and ultimate analysis (contents of elements: C, H, S, N and O). Both analyses are basically used by researcher for determining the compounds and elements in the biomass. In addition, calorific value is also conducted for examining the energy content of biomass.

### 2.3.1 Proximate Analysis

Proximate analysis is an important biomass characterization methods since every biomass have different chemical composition or combustion behaviour which consists of determination of moisture, volatile matter, fixed carbon, and ash (Garcia et al., 2013). A convenient method such as Thermogravimetric Analysis (TGA) which measures the weight changes in a material under specific temperature is suitable for providing proximate analysis data  (WOC, 2016).

#### 2.3.1.1 Moisture Content

The moisture content of biomass is the amount of water in the material expressed as a percentage of the material's weight (Fantini, 2010). This weight can be represented based on wet basis and based on dry ash free basis. The moisture content of a solid is expressed as the quantity of water per unit mass of the dry solid.

#### 2.3.1.2 Volatile Matter

Volatile matter refers to the part of the biomass that is released when the biomass is heated (usually up to 400 to 500 °C). During this heating process the biomass will decompose into volatile gases and solid char. Volatile matters may include combustible gases such as methane, hydrocarbons, hydrogen and carbon monoxide, as well as incombustible gases like carbon dioxide and nitrogen (Fantini, 2010). Thus, the volatile matter can be said as the main index of the gaseous fuels content.

#### 2.3.1.3 Fixed Carbon

The fixed carbon is the combustible residue left after driving off the volatile matter. The percentage of fixed carbon in a proximate analysis is obtained by subtracting 100 from the sum of the percentages of moisture, volatile matter and ash. Fixed carbon constitutes of mostly carbon but also contains traces of hydrogen, oxygen, sulphur and nitrogen (Fantini, 2010).

#### 2.3.1.4 Ash

The ash content is the inorganic matter or residue left out after complete combustion of the biomass. The ash content is determined by combustion of the fixed carbon and is expressed based on dry basis. The amount of ash is obtained by subtracting the total 100 from the sum of moisture, volatile matter and fixed carbon (Fantini, 2010).

### 2.3.2 Ultimate Analysis

The ultimate analysis is the second methods to represent the components in the organic parts especially for biomass. Ultimate analysis provides the main elements in biomass. The main or primary elements in biomass consist of carbon, hydrogen and oxygen while the secondary elements like nitrogen, sulphur and chlorine (Jones et al., 2014). The amount of these secondary elements is basically less than primary elements. The ultimate analysis is expressed based on dry basis. This ultimate analysis is necessary for indicating the quantitative analysis of various elements present in the biomass samples.

### 2.3.3 Calorific Value

The calorific value is one of the most significant characteristics of a biomass which indicates the amount of heat that produced from the mass (weight) of biomass in its complete combustion with oxygen in a calorimeter equipment (Moka, 2012). It is described as the amount of heat energy released during the complete combustion of unit mass of biomass. There are two types of calorific value (usually expressed in kcal/kg or MJ/kg) which are higher heating value (HHV) and lower heating value (LHV). HHV is the amount of heat released by a complete combustion of a mass unit of a sample at fixed volume in an oxygen atmosphere and at the standard conditions (101.3 kPa, 25 °C). The difference between the HHV and the LHV is the latent heat of condensation of the water vapor produced during the combustion process (Q. Zhu, 2010). Basically, HHV takes into account the latent heat of vaporization of water, and it assumes that the water component is in liquid state at the end of combustion. LHV does not include the water condensation heat. The LHV assumes that the water is removed with the combustion products without being fully condensed. The HHV can be determined experimentally in the laboratory by using adiabatic bomb calorimeter. The LHV is calculated based on the net of fuel moisture and water that forms in the combustion reaction. In practice, the value is obtained by subtracting the HHV with the heat water condensation produced during combustion.

## 2.4 Biomass as a Fuel Sources

Biomass can be converted into useful forms of energy by using a number of different thermochemical conversion processes which are classified into three categories namely combustion, gasification and pyrolysis. Thermochemical conversion process is the process where biomass wastes are converted into several products which are heat, bio-oil, char and synthesis gas. Figure 2.2 shows the thermochemical conversion processes and their primary products obtained based on biomass conversion process.

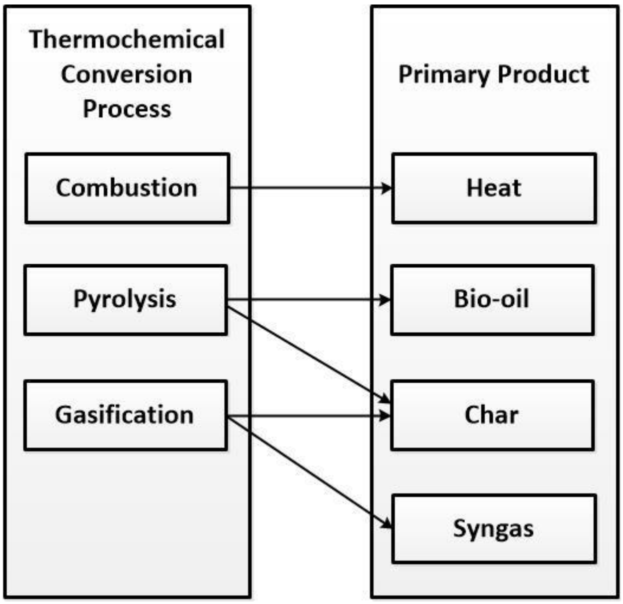

Figure 2.2 Thermochemical conversion and primary products

### 2.4.1 Combustion

Combustion is a thermochemical conversion process type that employs biomass feedstock such as wood, agricultural waste, municipal solid and residential waste to produce energy that can be used for power generation. In general combustion models of biomass can be classified as macroscopic or microscopic (Ragland et al., 1991). The macroscopic properties of biomass are given with for macroscopic analysis, such as ultimate and proximate analysis, heating value, moisture content, particle size, and ash fusion temperature. The properties for microscopic analysis include chemical kinetic, thermal, and mineral data (Demirbas, 2004). Combustion is broadly used on numerous scales to convert biomass into heat and/or electricity with the help of a steam cycle such as boilers, stoves, and power plants (Adams, 2013). The advantage of combustion is good overall electrical efficiency can be obtained up to 40 %. Usually combustion of biomass produces hot gases at temperatures around 800–1000 °C. However, the disadvantage of combustion is the process is practical only for biomass with moisture content lower than 50 %. Besides, the present of excess oxygen in the combustion are making the efficiency of the energy is decreasing (Faaij, 2004). This making combustion is not as the main energy conversion technology for biomass.

### 2.4.2 Pyrolysis

Pyrolysis is defined as the process to convert biomass to liquid (bio-oil), gaseous and solid (charcoal) fraction at operating temperature around 500 °C in the absence of oxygen. The products of pyrolysis are in solid (charcoal), liquid (pyrolysis oil) and gaseous form. For biomass, the pyrolysis is basically referring to lower temperature thermal processes producing liquids as the primary product. In this process, dry biomass is converted into liquid fuels via a fast pyrolysis process in which biomass is rapidly heated up to 500 °C in the absence of oxygen and then quickly cooled in the reactor. The process converts the biomass into carbohydrate-based compounds that include condensable gas and then these gases are condensed into liquid bio-oil which is the primary product of pyrolysis.

### 2.4.3 Gasification

Gasification is the conversion of biomass into a synthesis gas by partial oxidation at high temperatures, typically in the range 800–1100 °C. The synthesis gas is consists of mainly carbon dioxide, carbon monoxide, hydrogen and traces of methane. The low calorific value of synthesis gas produced around 4–6 MJ/N $m^3$ can be burnt directly or used as a fuel for gas engines and gas turbines (Susastriawan et al., 2017). In addition the synthesis gas can be used as a feedstock for the production of chemicals (e.g. methanol) (McKendry, 2002). According to Muslim et al. (2017), there are 9 general gasification reactions which occurred during the process as shown below:

$$C + O_2 \rightarrow CO_2 \qquad \Delta H^{\circ}_{298}: -393\ \text{kJ/mol} \qquad 2.1$$

$$C + 0.5O_2 \rightarrow CO \qquad \Delta H^{\circ}_{298}: -111\ \text{kJ/mol} \qquad 2.2$$

$$H_2 + 0.5O_2 \rightarrow H_2O \qquad \Delta H^{\circ}_{298}: -242\ \text{kJ/mol} \qquad 2.3$$

$$C + CO_2 \leftrightarrow 2CO \qquad \Delta H^{\circ}_{298}: +172\ \text{kJ/mol} \qquad 2.4$$

$$C + H_2O \leftrightarrow CO + H_2 \qquad \Delta H^{\circ}_{298}: +131\ \text{kJ/mol} \qquad 2.5$$

$$C + 2H_2 \rightarrow CH_4 \qquad \Delta H^{\circ}_{298}: -75\ \text{kJ/mol} \qquad 2.6$$

$$CO + H_2O \leftrightarrow CO_2 + H_2 \qquad \Delta H^{\circ}_{298}: -41\ \text{kJ/mol} \qquad 2.7$$

$$CH_4 + H_2O \leftrightarrow CO + 3H_2 \qquad \Delta H^{\circ}_{298}: +206\ \text{kJ/mol} \qquad 2.8$$

$$CH_4 + 2H_2O \leftrightarrow CO_2 + 4H_2 \qquad \Delta H^{\circ}_{298}: -111\text{kJ/mol} \qquad 2.9$$

Among all the processes, gasification is often chosen as main biomass thermochemical process since the process has a high advantageous in terms of carbon conversion and provides high calorific value in synthesis gas compared to combustion and pyrolysis. Another advantage of gasification is its capability to produce a high purity of fuel and therefore it could reduce pollution problems during burning process. Besides, the gasification process has higher efficiency to remove contaminants such as sulphur and nitrogen in the synthesis gas which resulting into lower emissions compare to combustion and pyrolysis. Moreover, the synthesis gas produced from the gasification reaction is a potential clean fuel which can be employed as substitution of oil and petroleum in conceivable future. Apart from that, the synthesis gas produced also can be used for power production purposes. The synthesis gas produced from gasification can be used by applying fuel cell-based cycles with yet even higher efficiencies and exceptionally low emissions of pollutants which can be used to produce electricity and heat. In fact, the synthesis gas can be clean relatively easily, given the much lower volume of raw synthesis gas to be treated compared to the large volume of flue gases that need to be treated in another thermochemical conversion processes.

## 2.5 Biomass Torrefaction

Biomass torrefaction is a mild pyrolysis and known as thermo-chemical treatment, where the biomass is heated under inert condition in the range of temperature from 200 °C to 300 °C, for upgrading the properties of biomass (Chen et al., 2015). Biomass torrefaction is a thermo-chemical process for upgrading the properties of biomass and biomass conversion to achieve a set of desirable chemical and physical properties. When biomass undergo torrefaction, the pretreatment can be further classified into light, mild and severe torrefaction processes, corresponding to the temperatures of approximately 200-235 °C, 235-275 °C and 275-300 °C, respectively (Chen and Kuo, 2011). During the process, the biomass partly decomposes giving off various condensable and non-condensable gases. The final product of the torrefaction process is a carbon rich solid, which is referred as torrefied biomass. For example, in elemental analysis of biomass properties, the weight percentage of carbon (C) element in the products of torrefied biomass will be increased after undergo torrefaction process. In contrast, the weight percentages of hydrogen (H) and oxygen (O) elements will be decreased. These weight percentages decrement in H and O elements are due to dehydration and de-carbon dioxide from the biomass during torrefaction (Poudel and Oh, 2014). As the biomass is torrefied, more generation of volatiles such as carbon monoxide (CO), carbon dioxide ($CO_2$) and water ($H_2O$) are expected and thus resulting into the decrease in the H and O contents for the biomass. Due to the torrefaction, the O/C and H/C ratios of torrefied biomass are lesser than raw biomass and as consequence, a high carbon converion is expected which resulting into the higher yield of synthesis gas for torrefied biomass compare to raw biomass. As the result, the torrefaction process will upgrade the properties of biomass.

## 2.6 Thermochemical Gasification of Biomass

There are three types of gasification technologies commonly used which are fixed bed gasifier, fluidized bed gasifier and entrained flow gasifier as shown in Figure 2.3.

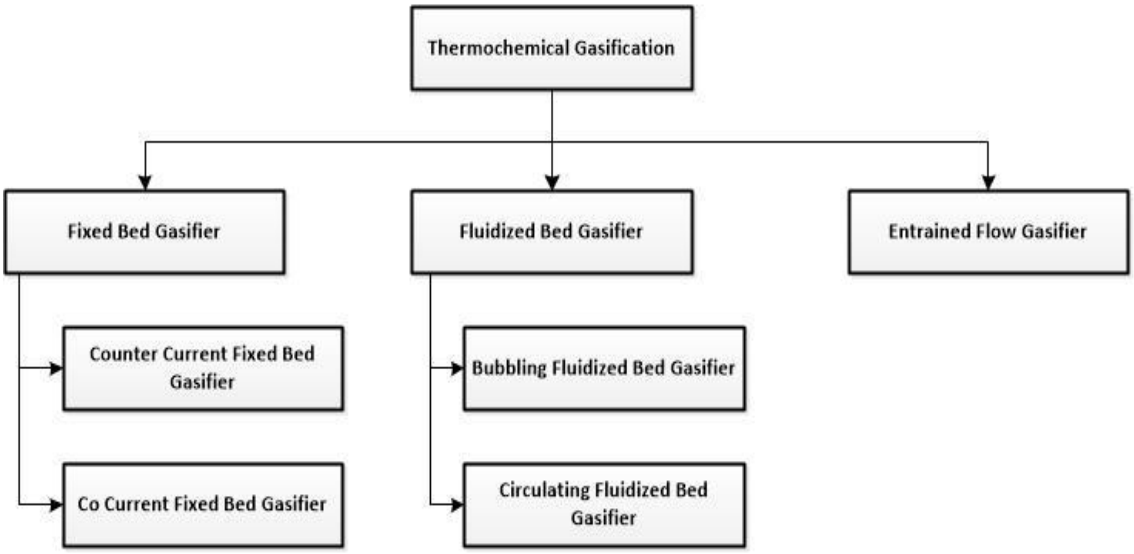

Figure 2.3 Types of gasification gasifier

### 2.6.1 Fixed-bed Gasifier

Fixed-bed gasifier is commonly used in gasification process due to its simplicity in design and operation. The gasifier is classified based on the modes of air flow direction. The updraft and downdraft gasifiers are shown in Figures 2.4 and 2.5. In updraft and downdraft gasifiers, the gas composition obtained in volume percentages based on the following ranges: CO (20-30 %), $H_2$ (5-15 %), $CH_4$ (1-3 %) and $CO_2$ (5-15 %) (Gordillo et al., 2009). The distribution of the reaction regions in a fixed-bed reactor is different depending on the design of gasifier.

#### 2.6.1.1 Counter-current (Updraft Gasifier)

In updraft mode, the biomass and air move counter-currently or opposite direction where the biomass moves downward from the top and gasifying agent from the bottom as shown in Figure 2.4.

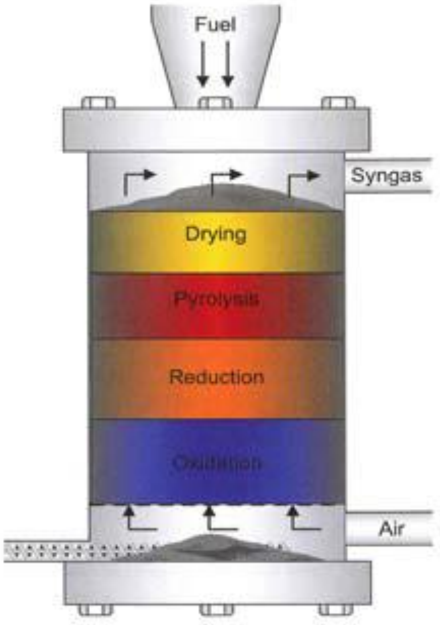

Figure 2.4 Updraft fixed bed gasifier
Source: Arnavat (2011)

The updraft gasifier has four distinct zones: (1) upper - drying zone, (2) upper medium - pyrolysis zone, (3) lower medium - oxidation zone and (4) lower - reduction zone. When the biomass is fed in the top section of the gasifier, firstly the biomass will enter the drying zone for reducing the moisture content of biomass and subsequently moving downward to reach the pyrolysis zone. In the pyrolysis zone, biomass is decomposed into volatiles and considerable quantities of char are formed. The air as gasifying agents interacts with the char and produces the required synthesis gas and these hot product gas moving upwards and reach drying zone. The heat from the gas evaporates the volatile compounds in the pyrolysis zone and then, the remaining heat of the product gas is used to evaporate the moisture. The temperature in the gasification zone can also be controlled by co-feeding steam and air or by humidifying the air. Because of the low temperature of the gas leaving the gasifier the formed gases are cooled down to 200-300 ºC. However, the tar from the char reaction which is in pyrolysis zone is condensed where it is further cracked to synthesis gas and soot (Nagel et al., 2009). The removal of tar is required if the gasifier is to be used in engine and synthesis application which represents the disadvantage of this gasifier.

### 2.6.1.2 Co-current (Downdraft Gasifier)

The design of the downdraft gasifier is basically similar as the updraft except in the downdraft design, the air is supplied at the oxidation layer in the co-current directions of the biomass into the bottom of the gasifier as shown in Figure 2.5.

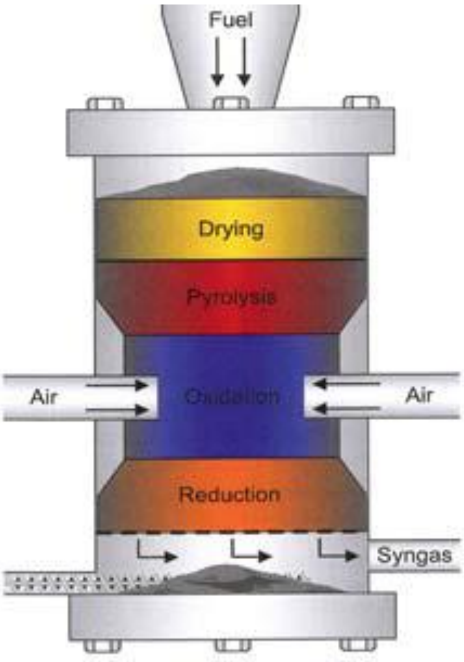

Figure 2.5 Downdraft fixed bed gasifier
Source: Arnavat (2011)

The biomass for in downdraft gasifier will undergo drying and pyrolysis stages as in the updraft gasifier. The water vapour and pyrolysis product then pass through oxidation zone where the oxidation agent such as air is supplied to ignite the combustion process. All products from the oxidation zone will pass to the reduction zone which lies under the oxidation zone. Here, the gases react with hot char and produce synthesis gas such as $CO_2$, $H_2$, $CH_4$ and CO. The downdraft gasifier is preferable compare to updraft gasifier due to its ability to produce clean synthesis gas (Sheth and Babu, 2009). In the downdraft gasifier, less tar production is usually obtained which contributing to the production of clean synthesis gas. However, low thermal efficiency usually obtained by using this gasifier.

### 2.6.2 Fluidized Bed

Fluidized bed gasification has been widely used for biomass gasification over the years. The main advantage of fluidized bed gasifier over fixed bed gasifier is the uniform temperature distribution that took place in the reduction zone. The consistency of temperature can be obtained by using a bed of fine granular material such as silica sand into the fluidization medium where the biomass is circulated and fluidizing the bed. The feed and the bed are mixing together which behave like a fluid inside of the gasifier. The temperature is fairly low compared to the temperature of the oxidation zone in fixed bed gasifiers, which helps to prevent problems related to ash melting (Siedlecki et al., 2011). The main fluidized media for this gasifier is the use of air and steam. This is another advantages of the fluidized bed compared to fixed bed since the gasifier have the steam flow to the gasifier compared to fixed bed. Although there have some literature used steam as gasifying agent for fixed bed, the fixed bed gasifier needs to rebuild first for adding the steam flow which differ from fluidized bed that have air and steam flow originally. Fluidized beds are used for a broad variety of fuels which offer operation flexibility of fluidized bed (Bartels et al., 2008). There are two common types of fluidized bed gasifiers which are bubbling bed and circulating fluidized bed. The different between this gasifier is the velocity of the fluidization medium in the gasifier.

#### 2.6.2.1 Bubbling Bed

This gasifier design looks like a vessel with a grate in the bottom and the air introduced through grate as shown in Figure 2.6. Above the grate, biomass is fed into the moving bed of fine-grained material. Typically, the temperature in this type of gasifier is around 700-900 ºC which can be maintained by controlling the air/biomass ratio. As the biomass is fed into the gasifier, it is heated up very quickly to the bed temperature due to the large heat capacity and movement of the bed. This allows a fast reaction of drying and pyrolysis of the biomass. The char particles remain in the bed, where they are grounded by rasping effect of the bed material. Usually the char is partially combusted in the bed, thus producing heat for endothermic gasification reactions. In bubbling fluidized bed, the gasifying agent is injected at the bottom of the reactor at a velocity equal to the minimum fluidization velocity to ensure intense mixing of the hot bed material. Basically, bubbling beds operate at relatively low gas velocities which typically below 3 $ms^{-1}$ which dragging the solid particle upwards with the gas flow. Uniform temperature across the bed can be maintained by good mixing of feed and bed resulting in uniform product synthesis gas. The product synthesis syngas is extracted from the top after being cleaned in the cyclones.

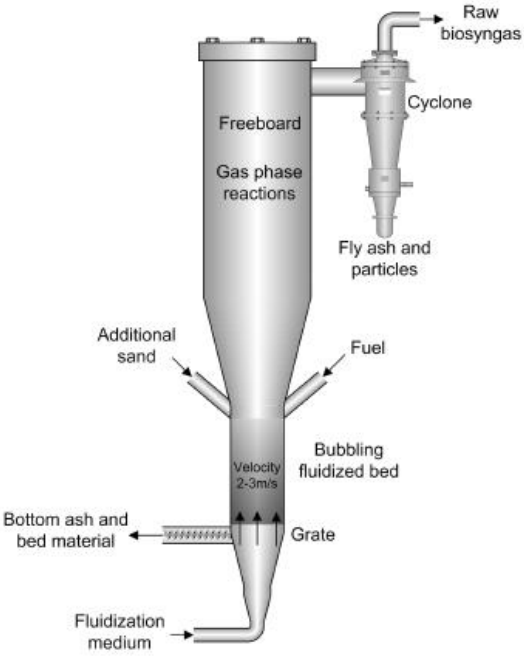

Figure 2.6 Bubbling fluidized bed gasifier
Source: Arnavat (2011)

#### 2.6.2.2 Circulating Bed

The circulating fluidized bed gasifier is shown Figure 2.7. The operating process for this type of gasifier is similar as bubbling fluidized bed. The biomass is fed into the bed, which is fluidized with gasification agent similarly to a bubbling fluidized bed installation. The different is this gasifier run with high fluidization velocity which around 5-10 $ms^{-1}$. The other different is the char particles that separated from the gasifier is recycled back to the bottom of the gasifier (Basu, 2013). Due to the high fluidization velocity, an entrainment of the particles in the product gas occurs. This exhaust stream is fed into a cyclone separator to isolate solids from the gas and the particles are separated in a cyclone at the exit of the reactor and the bed material is returned to the reactor as shown in Figure 2.7. Either one stage or multi-stage cyclone is used, depending on the solids concentration and size distribution. Circulation of the biomass particles is carried out until the particles are reduced in size due to combustion/gasification. The advantage of using the circulating fluidized bed design is the gasifier can be operated at elevated pressures. However, the circulating fluidized bed provides lower heat exchange compared to the bubbling fluidized bed gasifier and thus not suitable for a wide range of biomass particle sizes. Furthermore, bubbling fluidized bed gasifier with air is a relatively simple process for synthesis gas production.

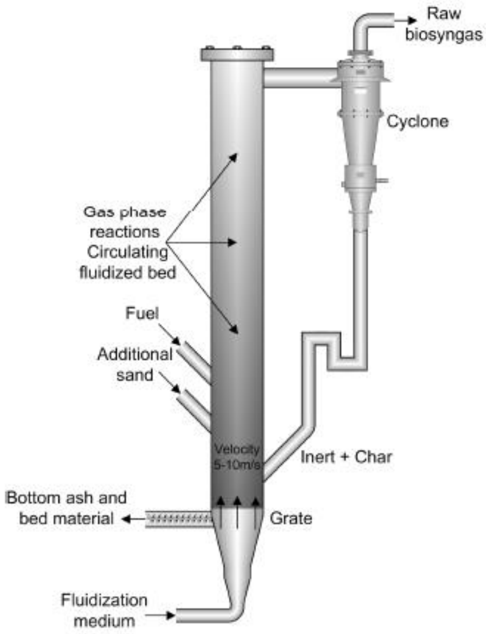

Figure 2.7 Circulating fluidized bed gasifier
Source: Arnavat (2011)

### 2.6.3 Entrained Flow

In the entrained flow gasifier as shown in Figure 2.8, the feedstock is introduced to the reactor as very fine particles, either dry or suspended in water. Entrained flow gasifier operates at much higher temperatures than the previously discussed gasifiers which are from ranges of 1200 to 1500 °C, usually with oxygen or with a mixture of oxygen and steam. The high temperature results in melting of the ash, which is then cooled and collected at the bottom of the gasifier. However, when biomass is used as a fuel, it is crushed into a powder which nearly to 50 µm in diameter before feeding. This is immediately the biggest disadvantage of entrained flow with respect to a biomass application where the size reduction of biomass is a very costly process in terms of energy. Finally, in order to reach high gasification temperature more product gas needs to be oxidized, which will reduce the cold gas efficiency (CGE) (Mikko, 2011). Hence, due to these disadvantages, this type of gasifier will not be chosen in this work. The comparison of the thermochemical gasification reactor is shown in Table 2.1.

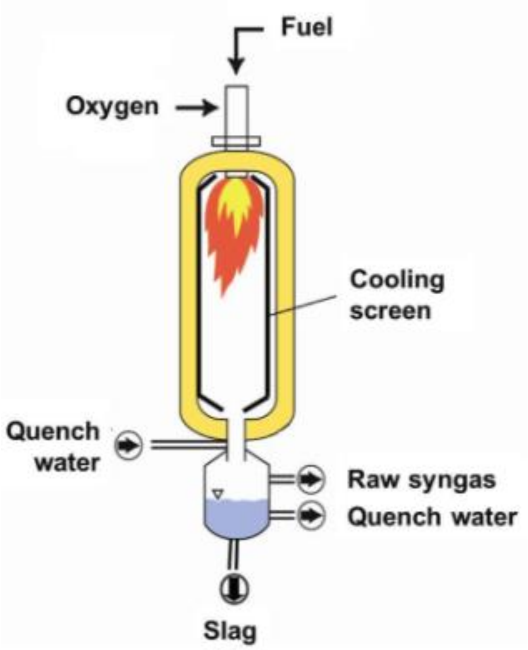

Figure 2.8 Entrained flow gasifier

Source: Arnavat (2011)

Table 2.1 Comparison on the different types gasifier

| Gasifier Types | Description | Advantages | Disadvantages |
|---|---|---|---|
| Updraft Fixed Bed | Fuel is fed from the top and gasification agent flows from the bottom of the reactor. The process steps are drying, pyrolysis, reduction and oxidation respectively. | - High charcoal burn-out<br>- Simple design<br>- Little scaling limitation | - High amount of tars produced<br>- Extensive gas cleaning needed if used for power production<br>- Stick ash can easily block the reactor<br>- Not used in large scale biomass gasification<br>- Limited ability to handle biomass fines |
| Downdraft Fixed Bed | Fuel is fed from the top of the reactor. The gasification agent is fed into the middle of the reactor. Synthesis gas is extracted from the bottom. The process steps are drying, pyrolysis, oxidation and reduction. | - Applicable for small-scale operations<br>- Produce gas with low tars | - Low thermal efficiency<br>- Limited scale-up<br>- High amounts of ash and dust<br>- Lumps easily to produce<br>- Fuel requirement are strict |
| Bubbling Fluidized Bed | Fuel is fed above the sand bed and the gasification agent enters the reactor from the bottom. The synthesis gas is extracted from the top after being cleaned in cyclones. | - Uniform temperature profile<br>- Accepts fuel size variation<br>- High ash melting point of biomass does not lead to clinker formation<br>- Uniform mixing of biomass<br>- High conversion rate of feedstock<br>- Catalyst are easily to replaced<br>- High cold gas efficiency<br>- Load flexibility and high heat transfer rates<br>- Compact construction | - Complex system due to low biomass hold up in the fuel bed<br>- Gas stream contains fine particles of dust |

| | | | |
|---|---|---|---|
| Circulating Fluidized Bed | Fuel is fed to the sand bed while the gasification agent enters the reactor from the bottom. Synthesis gas is partly extracted from the top and partly recycled to the bottom of the gasifier again. The fluidization velocity is higher than bubbling bed gasifier. | - Uniform temperature profile<br>- Fuel flexibility, can gasify a wide range of feedstock<br>- Scalable<br>- Short residence time | - High maintenance<br>- Easily to expose on erosion<br>- Produce high char content |
| Entrained Flow | Powder or slurry fuel is mixed with the gasification agent and enters to the reactor from the top. The gasification is aided by a powderized flame. Synthesis gas is extracted from the bottom | - Suitable for large pilot scale<br>- Product quality is high<br>- Can operate at high temperature | - Cannot operate at lab scale<br>- High cost for size reduction of biomass<br>- Low gas efficiency<br>- Large molten slag can be formed |

Sources : Mirmoshtaghi (2016)

According to Table 2.1, bubbling fluidized bed gasifier can be concluded as the best gasifier to run the gasification process since this kind of gasifier provides higher flexibility, having uniform temperature during the gasification process, high conversion of feedstock and higher efficiency compared to fixed bed gasifier. Since the fluidized bed allows an intensive mixing and a good heat transfer, there are no distinguished reaction zones. Hence, drying, pyrolysis, oxidation and reduction reactions take place simultaneously (Tripathy, 2013). Besides, this reactor also provides the higher efficiency compare to other gasifier. For entrained flow gasifier, it is not suitable for biomass application since high cost is needed for size reduction of biomass. Hence, in this study bubbling fluidized bed and downdraft fixed bed will be chosen as the gasifier for the gasification process.

Moreover, the gasification system can be constructed in several software in order to represent the actual experimental gasification work. The software such Aspen Plus have been widely used by the researcher for simulating the gasification process. The previous work based on simulation studies have been list in Table 2.2.

Table 2.2 Previous literature regarding on fixed and fluidized bed gasification simulation based study

| References | Gasifier Type | Work Description |
|---|---|---|
| Gómez-Barea & Leckner (2002) | Fluidized bed | Modelling of solid fuel gasification in fluidized bed with special emphasis on biomass and waste materials |
| Li et al. (2004) | Fluidized bed | Simulation of non-stoichiometric equilibrium model based on direct minimization of Gibbs free energy to predict the performance of the gasifier |
| Nikoo and Mahinpey (2008) | Fluidized bed | Simulation model which focusing on predicting the steady-state performance of an atmospheric fluidized bed gasifier. |
| Puig-Arnavat et al. (2010) | Fluidized bed | Analysed fluidized gasification model based on thermodynamic equilibrium, kinetics and artificial neural networks (ANN) |
| Sarkar & Bhattacharyya (2012) | Fixed bed | Simulation of fixed bed model for biomass gasification under steady-state and dynamic state conditions |
| Fatoni et al. (2014) | Fluidized bed | Studying the performance of biomass gasification in a circulating fluidized bed model process in Aspen Plus. |
| Begum et al. (2013) | Fixed bed | Studying the performance analysis of an integrated fixed bed gasifier model for different biomass feedstock |
| Mikulandrić et al. (2016) | Fixed bed | Develop a dynamic modelling of biomass gasification in a co-current fixed bed gasifier |
| Kaushal & Tyagi (2017) | Fixed bed | Investigating the performance of fluidized bed gasifier by focusing on kinetics of drying, devolatilization, tar |

| | | |
|---|---|---|
| | | cracking and char gasification coupled with the reactor hydrodynamic using Aspen Plus software. |
| Han et al. (2017) | Fixed bed | Developed a model of downdraft biomass gasification process by restricting chemical reaction equilibrium using Aspen Plus |
| Pala et al. (2017) | Fluidized bed | Develop an integrated model for steam gasification of biomass and subsequent synthesis gas adjustment using shift reaction in Aspen Plus to predict the synthesis gas composition from biomass. |

## 2.7 Fuel Cells

Fuel cells (FC) are electrochemical energy conversion devices for the alteration of primary energy of a fuel (usually hydrogen ($H_2$) gas or a mixture rich in $H_2$) into direct current electricity. The main benefit of this technology is the high efficiency of fuel conversion can be obtained through electrochemical reactions. Another advantage of fuel cell is their low environmental impact. In fact if the fuel is pure hydrogen, the by-products of the fuel cell are water and heat only.

A typical fuel cell system consists of a fuel cell stack where the fuel mono-cells are linked together in series to deliver useful power (Sattler, 2000). Each mono-cell, regardless of the fuel cell types, has the same main components. In Figure 2.9, a typical schematic of a fuel cell is presented with the main flows that characterize its operation. A generic cell is composed of two electrodes divided by a liquid or solid electrolyte and an external electric circuit. In the electrodes, the oxidation/reduction reactions take place. In some fuel cell types, the catalyst is needed for improving the kinetics of the reactions that occur at the electrodes. The importance role of catalyst increase as the operating temperature decreases. The electrode where the oxidation reactions take place is called “anode”, while the other, where the reduction reactions take place, is called “cathode” (Haile, 2003). The external circuit allows electrons to be carried between the two electrodes, while the electrolyte has to permit the transport of ions from one electrode to the other.

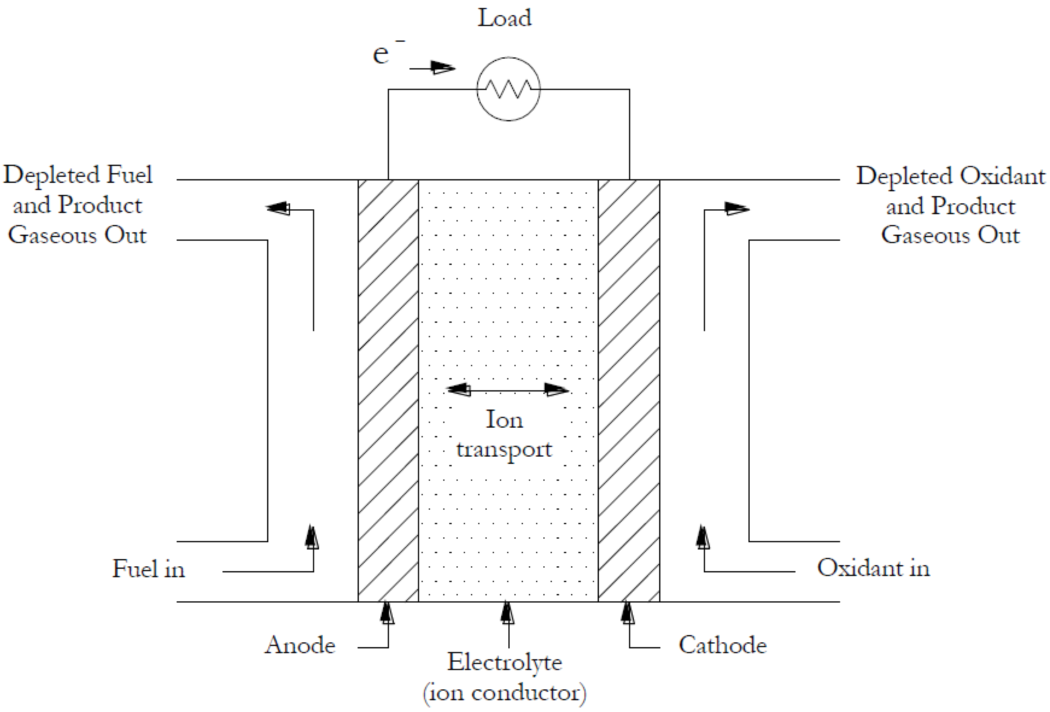

Figure 2.9 Schematic of a generic fuel cell
Source: Sardella (2013)

The main differences in the different types of fuel cells lie in materials and operating conditions. It is common to classify a fuel cell according to the type of the electrolyte used. There are several types of fuel cells such as Alkaline Fuel Cells (AFC), Phosphoric Acid Fuel Cells (PAFC), and Molten Carbonate Fuel Cells (MCFC), Solid Oxide Fuel Cells (SOFC) and Proton Exchange Membrane Fuel Cells (PEMFC).

### 2.7.1 Alkaline Fuel Cells (AFC)

Alkaline fuel cell (AFC) as shown in Figure 2.10 was one of the first fuel cell technologies developed, and they were the first type of fuel cell that widely used for space program to produce electrical energy and water on-board spacecraft. These fuel cells use a solution of potassium hydroxide in water as the electrolyte and can use a variety of non-precious metals as a catalyst at the anode and cathode (Sotouchi, 1984.). These fuel cells are closely similar to conventional PEM fuel cells, except that they use an alkaline membrane instead of an acid membrane. The high performance of AFC is depending on the rate at which electro-chemical reactions take place in the cell (Gulzow et al., 2002). They have also demonstrated efficiencies above 60 % in space applications. The electrode reactions for AFCs are shown as follows:

Cathode : $1/2O_2 + H_2O + 2e^- \rightarrow 2OH^-$ 2.10

Anode : $H_2 + 2OH^- \rightarrow 2H_2O + 2e^-$ 2.11

Overall : $H_2 + 1/2O_2 \rightarrow H_2O$ 2.12

Water has to move from the anode to the cathode; OH– ions have to move from the cathode to the anode. On their way they have to pass parts of the electrodes and the active separator. The active separator is placed in between the anode and the cathode. The reaction water has to pass two electrodes and one or two separators which depending on where the water leaves the cell (Kohnke et al., 2005).

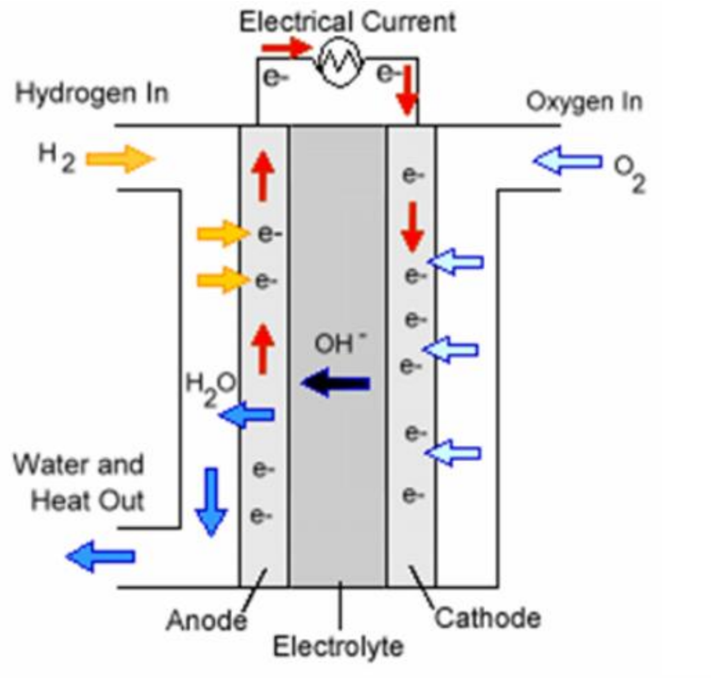

Figure 2.10 Schematic of a generic alkaline fuel cell
Source: Adapted from https://energy.gov/eere/fuelcells/types-fuel-cells

A key challenge for this fuel cell type is that it is vulnerable to be poisoned by carbon dioxide ($CO_2$). In fact, even the small amount of $CO_2$ in the air can dramatically affect overall cell performance and durability due to carbonate formation (Gulzow, 1996). Alkaline cells with liquid electrolytes can be run in a recirculating mode, which allows for electrolyte regeneration to help reduce the effects of carbonate formation in the electrolyte, but the recirculating mode introduces issues with bypass currents. The liquid electrolyte systems also have several difficulties which concerns wettability, increased corrosion, and difficulties in handling differential pressures. Alkaline membrane fuel cell (AMFC) addresses these concerns and has lower susceptibility to $CO_2$ poisoning than liquid-electrolyte AFC. However, $CO_2$ still affects performance and durability of the AMFCs which shows this fuel cell is still lag that of PEMFCs. Challenges for AMFCs include tolerance to carbon dioxide, membrane conductivity and durability, higher temperature operation, water management, power density, and anode electrocatalysis.

### 2.7.2 Phosphoric Acid Fuel Cells (PAFCs)

Phosphoric acid fuel cells (PAFCs) as shown in Figure 2.11 use liquid phosphoric acid as an electrolyte which the acid is contained in a teflon-bonded silicon carbide matrix and the porous carbon electrodes containing a platinum catalyst (Remick and Wheeler, 2010). The electro-chemical reactions that take place in the cell are shown in the Figure 2.11.The PAFC is believed as the "first generation" of modern fuel cells (Schudt et al., 2009). It is one of the most mature cell types and the first to be used commercially. This type of fuel cell is typically used for stationary power generation, but some of this fuel cell has been used to supply power for large vehicles such as city buses.

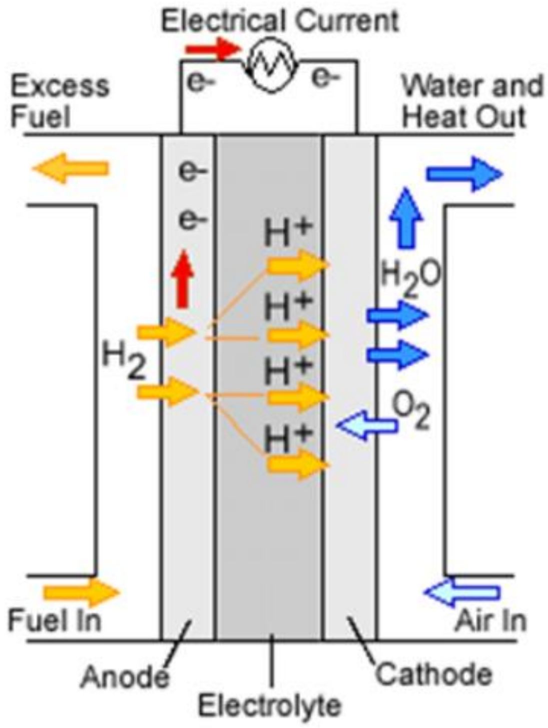

Figure 2.11 Schematic of a generic phosphoric acid fuel cell
Source: Adapted from https://energy.gov/eere/fuelcells/types-fuel-cells

The electrode reactions for PAFCs are shown as follows:

$$\text{Cathode}: O_2 + 4H^+ + 4e^- \rightarrow 2H_2O \qquad 2.13$$

$$\text{Anode}: 2H_2 \rightarrow 4H^+ + 4e^- \qquad 2.14$$

$$\text{Overall}: 2H_2 + O_2 \rightarrow 2H_2O \qquad 2.15$$

PAFCs are more lenient of impurities in fossil fuels that have been reformed into hydrogen than PEM cells, which are easily "poisoned" by carbon monoxide because carbon monoxide binds to the platinum catalyst at the anode, decreasing the fuel cell's efficiency. PAFCs are more than 85 % efficient when used for the co-generation of electricity and heat but they are less efficient at generating electricity alone (37 – 42 %). PAFC efficiency is only slightly more efficient than combustion-based power plants, which typically operate at around 33 % efficiency. PAFCs are also less powerful than other fuel cells, given the same weight and volume. As a result, these fuel cells are typically large and heavy. Besides, PAFCs are also expensive. They require much higher loadings of expensive platinum catalyst than other types of fuel cells, which raise the cost considerably.

### 2.7.3 Molten Carbonate Fuel Cells (MCFCs)

Molten carbonate fuel cell (MCFC) as shown in Figure 2.12 is currently being established for natural gas and coal-based power plants for industrial, electrical utility and military applications. MCFC is high-temperature fuel cell that use an electrolyte composed of a molten carbonate salt mixture suspended in a porous, chemically inert ceramic lithium aluminum oxide matrix (Rexed, 2014). Since they operate at high temperatures of 650 °C (roughly 1,200 °F), the non-precious metals can be used as catalysts at the anode and cathode and this can reduce operational costs.

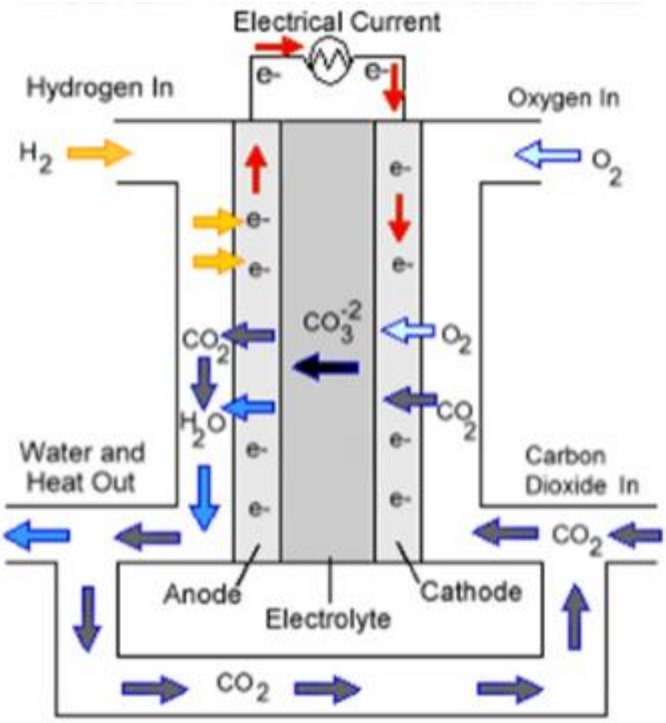

Figure 2.12 Schematic of a generic molten carbonate fuel cell
Source: Adapted from https://energy.gov/eere/fuelcells/types-fuel-cells

The electrode reactions for MCFCs are shown as follows:

$$\text{Cathode}: 2CO_2 + O_2 + 4e^- \rightarrow 2CO_3^{2-} \qquad 2.16$$

$$\text{Anode}: 2H_2 + 2CO_3^{2-} \rightarrow 2H_2O + 2CO_2 + 4e^- \qquad 2.17$$

$$\text{Overall}: 2H_2 + O_2 \rightarrow 2H_2O \qquad 2.18$$

From the equation above, the overall reaction is water producing reaction between oxygen and hydrogen, with the carbonate ions $CO_3^{2-}$ is acting as intermediate agent to transfer oxide ion from cathode to anode. Electrons produced at the anode pass through an external circuit before flowing to the cathode, and thus electric power can be extracted (Takizawa, 1988).

Improved efficiency is another reason MCFCs offer important cost reductions over phosphoric acid fuel cells. Molten carbonate fuel cells, when set with a turbine, can reach efficiencies approaching 65 %, considerably higher than the 37 – 42 % efficiencies of a phosphoric acid fuel cell. When the waste heat is captured and used, overall fuel efficiencies can be over 85 %. Unlike alkaline, phosphoric acid, and PEM fuel cells, MCFCs do not require an external reformer to convert fuels such as natural gas and biogas to hydrogen. At the high temperatures at which MCFCs operate, methane and other light hydrocarbons in these fuels are converted into hydrogen within the fuel cell itself by a process called internal reforming, which also reduces cost. The primary disadvantage of current MCFC technology is its durability. The high temperatures at which these cells operate and the corrosive electrolyte used accelerate component breakdown and corrosion which contributing to the decreasing of cell life.

### 2.7.4 Solid Oxide Fuel Cells (SOFCs)

Solid oxide fuel cell (SOFC) as shown in Figure 2.13 uses a hard, non-porous ceramic compound as the electrolyte (Singhal, 2000). SOFC is able to produce around 60 % efficiency for converting fuel to electricity. In applications designed to capture and utilize the systems waste heat (co-generation), overall efficiencies could reach as high as 85 %. SOFC operate at very high temperatures as high as 1,000 °C (1,830 °F) (Singhal, 2007). High temperature operation removes the need for precious-metal catalyst, which ultimately reduces the operational cost. It also allows SOFCs to reform fuels internally, which enables the use of a variety of fuels and reduces the cost associated with adding a reformer to the system.

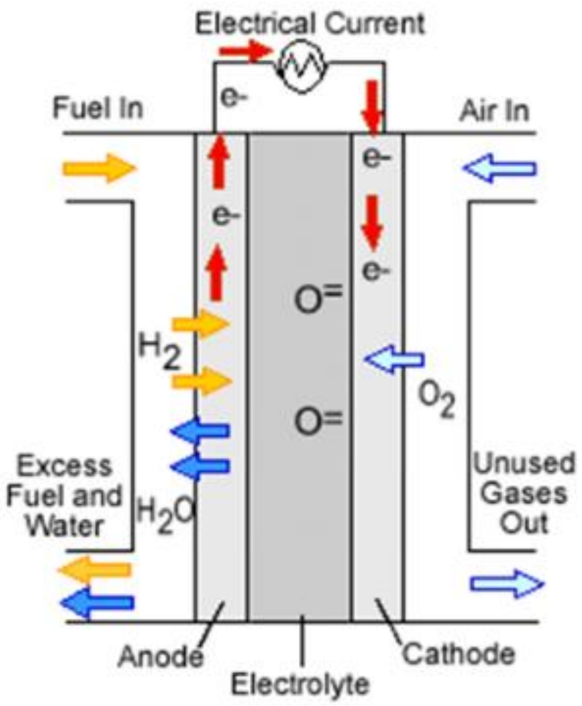

Figure 2.13 Schematic of a solid oxide fuel cell
Source: Adapted from https://energy.gov/eere/fuelcells/types-fuel-cells

The electrode reactions for SOFCs are shown as follows:

$$\text{Cathode : } 1/2O_2 + 2e^- \rightarrow O^{2-} \qquad 2.19$$

$$\text{Anode : } H_2 + O_3^{2-} \rightarrow H_2O + 2e^- \qquad 2.20$$

$$\text{Overall : } H_2 + 1/2O_2 \rightarrow H_2O \qquad 2.21$$

Based on the equation above, the $O^{2-}$ ion is drawn through the electrolyte from the cathode to the anode by the reactive attraction of hydrogen and carbon monoxide to oxygen, while electrons are forced through an external circuit from the anode to the cathode. Thus, the fuel cell will produces water regardless of fuel in the end of reaction (Fontes et al., 2012).

SOFC is also employing sulphur-resistant which enabling to endure several orders of sulphur than other fuel cell. In addition, they are not poisoned by carbon monoxide. This property allows SOFC to use natural gas, biogas, and gases made from coal. However, SOFC still have main disadvantage compare to another fuel cells. The high-temperature operation of SOFC causes a slow start up and requires significant thermal shielding to retain heat and protect personnel, which may be acceptable for utility applications but not for transportation. The high operating temperatures also place stringent durability requirements on materials (Zhu and Deevi, 2003). The development of low-cost materials with high durability at cell operating temperatures is the key technical challenge using this technology.

### 2.7.5 Proton Exchange Membrane (PEM) Fuel Cell

Proton exchange membrane (PEM) fuel cell also called polymer electrolyte membrane (PEM) fuel cell deliver high power density and offer the advantages of low weight and volume compare to other fuel cells. PEM fuel cell as shown in Figure 2.14 uses a solid polymer as an electrolyte and porous carbon electrodes containing a platinum or platinum alloy catalyst (Basualdo et al., 2012). They need only hydrogen, oxygen from the air, and water to operate. They are typically fuelled with pure hydrogen supplied from storage tanks or reformers.

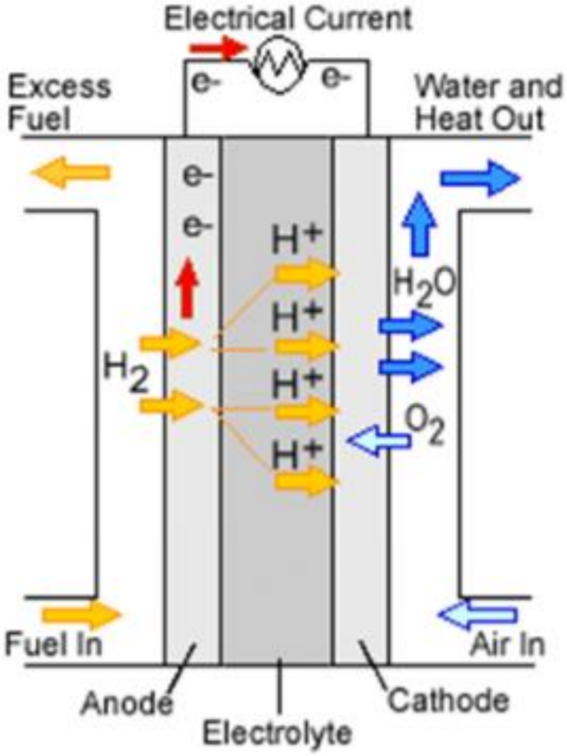

Figure 2.14 Schematic of a generic proton exchange membrane (PEM) fuel cell
Source: Adapted from https://energy.gov/eere/fuelcells/types-fuel-cells

The electrode reactions for PEMFCs are shown as follows:

$$\text{Cathode : } 1/2O_2 + 2e^- + 2H^+ \rightarrow H_2O \quad 2.22$$

$$\text{Anode : } H_2 \rightarrow 2H^+ + 2e^- \quad 2.23$$

$$\text{Overall : } H_2 + 1/2O_2 \rightarrow H_2O \quad 2.24$$

For PEMFC, the $H^+$ ion is drawn through the electrolyte from the anode to the cathode by the reactive attraction of hydrogen to oxygen, while electrons are forced through an external circuit. Thus, for overall reaction, the fuel cell will produces water which accumulates at the cathode (Eysenbach, 2008).

PEM fuel cell operates at relatively low temperatures around 80 °C (176 °F). Low-temperature operation allows them to start quickly (less warm-up time) and resulting into less wear on system components which provides better durability (Mert et al., 2011). The main advantage of PEM fuel cell is their high efficiency which comparable with other energy conversion devices (Sharaf and Orhan, 2014). However, it requires noble-metal catalyst (typically platinum) for separating the hydrogen's electrons and protons. The platinum catalyst is also extremely sensitive to carbon monoxide poisoning, making it necessary to employ an additional reactor to reduce carbon monoxide in the fuel gas if the hydrogen is derived from a hydrocarbon fuel. PEM fuel cells are used primarily for transportation applications and some stationary applications. This high efficiency of a fuel cell is beneficial for vehicle related application (Rajashekara, 2000). Moreover, due to their fast start-up time and favourable power-to-weight ratio, PEM fuel cell is particularly suitable for use in passenger vehicles such as cars and buses. There are several studies done by previous researcher regarding to model PEMFC. The previous work based on simulation studies on fuel cell have been list in Table 2.3.

Table 2.3 Previous literature regarding on simulation based study on fuel cells

| References | Fuel Cell Types | Work Description |
|---|---|---|
| Angelika Heinzela et al. (2001) | Proton Exchange Membrane | Developed and simulating Aspen Plus model for 3.3 Kw power production by applying PEM fuel cell |
| Kivisaari (2001) | Alkaline | Simulating the alkaline fuel cell with high pressure- |

|  |  |  |
|---|---|---|
|  |  | gasification for efficiency and economic purposes. |
| Fermeglia et al. (2005) | Molten Carbonate | Investigating the dynamic behaviour of a two dimensional model of Molten carbonate Fuel Cell by undergo simulation process. |
| Steward et al. (2010) | Phosphoric Acid | Develop a modelling based on Aspen software for investigating the production of electricity, heat, and hydrogen generation from Phosphoric Acid Fuel Cell |
| Rabbani and Rokni (2012) | Proton Exchange Membrane | Performing dynamic simulation of Proton Exchange Membrane Fuel Cell system for automotive applications using Aspen Plus as main base simulator. |
| Doherty (2014) | Solid Oxide | Modelling of biomass gasification integrated with a solid oxide fuel cell system by using Aspen Plus. |
| Paengjuntuek et al. (2015) | Solid Oxide | Develop a Aspen Plus modelling of integrated gasification with solid cycle of fuel cell for energy analysis. |
| Chutichai and Arpornwichanop (2015) | Proton Exchange Membrane | Investigate the ability of integrated biomass gasification and PEMFC based system analyze the effect of primary parameters of power production on the system energy efficiency using Aspen Plus software. |

For fuel cell comparison, the overall comparisons of the fuel cells are summarized in Table 2.4. Based on this comparison, PEM fuel cell gives more advantages and compatibility compare to other types of fuel cell. The higher efficiency of energy conversion is needed in specific fuel cell during energy production and this criterion is available from PEM fuel cell.

Table 2.4 Summary of major differences of the fuel cell types

| Fuel Cell Types | Alkaline (AFC) | Phosphoric Acid (PAFC) | Molten Carbonate (MCFC) | Solid Oxide (SOFC) | Proton Exchange Membrane (PEM) |
|---|---|---|---|---|---|
| Common Electrolyte | Alkaline polymer Membrane | Phosphoric acid soaked in a polymer membrane | Molten lithium, sodium, and/or potassium carbonates, soaked in a porous matrix | Yttria stabilized zirconia | Perfluorosulfonic acid |
| Operating Temperature | <100 °C | 150 – 200 °C | 600 – 700 °C | 500 – 1000 °C | <120 °C |
| Electrical Efficiency | 60 % | 40 % | 50 % | 60 % | 60 % direct $H_2$;<br>40 % reformed fuel |
| Advantages | • Low temperature<br>• Quick start-up | • Increased tolerance to fuel impurities | • High efficiency<br>• Fuel flexibility<br>• Hybrid/gas turbine cycle | • High efficiency<br>• Fuel flexibility<br>• Solid electrolyte | • Solid electrolyte reduces corrosion & electrolyte management problems<br>• Low temperature<br>• Quick start-up<br>• High efficiency |
| Challenges | • Sensitive to $CO_2$ in fuel and air<br>• Electrolyte management (aqueous)<br>• Electrolyte conductivity (polymer) | • Expensive catalysts<br>• Long start-up time<br>• Sulfur sensitivity | • High temperature corrosion and breakdown of cell components<br>• Long start-up time<br>• Low power density | • High temperature corrosion and breakdown of cell components<br>• Long start-up time<br>• Limited number of shutdowns | • Expensive catalysts<br>• Sensitive to CO |

Source: U.S. Department of Energy (2011)

## 2.8 Hydrogen Purification

Fuel cells such as PEMFC have attracted significant interest due to their low temperature of operation (80 °C), high power density, high efficiency and the environmentally benign nature of their exhaust. The PEMFC ideal fuel is hydrogen. One of the feasible sources to generate hydrogen is by using gasification but the difficulty is the hydrogen produced usually comes with another synthesis gas component such as CO and $CO_2$. However, the anode catalysts of PEMFC which are operated at relatively low temperatures (80-120 °C) have been demonstrated to be easily poisoned by traces of CO even the amount exists is around 10 ppm in the hydrogen rich feed gas. Therefore it is necessary to eliminate the traces of CO in the hydrogen stream with a minimum hydrogen loss (Schonbrod et al., 2009). There are several methods for CO removal from the synthesis gas stream which are: i) purification with hydrogen selective membrane, ii) CO methanation, iii) pressure swing adsorption, and iv) preferential oxidation (PROX) of CO.

### 2.8.1 Purification with Hydrogen Selective Membrane

One alternative to purify hydrogen is the use of hydrogen selective membranes due to their easy preparation, low energy consumption and cost effectiveness at low gas volumes (Holmes, 2010). Figure 2.15 shows a schematic of the semipermeable membrane separation process, in which the driving force is often pressure or concentration gradient across the membrane. Hydrogen separations from highly supercritical gases, such as methane, carbon monoxide, and nitrogen are easy to achieve by using polymeric membranes, because of the extremely high diffusion coefficient of hydrogen relative to all other molecules except helium.

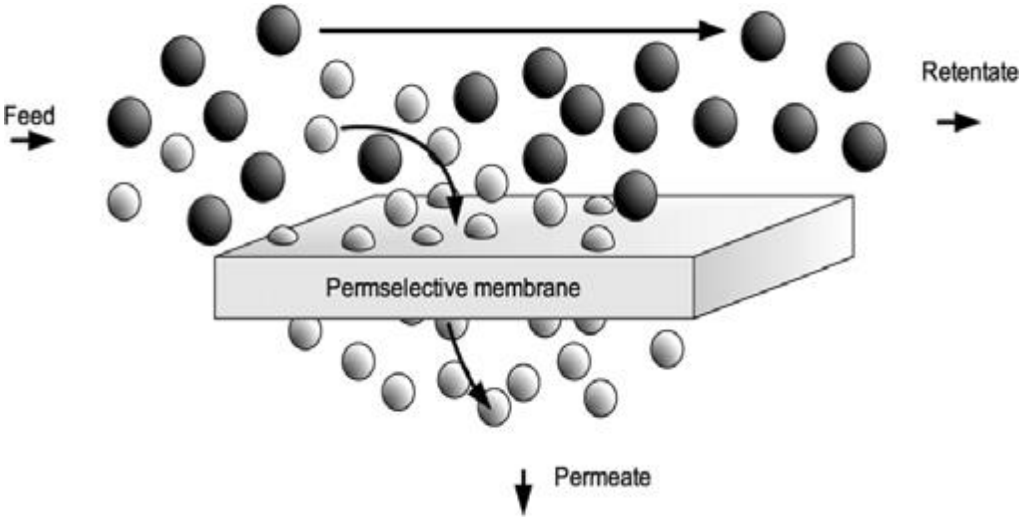

Figure 2.15 Simplified concept schematic of membrane separation
Source: Mishra and Prasad (2011)

In order to meet the best requirements of PEMFC feed such as a high permeability selectivity for $H_2$, the dense phase metal membrane in which the solution diffusion is dominant has been considered to be most feasible. However, in recent work, Varela et al. (2010) found that the selectivity for hydrogen purification was very high but further efforts need to be undertaken in order to improve the flux through the composite membrane materials.

### 2.8.2 CO Methanation

CO methanation is another methods for the purification of hydrogen gas mixture. The following reactions (Equations 2.25 and 2.26) can be carried out in the presence of CO, $CO_2$, and $H_2$ which are the main gaseous components in the exit of water-gas shift reactor.

$$CO(g) + 3H_2(g) \rightarrow CH_2(g) + H_2O(g) \qquad \Delta H^{\circ}_{298}: -205.813 \text{ kJ/mol} \qquad 2.25$$

$$CO_2(g) + 4H_2(g) \rightarrow CH_4(g) + 2H_2O(g) \qquad \Delta H^{\circ}_{298}: -164.647 \text{ kJ/mol} \qquad 2.26$$

The use of catalysts such as Nickel-Zirconium dioxide ($Ni/ZrO_2$) and Ruthenium-Titanium dioxide ($Ru/TiO_2$) can decrease a concentration of CO from 0.5 % to 20 ppm in the gases formed by the steam reforming of methane with a significantly low conversion of $CO_2$ into methane (Takenaka et al., 2004). Generally, all catalysts used for CO methanation are noble metal based which are very costly and temperature (300-340 °C) for the reaction was also very high. Besides, in CO methanation, hydrogenation of CO takes place in which hydrogen is consumed in large amount so popularity of this method is less than preferential oxidation of carbon monoxide (Park et al., 2009).

### 2.8.3 Pressure Swing Adsorption

The current technology used to purify hydrogen from synthesis gas is pressure swing adsorption (PSA). It is a technology used to separate some gas species from a mixture of gases under pressure according to the species molecular characteristics and affinity for an adsorbent material (Lawrence, 2010). Pressure swing adsorption processes rely on the fact that under pressure, gases tend to be attracted to solid surfaces, or "adsorbed". The higher the pressure, the more gas is adsorbed; when the pressure is reduced, the gas is released, or desorbed. PSA processes can be used to separate gases in a mixture because different gases tend to be attracted to different solid surfaces more or less strongly. Although many adsorbents are commercially available, there are still demand for robust (high chemical stability against other contaminants, high mechanical stability against attrition), cheap (low synthesis cost since adsorbent cost represents a significant part of the investment cost) and energy efficient materials (Barelli et al., 2008). In addition, it is not suitable for non-stationary applications, due to the large dimensions and high costs of the compressor (Tagliabue et al., 2009).

### 2.8.4 Preferential Oxidation of CO

The preferential oxidation (PROX) process is one of the most effective methods for the removal of CO trace from the reformate stream. PROX of CO involves a reaction to convert CO in a $H_2$-rich gas mixture to $CO_2$ with minimal $H_2$ consumption. Therefore, preferential oxidation process is an indispensable step to reduce the concentration of CO to 10 ppm level in a $H_2$ generation process (Park et al., 2009). The flow diagram of hydrogen purification by preferential oxidation of CO is shown in Figure 2.16.

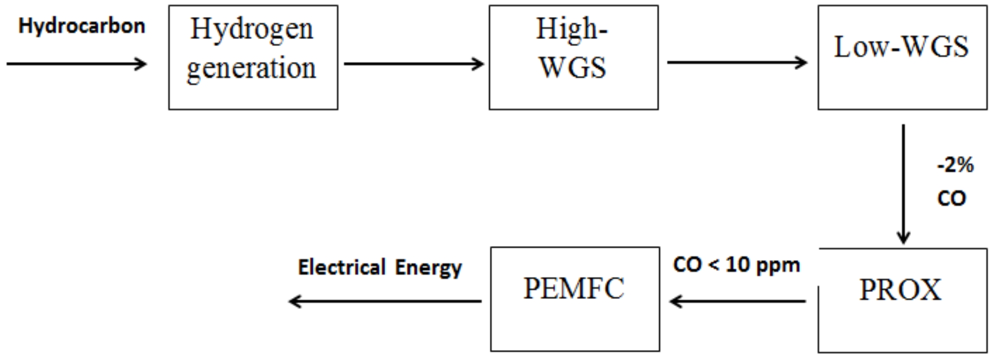

Figure 2.16 Flow diagram of hydrogen purification by CO-PROX

The following reaction which is shown in Equation 2.27 is occurred in the PROX system.

$$CO + 0.5O_2 \leftrightarrow CO_2 \qquad \Delta H^{\circ}_{298}: -283 \text{ kJ/mol} \qquad 2.27$$

From Equation 2.27, an excess of oxygen is provided, at around a factor of two, and about 90 % of the CO is transformed. In the second step a substantially higher oxygen excess is used, at approximately a factor of 4, which is then processed with the remaining CO, in order to reduce the CO concentration to be lesser than 10 ppm and to avoid excess CO-fraction loading. The instrumentation and process control complexity requirements are relatively high. The advantage of this technique over selective methanation is the higher space velocity, which reduces the required reactors size. The PROX of CO is a catalytic reaction where the catalyst plays a significant role in enhancing the CO oxidation and suppressing $H_2$ oxidation. The key factors to achieve very low CO concentration fuel, is synthesizing a highly active, stable, and selective catalyst for PROX reaction in $H_2$-rich gas mixture at the lower temperature range (Hulteberg et al., 2005).

## 2.9 Integrated Biomass Gasification and Fuel Cells

The gasification process is known as one of the best conversion routes for producing a renewable energy from biomass feedstock which produce high yield of syngas. However, biomass gasification cannot provide high energy efficiency. Meanwhile the fuel cell needs hydrogen as an input for the system. Therefore, the integrated biomass gasification and fuel cell can be done by combining both systems in order to obtain higher energy efficiency. Figure 2.17 shows an example of schematic diagram for the integrated biomass gasification and PEMFC system.

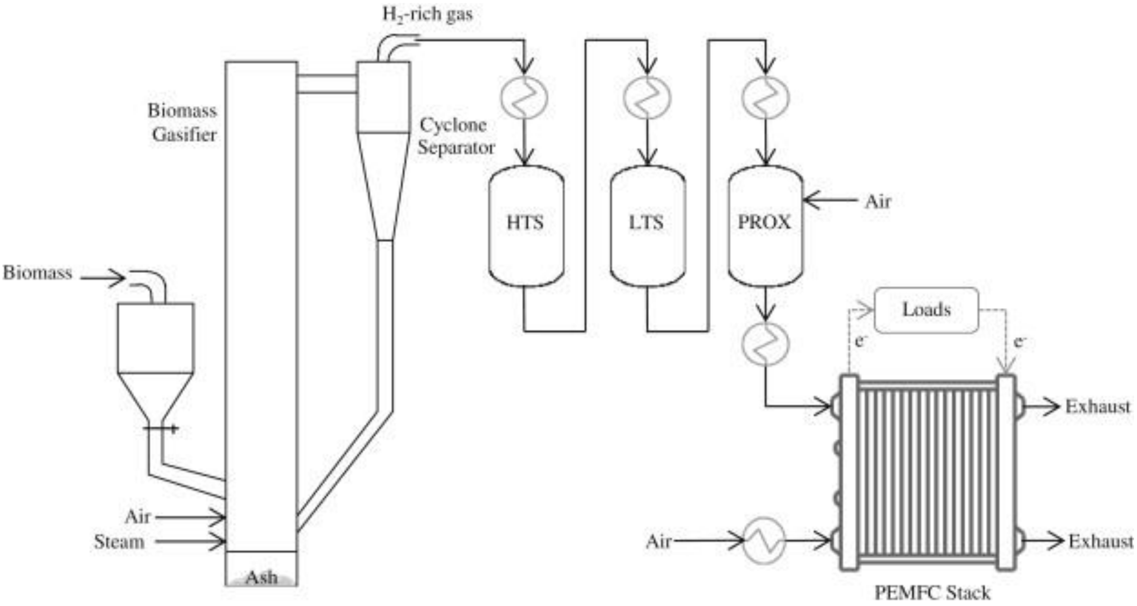

Figure 2.17 Schematic diagram of the biomass gasification and PEMFC integrated system

Source: Chutichai et al. (2013)

This integrated system consists of two main sections which are: (1) the hydrogen production and purification system, in which biomass is converted into an $H_2$-rich gas through gasification process; and (2) the PEMFC stack, in which electricity and power are generated from the electrochemical reaction of hydrogen and oxygen. The syngas produced from the gasification will be purified by the hydrogen purification system such as CO-PROX for producing the pure hydrogen and these pure hydrogen will be taken as input for PEMFC for power production and energy purpose (Chutichai and Arpornwichanop, 2015a).

## 2.10 Research Gap

Many previous studies have evaluated and focusing on biomass behavior in a gasification process especially for fluidized bed and fixed bed gasifiers. The modelling simulation works about gasification can be used to represent the experimental work of gasification process. Simulation modelling based analysis provides valuable insights to supplement experimental studies which are considered to be more reliable. The use of simulation models can considerably reduce the time and investment involved in exploring the favorable process conditions for sorbent incorporated gasification process. The previous work based on simulation studies have been list in Table 2.5.

Table 2.5 Previous literature regarding on fixed and fluidized bed gasification simulation based study

| References | Gasifier Types | Works Description |
|---|---|---|
| Gómez-Barea & Leckner (2002) | Fluidized bed | Modelling of solid fuel gasification in fluidized bed with special emphasis on biomass and waste materials |
| Li et al. (2004) | Fluidized bed | Simulation of non-stoichiometric equilibrium model based on direct minimization of Gibbs free energy to predict the performance of the gasifier |
| Nikoo and Mahinpey (2008) | Fluidized bed | Simulation model which focusing on predicting the steady-state performance of an atmospheric fluidized bed gasifier. |
| Puig-Arnavat et al. (2010) | Fluidized bed | Analysed fluidized gasification model based on thermodynamic equilibrium, kinetics and artificial neural networks (ANN) |
| Sarkar & Bhattacharyya (2012) | Fixed bed | Simulation of fixed bed model for biomass gasification under steady-state and dynamic state conditions |
| Fatoni et al. (2014) | Fluidized bed | Studying the performance of biomass gasification in a circulating fluidized bed model process in Aspen Plus. |
| Begum et al. (2013) | Fixed bed | Studying the performance analysis of an integrated fixed bed gasifier model for different biomass feedstock |
| Mikulandrić et al. (2016) | Fixed bed | Develop a dynamic modelling of biomass gasification in a co-current fixed bed gasifier |
| Kaushal & Tyagi (2017) | Fixed bed | Investigating the performance of fluidized bed gasifier by focusing on kinetics of drying, devolatilization, tar cracking and char gasification coupled with the reactor hydrodynamic using Aspen Plus software. |
| Han et al. (2017) | Fixed bed | Developed a model of downdraft biomass gasification process by restricting chemical reaction equilibrium using Aspen Plus |
| Pala et al. (2017) | Fluidized bed | Develop an integrated model for steam gasification of biomass and subsequent synthesis gas adjustment using shift reaction in Aspen Plus to predict the synthesis gas composition from biomass. |

All these previous studies in Table 2.5 used Aspen Plus software as main medium since this software is also very useful in predicting the behavior of a biomass gasification process as a sub-model with built-in solids properties. All these authors have shown reasonable agreement between equilibrium predictions and experimental data while using Aspen Plus as main software. Hence, this study will use Aspen Plus as main software for simulating the biomass gasification process. However, all this previous studies just focusing on one gasifier only either fluidized or fixed bed gasifier. There are limited of studies that cover the information about the comparison of fluidized and fixed bed gasifier in terms of performances such as hydrogen production, lower heating value and cold gas efficiency. It is very important to know which type of gasifier that can provide higher performances while implement oil palm waste as main biomass. Hence, in this research, both of gasifier will be stimulate and compared to study their optimum condition and performances.

In addition, all previous work mentioned before utilizing raw biomass as input for the gasifier. There have been ways to upgrade the biomass performance which is torrefaction process. There are not many previous work use torrefied biomass as an input for gasification process and compare the performance with the raw biomass. In a few recent studies, it has been reported that torrefied biomass can significantly increase the efficiency of biomass gasification. For example, previous study done by Prins, Ptasinski, & Janssen (2006) shows that the synthesis gas production for biomass underwent torrefaction process is higher than raw biomass. In another study, Batidzirai et al. (2013) provides the improvement of thermal efficiency in torrefied biomass compared to raw biomass. Furthermore, Dudyński et al. (2015) evaluated an industrial-scale gasification experiments for raw and torrefied biomass feedstock which resulting the increasing of higher calorific value of synthesis gas for torrefied biomass compared to raw biomass. In addition, Tapasvi et al. (2015) provides a biomass gasification study which using Aspen Plus with a two-stage gasification model based on Gibbs free energy minimization approach for comparing raw and torrefied biomass as feedstocks. It was reported that the carbon conversion and synthesis gas yield was higher for torrefied biomass than the raw biomass. Except for these few studies, there is a considerable lack of information on the behavior of torrefied biomass in terms of the best torrefaction temperature and residence time. In addition also often the synthesis gas produced usually depending on the types of biomass and the effects of torrefaction on the palm oil wastes as biomass is still not investigated yet which forms the basis of this work.

For fuel cell study, previous study done in literature is focusing on the power production such as Chutichai & Arpornwichanop (2015) where they used PEMFC to study the stack efficiency of PEMFC system. Besides, in the work done by Bhatia &

Wang (2004), the effects of carbon monoxide poisoning on PEMFC have been investigated. However, the previous studies did not focusing the hydrogen purification which can be employed for preventing carbon monoxide poisoning. This also becomes one of the subjects that will be further investigated in this study.

For integrated gasification and PEMFC, there is a lack of research on integrated gasification fuel cell systems. To date, the bulk of modelling work has focussed on biomass gasification or fuel cells alone. Although there are previous studies that carry out the integrated gasification process with PEMFC, they did not provide the evaluation data regarding to the impact of performance of torrified biomass in terms of efficiencies. For example, Chutichai et al. (2013) shows the good performance in terms of efficiency for an integrated biomass gasification and PEMFC system. In addition, Sordi et al. (2017) simulated the use of synthesis gas from sugarcane bagasse gasification for PEMFC application. However, their study only focuses on the raw biomass. Hence, this research will adding the research gap for evaluating the performances of raw and torrefied biomass on gasification and power production which will affecting the thermal, electrical, overall and stack efficiency for an integrated system.

## 2.11 Concluding Remark

In this chapter, the details about the biomass characteristics and properties have been reviewed. The properties such as proximate and ultimate analysis are deemed important for gasification. In order to extract the synthesis gas from the biomass, gasification have been chosen as the best process since this process can accept a wide variety of inputs and multiple useful products can be produced. Palm oil wastes have been review as the main input of gasification process since its presence abundantly in Malaysia. Both gasification technologies which are downdraft fixed bed and bubbling fluidized bed are selected for studying the gasification process. Besides, the review on integrated gasification and proton exchange membrane fuel cell (PEMFC) using fluidized bed gasifier and fixed bed gasifier also have been revised for power production purpose. Based on the literature, Aspen Plus software will be used as a tool to develop the selected modelling gasifier. In addition, the review of effectiveness of torrefaction process on biomass in terms of improving of biomass properties also will be evaluated through this research. Five types of fuel cells are presented where Proton

Exchange Membrane (PEM) fuel cell is chosen as the best fuel cell for power production since this fuel cell provides solid electrolyte which reduces corrosion and electrolyte management problems compare to other types of fuel cell. For avoiding CO poisoning for PEMFC, the preferential oxidation of CO is chosen for purifying the hydrogen and reduce the amount of CO which is essential for integrated PEMFC in producing the desired power.

# CHAPTER 3

# METHODOLOGY

## 3.1 Integrated Biomass Gasification and PEMFC Workflow

In this section, the systematic workflow for integration of biomass gasification and proton exchange membrane fuel cell (PEMFC) system has been developed as shown in Figure 3.1. By definition, the workflow is a real or conceptual structure intended to serve as a support or guide for the flow of the desired process in structural way. There are four main steps in the integrated workflow which consists of problem definition, process and product specifications, Aspen Plus modelling (gasification model and PEMFC model) and sensitivity analysis. The detailed of each step is explained in the subsequent section.

### 3.1.1 Problem Definition (Step 1)

The starting point of this workflow is problem definition in terms of the overall modelling objective and details of the process to be studied. In this step, basically three main objectives will be carry out which are 1) hydrogen production purpose which applying gasification stand-alone model as main model, 2) power production purpose which applying PEMFC as main model and 3) hydrogen and power production based on integrated gasification and PEMFC with purification as main models. All of these 3 objectives will be defined and chosen in this step which will be served as decision making in Step 2 for specifying process and product criteria.

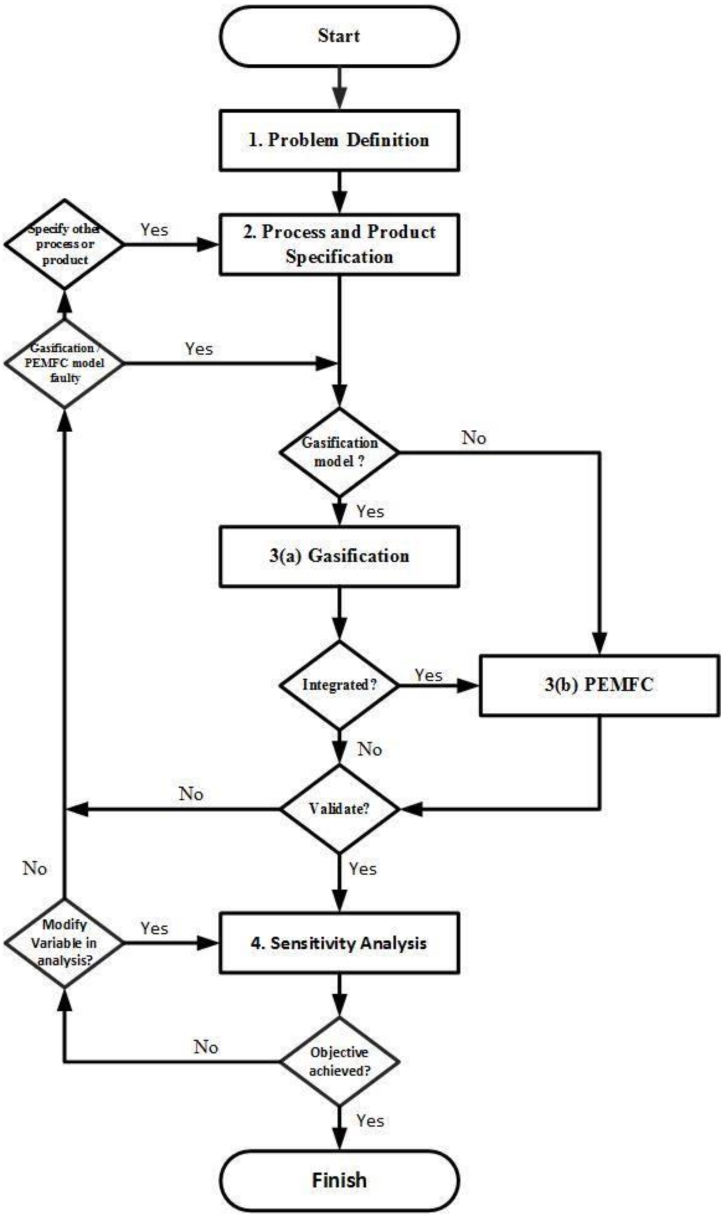

Figure 3.1 An integrated workflow of gasification and PEMFC

### 3.1.2 Process and Product Specifications (Step 2)

Step 2 involves the specification of desired process and product. Basically, in this step, all the raw materials specification and conditions that will be used in the simulation will be chosen based on the objective selected in Step 1. For process specification, the selections are divided into two parts which are the selection of biomass to be studied and the types of gasifier that will be used for the gasification simulation. For biomass selection, a biomass database has been developed in Excel software which acts as supporting tools of the workflow. All the collected biomasses which is palm oil wastes are arranged based on its ultimate analysis, proximate analysis and high heating value (HHV). All of these properties are essential and will be used in Aspen Plus for simulation process. The examples of collected biomass database based on proximate and ultimate analysis are shown in Figures 3.2 and 3.3.

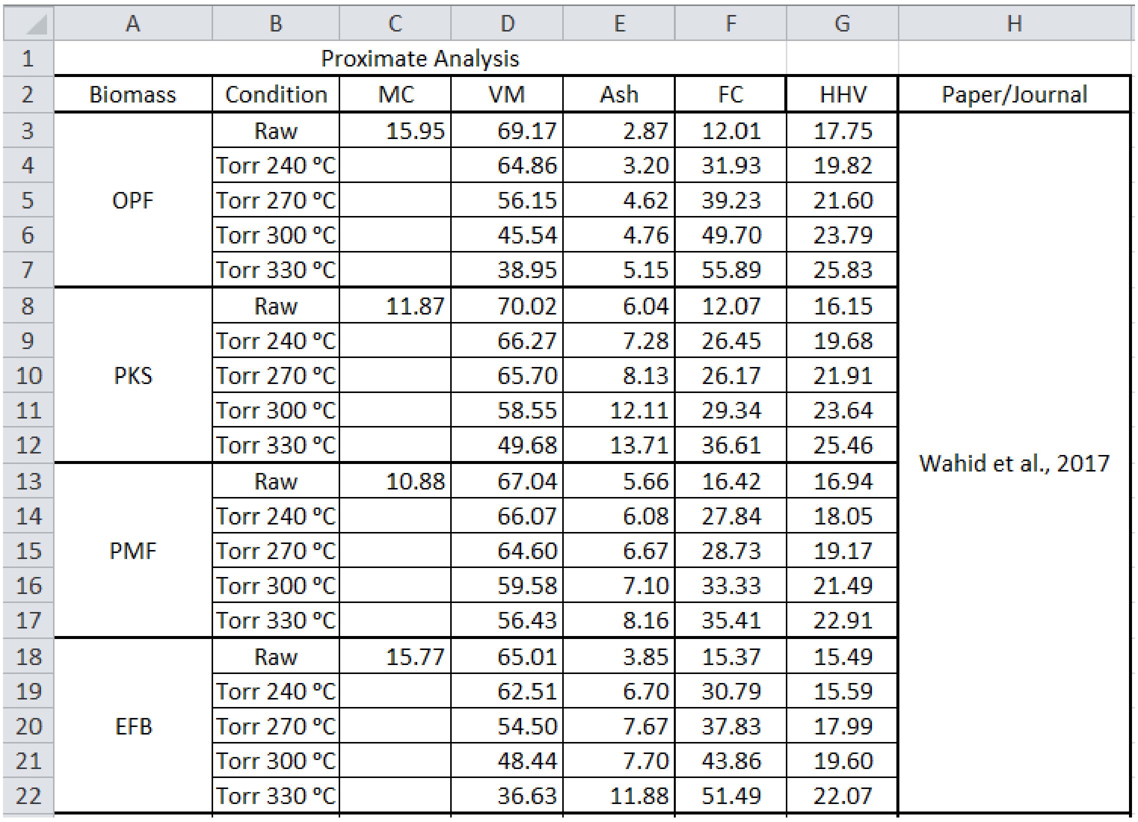

|  | A | B | C | D | E | F | G | H |
|---|---|---|---|---|---|---|---|---|
| 1 | Proximate Analysis |  |  |  |  |  |  |  |
| 2 | Biomass | Condition | MC | VM | Ash | FC | HHV | Paper/Journal |
| 3 | OPF | Raw | 15.95 | 69.17 | 2.87 | 12.01 | 17.75 | Wahid et al., 2017 |
| 4 |  | Torr 240 °C |  | 64.86 | 3.20 | 31.93 | 19.82 |  |
| 5 |  | Torr 270 °C |  | 56.15 | 4.62 | 39.23 | 21.60 |  |
| 6 |  | Torr 300 °C |  | 45.54 | 4.76 | 49.70 | 23.79 |  |
| 7 |  | Torr 330 °C |  | 38.95 | 5.15 | 55.89 | 25.83 |  |
| 8 | PKS | Raw | 11.87 | 70.02 | 6.04 | 12.07 | 16.15 |  |
| 9 |  | Torr 240 °C |  | 66.27 | 7.28 | 26.45 | 19.68 |  |
| 10 |  | Torr 270 °C |  | 65.70 | 8.13 | 26.17 | 21.91 |  |
| 11 |  | Torr 300 °C |  | 58.55 | 12.11 | 29.34 | 23.64 |  |
| 12 |  | Torr 330 °C |  | 49.68 | 13.71 | 36.61 | 25.46 |  |
| 13 | PMF | Raw | 10.88 | 67.04 | 5.66 | 16.42 | 16.94 |  |
| 14 |  | Torr 240 °C |  | 66.07 | 6.08 | 27.84 | 18.05 |  |
| 15 |  | Torr 270 °C |  | 64.60 | 6.67 | 28.73 | 19.17 |  |
| 16 |  | Torr 300 °C |  | 59.58 | 7.10 | 33.33 | 21.49 |  |
| 17 |  | Torr 330 °C |  | 56.43 | 8.16 | 35.41 | 22.91 |  |
| 18 | EFB | Raw | 15.77 | 65.01 | 3.85 | 15.37 | 15.49 |  |
| 19 |  | Torr 240 °C |  | 62.51 | 6.70 | 30.79 | 15.59 |  |
| 20 |  | Torr 270 °C |  | 54.50 | 7.67 | 37.83 | 17.99 |  |
| 21 |  | Torr 300 °C |  | 48.44 | 7.70 | 43.86 | 19.60 |  |
| 22 |  | Torr 330 °C |  | 36.63 | 11.88 | 51.49 | 22.07 |  |

Figure 3.2 Examples of proximate analysis in biomass database

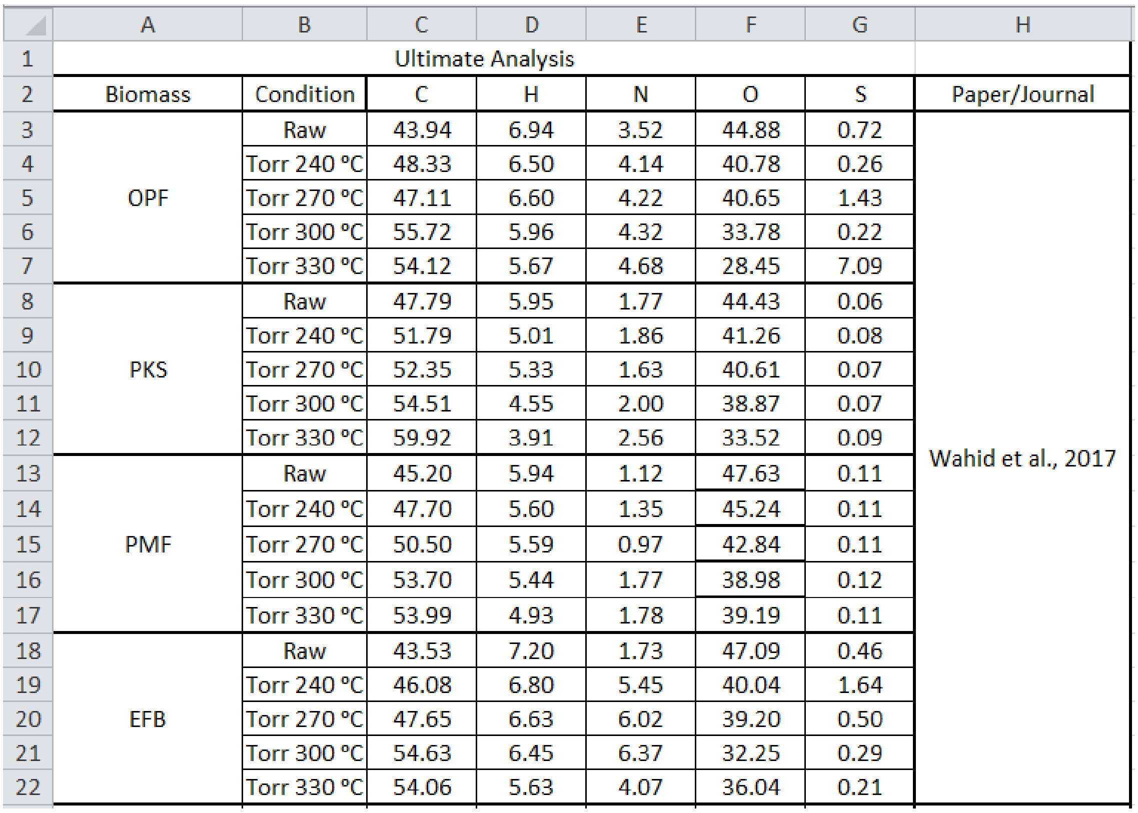

| | A | B | C | D | E | F | G | H |
|---|---|---|---|---|---|---|---|---|
| 1 | Ultimate Analysis | | | | | | | |
| 2 | Biomass | Condition | C | H | N | O | S | Paper/Journal |
| 3 | OPF | Raw | 43.94 | 6.94 | 3.52 | 44.88 | 0.72 | Wahid et al., 2017 |
| 4 | | Torr 240 °C | 48.33 | 6.50 | 4.14 | 40.78 | 0.26 | |
| 5 | | Torr 270 °C | 47.11 | 6.60 | 4.22 | 40.65 | 1.43 | |
| 6 | | Torr 300 °C | 55.72 | 5.96 | 4.32 | 33.78 | 0.22 | |
| 7 | | Torr 330 °C | 54.12 | 5.67 | 4.68 | 28.45 | 7.09 | |
| 8 | PKS | Raw | 47.79 | 5.95 | 1.77 | 44.43 | 0.06 | |
| 9 | | Torr 240 °C | 51.79 | 5.01 | 1.86 | 41.26 | 0.08 | |
| 10 | | Torr 270 °C | 52.35 | 5.33 | 1.63 | 40.61 | 0.07 | |
| 11 | | Torr 300 °C | 54.51 | 4.55 | 2.00 | 38.87 | 0.07 | |
| 12 | | Torr 330 °C | 59.92 | 3.91 | 2.56 | 33.52 | 0.09 | |
| 13 | PMF | Raw | 45.20 | 5.94 | 1.12 | 47.63 | 0.11 | |
| 14 | | Torr 240 °C | 47.70 | 5.60 | 1.35 | 45.24 | 0.11 | |
| 15 | | Torr 270 °C | 50.50 | 5.59 | 0.97 | 42.84 | 0.11 | |
| 16 | | Torr 300 °C | 53.70 | 5.44 | 1.77 | 38.98 | 0.12 | |
| 17 | | Torr 330 °C | 53.99 | 4.93 | 1.78 | 39.19 | 0.11 | |
| 18 | EFB | Raw | 43.53 | 7.20 | 1.73 | 47.09 | 0.46 | |
| 19 | | Torr 240 °C | 46.08 | 6.80 | 5.45 | 40.04 | 1.64 | |
| 20 | | Torr 270 °C | 47.65 | 6.63 | 6.02 | 39.20 | 0.50 | |
| 21 | | Torr 300 °C | 54.63 | 6.45 | 6.37 | 32.25 | 0.29 | |
| 22 | | Torr 330 °C | 54.06 | 5.63 | 4.07 | 36.04 | 0.21 | |

Figure 3.3 Examples of ultimate analysis in biomass database

Once the biomass is selected, the gasifier to be used to represent the gasification process needs to be selected. In this workflow, there are two types of gasifier available which consists of downdraft fixed bed gasifier and bubbling fluidized bed gasifier. It is also possible to choose both gasifiers in order to compare the performance of different gasifiers. In terms of the product specification, the user needs to specify the desired gas to be produced. Usually in the gasification process, the term synthesis gas (syngas) is commonly used when describing the product of gasification process. It consists of several types of gas components for example hydrogen, carbon monoxide, carbon dioxide and traces of methane. For this part, the production of hydrogen gas is the main focus as it will act as the input for the fuel cell. Meanwhile for PEMFC, the total power produced and overall efficiency are considered as the main product of PEMFC.

### 3.1.3 Aspen Plus Modelling (Step 3)

For Step 3, this step is divided into three parts which are modelling of gasification system (Step 3(a)), PEMFC model (Step 3(b)) and modelling of both gasification and PEMFC models (Step 3(c)). If the objective is focusing on gasification purpose only, the Step 3(a) which is modelling of gasification will be conducted. If the objective is concentrating on PEMFC purpose only, the Step 3(b) which is modelling of PEMFC will be operated. Meanwhile, if the objectives is selected on integrated gasification and PEMFC, both steps which are Step 3(a) and Step 3(b) will be conducted simultaneously which are known as Step 3(c) for integrated gasification and PEMFC modelling.

#### 3.1.3.1 Gasification Model (Step 3(a))

Step 3(a) is focusing on the modelling of stand-alone gasification system. The gasification model has been developed in the Aspen Plus software due to its capabilities of process decomposition into its constituent elements for individual study of performance (Eden, 2012). In addition, Aspen Plus software is based on “blocks” related to unit operations as well as chemical reactors, through which most industrial operations can be simulated. In this step, the user is able to choose to develop the gasification model only or with purification which depending on the specified objective. For example the purification is only needed to be applied if the objective is to integrate the biomass gasification and PEMFC for power production. For gasification, there are two types of gasifier available in the framework which is downdraft fixed bed gasifier and bubbling fluidized bed gasifier. Both of this gasifier is chosen as main gasification model in this work since they are usually used for gasification in real industry (Basu, 2013).

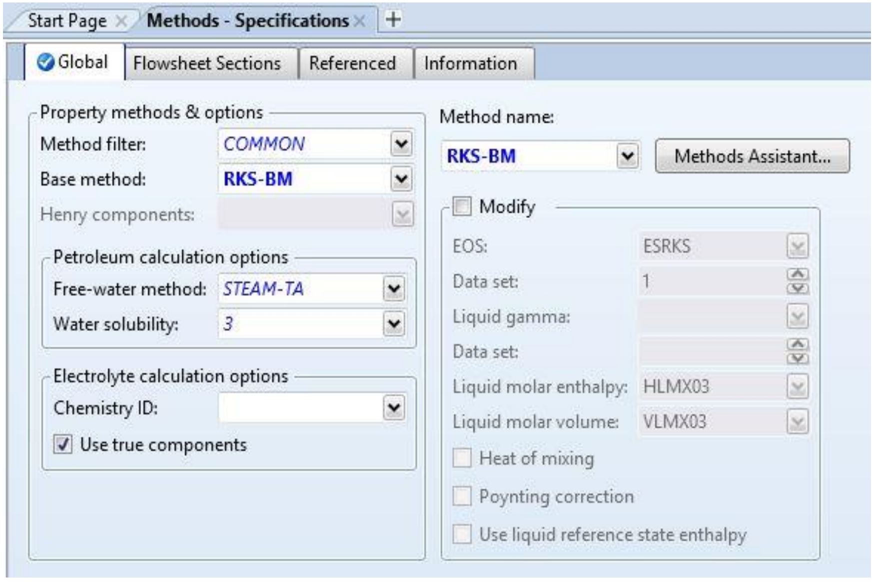

Property methods & options
Method filter: COMMON
Base method: RKS-BM
Henry components:

Petroleum calculation options
Free-water method: STEAM-TA
Water solubility: 3

Electrolyte calculation options
Chemistry ID:
☑ Use true components

Method name: RKS-BM

☐ Modify
EOS: ESRKS
Data set: 1
Liquid gamma:
Data set:
Liquid molar enthalpy: HLMX03
Liquid molar volume: VLMX03
☐ Heat of mixing
☐ Poynting correction
☐ Use liquid reference state enthalpy

Figure 3.4 Sectional part of method specification in Aspen Plus

For physical property method, the Redlich-Kwong-Soave cubic equation of state with Boston-Mathias alpha function (RKS-BM) has been used to estimate all physical properties of the conventional components in the gasification process as shown in Figure 3.4. This property method is comparable to the Peng Robinson cubic equation of state with the Boston-Mathias alpha function (PR-BM) property method. RKS-BM is mostly recommended since it is applicable for gas-processing, refinery and petrochemical applications such as gas plants, crude towers and ethylene plants (Aspen Technology Inc, 2010). This method is generally used for non-polar or mildly polar mixtures, like hydrocarbons and light gases such as $CO_2$ and $H_2$. Using RKS-BM, reasonable results can be expected at all temperatures and pressures. The RKS-BM property method is consistent in the critical region. Here, the enthalpy and density model selected for both feed and ash are non-conventional components denoted as HCOALGEN and DCOALIGT in Aspen Plus software as shown in Figure 3.5. Aspen Plus software basically uses component attributes to represent non-conventional components in terms of identifiable constituents needed to calculate the physical properties. In this case, HCOALGEN is selected since HCOALGEN uses the proximate analysis, ultimate analysis, and sulfur analysis to calculate the enthalpy of input material (Johansson, 2013). HCOALGEN is the general input material model for computing, and it includes correlations for four processes which consist of heat of combustion, heat capacity, standard heat of formation and enthalpy basis which has been defined in terms of the option code value fields as shown in Figure 3.5. The calculation method represented by the option value defaults of 1, 1, 1 and 1 will be selected if HCOALGEN is employed since it is representing all the four processes before (Aspen Technology, 2004). Similarly, the densities of these solids were specified using another pre-specified model called, DCOALIGT.

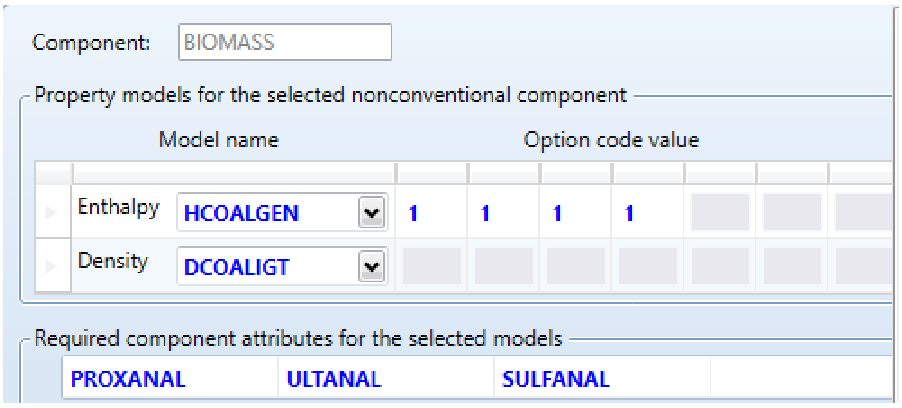
Component: BIOMASS

Property models for the selected nonconventional component

| | Model name | Option code value | | | |
|---|---|---|---|---|---|
| Enthalpy | HCOALGEN | 1 | 1 | 1 | 1 |
| Density | DCOALIGT | | | | |

Required component attributes for the selected models

PROXANAL ULTANAL SULFANAL

Figure 3.5 Sectional part of biomass definition in Aspen Plus

In this study, the biomass to be studied in gasification process is defined as non-conventional components. In addition the information of the proximate and ultimate analysis needs to be supplied during model development where this information can be extracted from the developed biomass database. The proximate analysis (PROXANAL) as shown in Figure 3.6 is the proximate analysis of the component where the contents of moisture, fixed carbon, volatile matter and ash are specified. This data helps Aspen Plus software to determine the amount of potential volatile and non-volatile matter presence in the solid. Meanwhile the ultimate analysis (ULTANAL) consists of ash, carbon, hydrogen, nitrogen, chlorine, sulphur, and oxygen elements as shown in Figure 3.7.

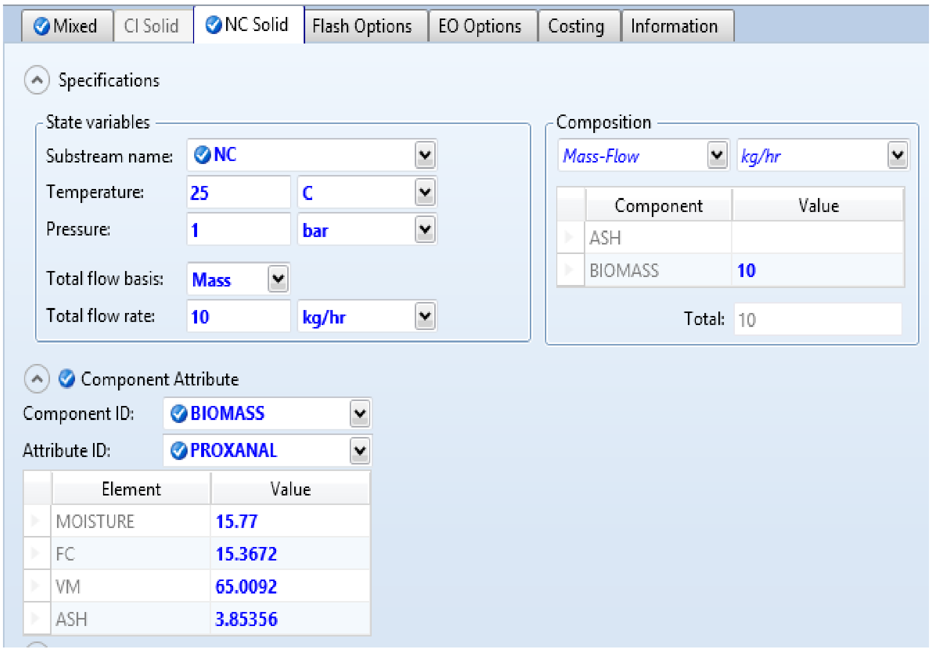

State variables

Substream name: NC

Temperature: 25 C

Pressure: 1 bar

Total flow basis: Mass

Total flow rate: 10 kg/hr

Composition

Mass-Flow kg/hr

| Component | Value |
|---|---|
| ASH | |
| BIOMASS | 10 |

Total: 10

Component Attribute

Component ID: BIOMASS

Attribute ID: PROXANAL

| Element | Value |
|---|---|
| MOISTURE | 15.77 |
| FC | 15.3672 |
| VM | 65.0092 |
| ASH | 3.85356 |

Figure 3.6 Sectional part of component attribute of proxanal in Aspen Plus

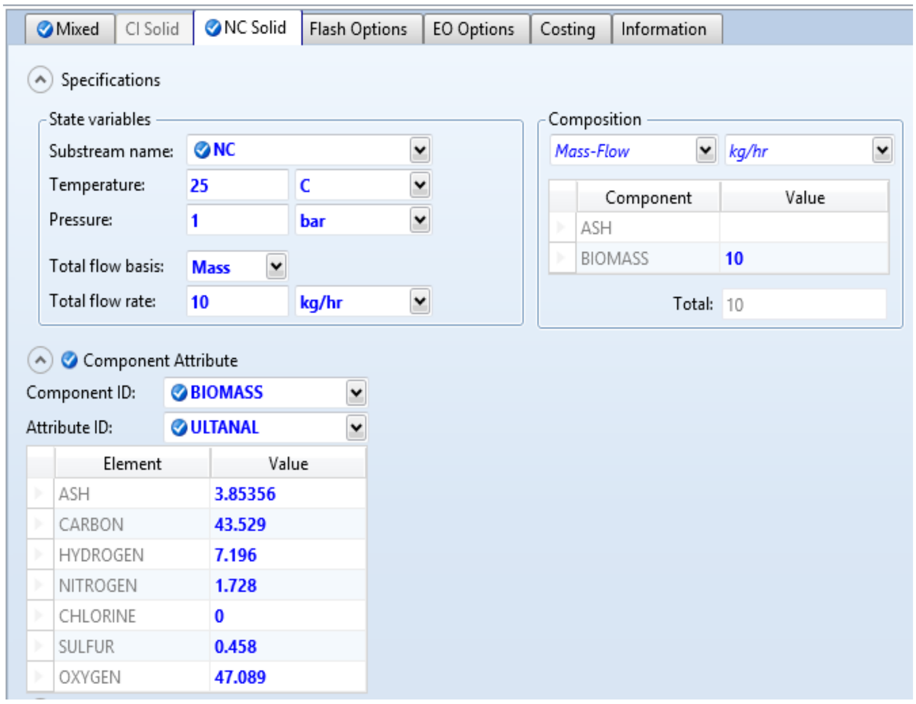

State variables

Substream name: NC

Temperature: 25 C

Pressure: 1 bar

Total flow basis: Mass

Total flow rate: 10 kg/hr

Composition

Mass-Flow kg/hr

| Component | Value |
|---|---|
| ASH | |
| BIOMASS | 10 |

Total: 10

Component Attribute

Component ID: BIOMASS

Attribute ID: ULTANAL

| Element | Value |
|---|---|
| ASH | 3.85356 |
| CARBON | 43.529 |
| HYDROGEN | 7.196 |
| NITROGEN | 1.728 |
| CHLORINE | 0 |
| SULFUR | 0.458 |
| OXYGEN | 47.089 |

Figure 3.7 Sectional part of component attribute of ultanal in Aspen Plus

The sulfanal is the composition of sulphur in ultimate analysis. Sulfanal analysis differentiates between various forms of sulfur that is present in the non-conventional item (Fatoni et al., 2014). Sulfanal consists of pyritic, sulphate and organic as shown in

Figure 3.8. The amount of pyritic is 10 % from the amount of sulfur meanwhile the sulphate and organic are 45 % each from the sulfur (Aspen, 2004).

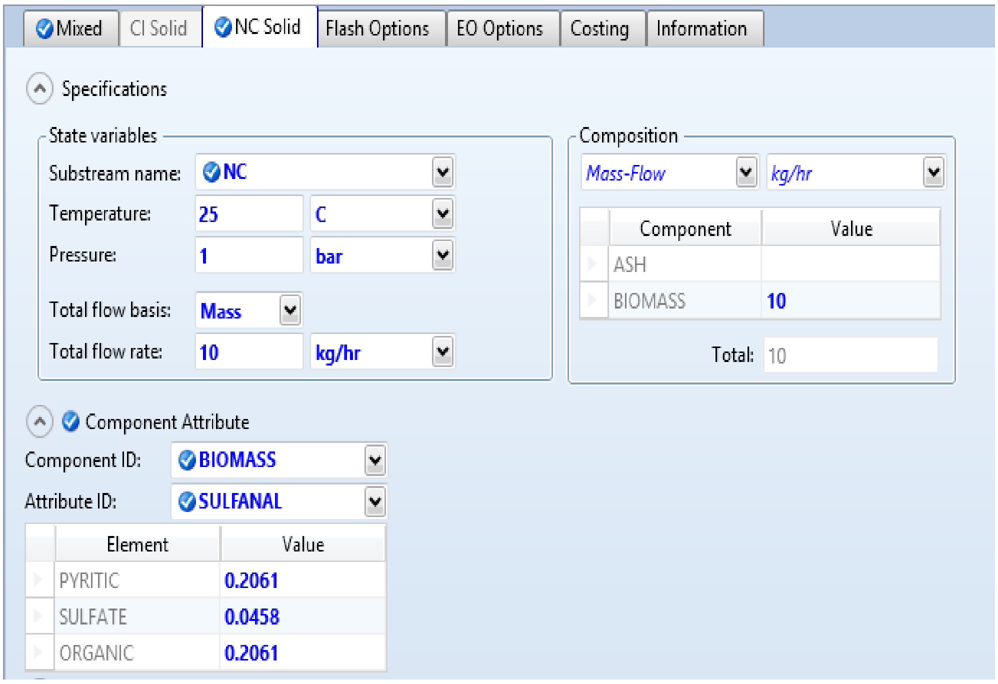

Substream name: NC
Temperature: 25 C
Pressure: 1 bar
Total flow basis: Mass
Total flow rate: 10 kg/hr

Mass-Flow kg/hr

| Component | Value |
|---|---|
| ASH | |
| BIOMASS | 10 |

Total: 10

Component ID: BIOMASS
Attribute ID: SULFANAL

| Element | Value |
|---|---|
| PYRITIC | 0.2061 |
| SULFATE | 0.0458 |
| ORGANIC | 0.2061 |

Figure 3.8 Sectional part of component attribute of sulfanal in Aspen Plus

The empirical molecular formula $C_{a1}H_{a2}O_{a3}N_{a4}$ for each biomass can be calculated by assuming the value of $a_1$is equal to 1.0 and by applying the following Equations (3.1) to (3.3) (Tapasvi et al., 2015). All these molecular formula will be collected in biomass database and can be used to define the non-conventional biomass in Aspen Plus.

$$a_2 = \frac{mass\ fraction(H)\ \times Molecular\ weight\ (C)}{mass\ fraction\ (C) \times Molecular\ weight\ (H)} \tag{3.1}$$

$$a_3 = \frac{mass\ fraction(O)\ \times Molecular\ weight\ (C)}{mass\ fraction\ (C) \times Molecular\ weight\ (O)} \tag{3.2}$$

$$a_4 = \frac{mass\ fraction(N)\ \times Molecular\ weight\ (C)}{mass\ fraction\ (C) \times Molecular\ weight\ (N)} \tag{3.3}$$

Subsequently the combustion process oxidizes fuel constituents in an exothermic reaction, while the gasification process reduces them to combustible gases in an endothermic reaction. The combustion process involves reaction with oxygen, which may be supplied as pure oxygen or from air, and forms carbon monoxide and carbon dioxide. The reactions of combustion are shown below:

$$C + O_2 \rightarrow CO_2 \qquad \Delta H^{\circ}_{298}: -393 \text{ kJ/mol} \qquad 3.4$$

$$C + 0.5O_2 \rightarrow CO \qquad \Delta H^{\circ}_{298}: -111 \text{ kJ/mol} \qquad 3.5$$

The heat of reaction for both reactions are shown in Equations (3.4) and (3.5) where the minus (-) sign indicates for exothermic reaction and plus (+) sign indicates for endothermic reaction. For gasification process, the reactions involved are shown in Equations (3.6) to (3.12):

$$H_2 + 0.5O_2 \rightarrow H_2O \qquad \Delta H^{\circ}_{298}: -242 \text{ kJ/mol} \qquad 3.6$$

$$C + CO_2 \leftrightarrow 2CO \qquad \Delta H^{\circ}_{298}: +172 \text{ kJ/mol} \qquad 3.7$$

$$C + H_2O \leftrightarrow CO + H_2 \qquad \Delta H^{\circ}_{298}: +131 \text{ kJ/mol} \qquad 3.8$$

$$C + 2H_2 \rightarrow CH_4 \qquad \Delta H^{\circ}_{298}: -75 \text{ kJ/mol} \qquad 3.9$$

$$CO + H_2O \leftrightarrow CO_2 + H_2 \qquad \Delta H^{\circ}_{298}: -41 \text{ kJ/mol} \qquad 3.10$$

$$CH_4 + H_2O \leftrightarrow CO + 3H_2 \qquad \Delta H^{\circ}_{298}: +206 \text{ kJ/mol} \qquad 3.11$$

$$CH_4 + 2H_2O \leftrightarrow CO_2 + 4H_2 \qquad \Delta H^{\circ}_{298}: -111\text{kJ/mol} \qquad 3.12$$

Based on the given reactions, the gasification process will produces combustible gases such as hydrogen, carbon dioxide, carbon monoxide and methane (Tapasvi et al., 2015). The main reactions of gasification process are Boudouard reaction (Equation 3.7), steam reforming reaction (Equation 3.8), methanation (Equation 3.9) and water-gas shift reaction (Equation 3.10). Boudouard reaction known as the reaction of carbon dioxide present in the gasifier reacts with char to produce carbon monoxide gas under endothermic condition. Steam reforming reaction is the partial oxidation of carbon by steam, which could come from a host of different sources, such as water vapour associated with the incoming air, vapour produced from the evaporation of water, and pyrolysis of the solid fuel. Steam reacts with the hot carbon according to the heterogeneous water–gas reaction. Methane also produced in the gasifier from the methanation process through hydrogasification of hydrogen and char (Lee, 2007). For water-gas shift reaction, the carbon monoxide will be reacted with steam to produce hydrogen gas.

In this work, different types of unit operation blocks are available in Aspen Plus software which can be employed to develop the gasification process. All the relevant unit operation blocks that can be used for gasification process and their description are shown in Table 3.1.

Table 3.1 Different unit blocks used for the gasification model

| **Block Name** | **Block Type** | **Block ID** | **Description** | **Reaction** |
|---|---|---|---|---|
| DRYER | RStoic | 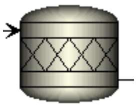 | Dryer reactor- convert water in the biomass into moisture based on the extent of reaction. | *Feed*→ $0.0555084H_2O$ |
| RYIELD | Ryield | 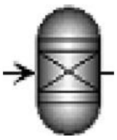 | Yield reactor – convert non-conventional biomass into conventional components based on mass balance | (Feed) →<br>C, H, O, N, S, ash |
| CHARSEPR | Separator | 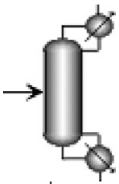 | Separation of volatiles (gas + char) from solids | - |
| DRY-SEP | Flash Separator |  | Separation of water and dry biomass | - |
| MIXER | Mixer | 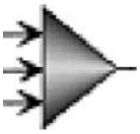 | Blending of volatile, non-volatile products, air and steam into one stream | - |
| RGIBBS | RGibbs | 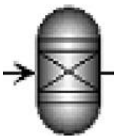 | Gibbs free-energy reactor – restricts chemical equilibrium of specified reactions to simulate the gasification | (3.4),(3.5),(3.6),(3.7),(3.8), (3.9), (3.10), (3.11), (3.12) |

Source: Muslim et al. (2017)

All the reaction shown in Equations (3.4) to (3.12) will be employed using different unit operations block in Aspen Plus. For pyrolysis process, the RYIELD block will be used since the specialized of this block is to convert non-conventional biomass into conventional components based on mass balance. For combustion reaction, RGIBBS block will be used since this block has the capability to run several restricts chemical equilibrium or simultaneous phase of specified reactions in order to simulate the gasification.

In typical gasifiers, there are three main thermochemical processes take place which are pyrolysis (>150 °C), combustion (150 °C – 170 °C) and gasification (600 °C -1100 °C). The pyrolysis process separates the water vapour, organic liquids and non-condensable gases from the char or solid carbon of the fuel. This process involves the degradation of biomass by heat under absence of oxygen. The devolatilization or pyrolysis processes start slowly at less than 350 °C, accelerating to an almost instantaneous rate above 700 °C. The composition of the evolved products is a function of the temperature, pressure and gas composition during devolatilization. The feed will then decompose in this stage to specific components such as hydrogen, oxygen, nitrogen and carbon based on the yield distribution. In addition, some product gas such as CO, $H_2$, $CH_4$, and $H_2O$ will be produced during this stage. Char (C), a solid residue from biomass mainly containing carbon element also will be produced from the pyrolysis process (Basu, 2013).

For the purpose of model development in Aspen Plus, the assumptions used for both gasification models are: (i) the processes are in the isothermal and steady state conditions; (ii) the composition of char consists only carbon, void and ash; (iii) all chemical reactions occur under equilibrium state in the gasifier and there is no pressure loss; (iv) all the particles are assumed in the spherical shape, uniform size and the average diameter remains constant during the gasification meaning that no species concentration or thermal gradients exist within the particles; (v) the synthesis gas produced in the ideal gases state, including $H_2$, CO, $CO_2$, steam ($H_2O$) and $CH_4$; (vi) all hydrogen and oxygen components contained in the biomass are assumed to be released during devolatilization; (vii) The pressure drop and heat losses from the equipment and pipelines were not included.

Once the gasification model has been developed, the model will undergo validation. Here, all the collected data from the model simulation are evaluated in terms of its behaviour which in accordance with the theory. In addition, the model validation can be performed in this step where the all the collected simulation results obtained are compared with experimental or literature data. For model validation purpose, the root mean square error (RMSE) will be applied based on the following equations:

$$RMSE = \frac{\sqrt{\frac{\sum (y_{ie} - y_{ip})^2}{y_{ie}}}}{N} \qquad 3.13$$

Where $y_{ie}$ is experimental values, $y_{ip}$ is the predicted values, $N$ is the number of data points. For the model validation, the model is concluded as validated and reliable when the RMSE values obtained is lesser than 0.3 (Veerasamy et al., 2011). Besides, the model also can be verified as validated model if the output data of the simulation model are very close to the data that provided by the literature data.

### 3.1.3.2 PEMFC Model (Step 3 (b))

This step is focused when the PEMFC case study is needed to carry out as stand-alone models in the objectives. For PEMFC modelling, a mathematical model of PEMFC is developed. This model will describe the behavior of PEMFC under steady-state and transient conditions. The PEMFC systems consisting of three main parts which are the fuel cell body, the cathode and anode gas chamber (Xue et al., 2006). According to Chutichai et al. (2013), the cells are connected in series via plates which called as anode and cathode. The electrochemical reactions will takes places as the gases pass from flow field plate through the electrode. At anode, the hydrogen will be ionized to form hydrogen ion and electron as shown in the reaction below:

$$H_2 \rightarrow 2H^+ + 2e^- \qquad 3.14$$

The hydrogen ion from the anode will transfer through the membrane into the cathode side of the cell while the electrons travel in an external circuit for generating the electrical output of the cell. On the cathode side, the transferred hydrogen ion from anode will react with electron and oxygen from air to generate water as shown in the reaction below:

$$0.5O_2 + 2H^+ + 2e^- \rightarrow H_2O \qquad 3.15$$

The combination of hydrogen and oxygen inside the PEMFC will produce a total reaction which generating the electrical power. Besides, pure water also will be produced as shown in the reaction below:

$$H_2 + 0.5O_2 \rightarrow H_2O \qquad 3.16$$

Bhatia & Wang (2004) presents a mathematical model in order to find the cell voltage of PEMFC. In PEMFC, the basic relation for voltage and current density are shown in Equations (3.17) until (3.20).

$$E_{cell} = E_R - \eta_a - \eta_c - \eta_{ohmic} \qquad 3.17$$

$$\eta_a = \frac{RT}{\alpha F}\sinh^{-1}\left(\frac{i}{2k_{eh}\theta_h}\right) \qquad 3.18$$

$$\eta_c = \frac{RT}{\alpha F}\ln\left(\frac{i}{i_{oc}}\right) \qquad 3.19$$

$$\eta_{ohmic} = iR_{ohmic} \qquad 3.20$$

The cell voltage ($E_{cell}$) can be calculated by subtracting the reversible cell potential ($E_R$) which is the maximum amount of voltage that can be achieved by a membrane fuel cell at specific condition by various voltage losses with the activation loss at the anode ($\eta_a$), the activation loss at the cathode($\eta_c$), and Ohmic loss ($\eta_{ohmic}$). All variables that used in mathematical model are taken from Bhatia and Wang (2004) as shown in Table 3.2.

Table 3.2 The known variables used for PEMFC mathematical model

| **Constants** | **Values** |
|---|---|
| $E_R$ | 1.2 V |
| R | 8.314 J mol$^{-1}$ K$^{-1}$ |
| T | 353 K |
| $\alpha$ | 0.5 |
| F | 96485 Cmol$^{-1}$ |
| $k_{eh}$ | 4 Acm$^{-2}$ |

|  |  |
|---|---|
| $i_{oc}$ | $7.0 \times 10^{-4}$ Acm$^{-2}$ |
| $R_{ohmic}$ | 0.3 Ω cm$^2$ |

Source: Bhatia and Wang (2004)

At steady-state conditions, the quantity of current density ($i$) that has been consumed by the electrochemical reactions in Equation (3.18), Equation (3.19) and Equation (3.20) can be calculated from Equation (3.21):

$$i = nFN_{H_2} \tag{3.21}$$

Where $n$ is the number of cells, $F$ is Faraday constant and $N_{H_2}$ is percentage of hydrogen that comes from gasification model. The unit of current density is Acm$^{-2}$. When the PEMFC models have been developed, the model will be evaluated and validated. Here, all the collected simulation results obtained are compared with experimental or literature data. For PEMFC model validation, the experimental data from Bhatia & Wang (2004) as shown in Figure 3.9 is used for comparison and validation. The root mean square error (RMSE) (Equation 3.13) will be applied for this validation purpose and the model can be justified as validated if the RMSE values obtained is lesser than 0.3 (Veerasamy et al., 2011).

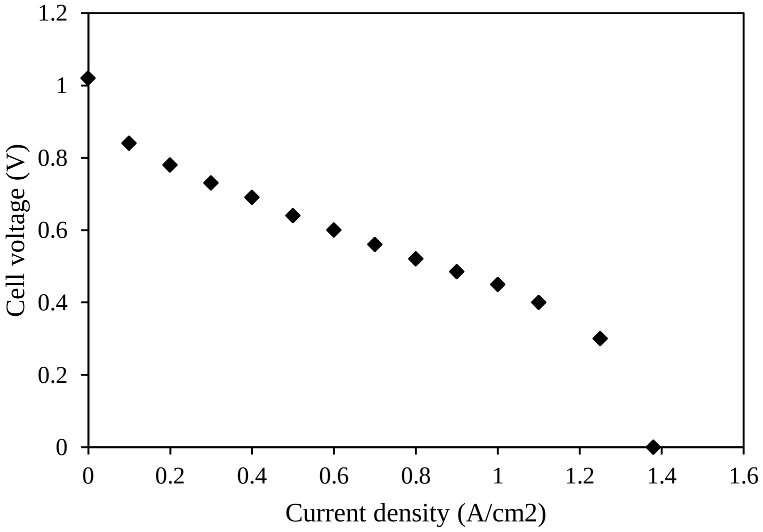

Figure 3.9 Steady state of cell potential from previous study
Source: Yan et al. (2006)

### 3.1.3.3 Integrated Biomass Gasification and PEMFC (Step 3(c))

For Step 3(c), this step will be implemented when both gasification and PEMFC models were applied together in order to find the amount of power (kW) produced. Here, the hydrogen purification and CO removal will be applied in order to reduce the CO poisoning for the PEMFC membrane.

### 3.1.3.4 Hydrogen Purification and Preferential Oxidation of CO

This step is performed for integrating biomass gasification and PEMFC in order to produce the power. For integrated system, hydrogen purification and CO removal stages will be implemented in this step since the amount of carbon monoxide (CO) is corrosive to PEMFC layer and the amount is needed to be reduced to 10 ppm. Hence, the integrated biomass system and PEMFC will undergo hydrogen purification for reducing the amount of CO gas.

For purification, there are two main reactions occurs which consists of:

$$CO + H_2O \leftrightarrow CO_2 + H_2 \qquad \Delta H^{\circ}_{298}: 41 \text{ kJ/mol} \qquad 3.22$$

$$CO + 0.5O_2 \leftrightarrow CO_2 \qquad \Delta H^{\circ}_{298}: -283\text{kJ/mol} \qquad 3.23$$

The hydrogen purification is carried out by implementing water gas shift reactor and CO-PROX reactor. In order to produce a hydrogen-rich fuel, water-gas shift reactor is implemented by carrying out reaction (3.22) which reduces the amount of CO and increasing the hydrogen gas. For CO removal, the CO-PROX reactor is used for process of preferential oxidation (PROX) of CO to $CO_2$ in the presence of an excess of $O_2$ (Equation 3.23) that can reduce the carbon monoxide concentration in the feed to PEMFC down to few ppm state. Both reactors will use RSTOIC block since this reactor used stoichiometry and extent of reaction in order to perform simulation.

Table 3.3 Different unit blocks used for the gasification model

| Block Name | Block Type | Block ID | Description | Reaction |
|---|---|---|---|---|
| HTS, LTS | RStoic | 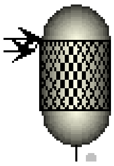 | Water gas shift reactor-reducing the amount of CO and increase hydrogen yield. | (3.25) |
| CO-PROX | RStoic | 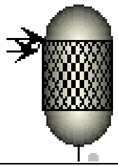 | CO-PROX reactor–reducing the carbon monoxide concentration in the feed to few ppm units before PEMFC. | (3.26) |

Source: Muslim et al. (2017)

#### 3.1.3.5 PEMFC Performances

The hydrogen rich production is obtained once the amount of CO is lesser than 10 ppm after hydrogen purification and CO removal and subsequently be fed into the PEMFC for power production. The output power produced by PEMFC can be calculated by multiplying the amount of $E_{cell}$ with the current density ($i$), number of cell used in PEMFC ($n$) and the area of the active cell ($A$) as shown in Equation (3.24):

$$P_{FC} = i * n * A * E_{cell} \qquad 3.24$$

In order to evaluate the performance of integrated biomass gasification and PEMFC system, the efficiency in terms of thermal, electrical and overall are calculated. This efficiency is essential for the integrated system in order to evaluate its ability to convert the chemical energy stored in biomass into electrical and thermal power. Equations (3.25) – (3.27) are employed for calculating the electrical, thermal and overall efficiency.

$$\eta_{electrical} = \frac{P_e(W)}{m_{biomass} \times HHV_{biomass}} \times 100 \qquad 3.25$$

$$\eta_{thermal} = \frac{P_h}{m_{biomass} \times HHV_{biomass}} \times 100 \qquad 3.26$$

$$\eta_{overall} = \frac{P_h + P_h(W)}{m_{biomass} \times HHV_{biomass}} \times 100 \qquad 3.27$$

Where $P_e$ is the amount of power produced from the PEMFC and $P_h$ is amount of thermal energy from the PEMFC (Chutichai et al., 2013). For stack efficiency of PEMFC, Equation (3.28) is used as shown below:

$$\eta_{stack} = \frac{\dot{m}_{H_2}\ LHV}{E} \times 100 \qquad 3.28$$

Where $\dot{m}_{H_2}$ the hydrogen mass flow rate from the PROX reactor, $LHV$ is the lower heating value for hydrogen and $E$ is electric energy input.

Based on this step 3, if the model is not validated, the user needs to go back to previous step in order to check either gasification model faulty (Step 3(a)), PEMFC model faulty (Step 3(b)) or both integrated models in Step 3(c), or wrong specification of process and product (Step 2). For example, for gasification model validation, if the RMSE value is higher than 0.3, the model can be said as not reliable with the literature data. Hence, the model needs to be checked again either having error during gasification modelling in Step 3(a). The step is then repeated until validated model is achieved.

### 3.1.4 Sensitivity Analysis (Step 4)

After the model from Step 3 has been developed, the next step is Step 4 which consists of sensitivity analysis. Sensitivity analysis is a common technique to determine how different values of an independent variable will impact output variables under a given set of assumptions. It is important to perform sensitivity analysis for investigating the effects of varying the values of key parameters on model performance in order to ascertain the validity of the approach (Perez et al., 2015). Several simulation trials will be conducted by varying the relevant parameter while all other parameters were kept constant. In this step, the model will undergo sensitivity analysis in specific range of operating condition. The relevant parameters selected for sensitivity analysis are gasification temperature, air to biomass ratio (ABR), and steam to biomass ratio (SBR). The air to biomass ratio is defined as the ratio of the actual air to biomass ratio divided by the stoichiometric air to biomass ratio required for complete combustion. In biomass gasification the range of air biomass ratio is varies from 0.20 to 1 (Tasma et al., 2007).

Steam to biomass ratio is defined as moles of steam as a gasifying agent per mole of biomass in the feedstock. Steam to biomass ratio has a significant effect on the output synthesis gas in gasification. The ranges for investigating the steam to biomass analysis are set between 0.1 and 1.0. In this work, the tested range for each process variables are shown in Table 3.4.

Table 3.4 Tested range for process variables

| **Process Variables** | **Low** | **Medium** | **High** |
|---|---|---|---|
| Temperature (°C) | 600 | 800 | 1000 |
| ABR | 0.2 | 0.6 | 1.0 |
| SBR | 0.1 | 0.55 | 1.0 |

In addition, the amount of lower heating value (LHV) and cold gas efficiency (CGE) are also calculated in this work. In this work, LHV is calculated for product synthesis gas and biomass as shown in Equations (3.29) – (3.31). The LHV for product synthesis gas is accounted for the amount of heat available from a fuel after the latent heat of vaporisation. Meanwhile LHV of biomass (MJ/kg) is calculated based on the HHV value and elemental composition of biomass. Meanwhile the cold gas efficiency (CGE) as shown in Equation (3.31) is defined as the fraction of the chemically bound energy in the biomass that is converted into chemically bound energy in the product gas from the gasification process.

$$LHV_{PG} = 0.126\chi_{CO} + 0.358x\chi_{CH_4} + 0.108\chi_{H_2} \quad 3.29$$

$$LHV_{bio} = HHV - 0.212 \times H - 0.00245 \times M - 0.008 \times O \quad 3.30$$

$$\eta_{cg} = \frac{\dot{m}_{PG}\ LHV_{PG}}{\dot{m}_{Bio}\ LHV_{Bio}} \times 100\% \quad 3.31$$

where $\dot{m}_{PG}$ and $\dot{m}_{Bio}$ is the mass flow rates of product gas and biomass in kg/h respectively. $\chi_{CO}$, $\chi_{CH_4}$, $\chi_{H_2}$ is the product composition of output carbon monoxide, methane and hydrogen (Arena, 2012). *HHV* is the high heating value of the biomass (MJ/kg), *H*, *M*, and *O* are the weight percentages of hydrogen, moisture content and oxygen obtained from ultimate analysis. Both of LHV and CGE is the important indicator to measure an efficiency of biomass conversion in the gasifier reactor (Jayathilake and Rudra, 2017).

At the end of the workflow, the final biomass gasification model, PEMFC model and final integrated biomass gasification and PEMFC model are obtained which subject to the objective specified in Step 1. If the objective is not achieved, then the user will have to repeat or go back to the previous steps either Step 2, 3 or 4 for model adjustment and improvement.

## 3.2 Concluding Remark

In this chapter, the integrated biomass gasification and PEMFC model-based workflow has been developed which consists of four main steps. Based on the proposed steps, this workflow covers wide ranges of application which are the model development of fluidized and fixed bed gasification, PEMFC and the possibility to integrate biomass gasification and PEMFC for power production. The applicability of this workflow will be demonstrated through different case studies in the next chapter.

# CHAPTER 4

# RESULTS AND DISCUSSIONS

## 4.1 Introduction

In this chapter, the application of the systematic integration biomass gasification and PEMFC model-based workflow is demonstrated through five different case studies. Case 1 is focusing on development and validation of fluidized bed gasification model meanwhile Case 2 covers the development and validation of fixed bed gasification model. For Case 3, this case is concentrating on applying the fluidized and fixed bed gasification models for sensitivity analysis which focusing on evaluation on the hydrogen ($H_2$) production using different palm oil wastes which includes the development of the fluidized bed and fixed bed gasification models, evaluation on the hydrogen ($H_2$) production using different palm oil wastes. For Case 4, this case covers the study on effect of torrefaction process on the $H_2$ production and for the Case 5, this case is focusing on developing the integration of fluidized and fixed bed biomass gasification with PEMFC for power production.

## 4.2 Case Study 1: Development of Fluidized Bed Gasification Model

The application of the model-based workflow is highlighted using gasification of pine sawdust in bubbling fluidized bed model. The relevant data from Schuster et al (2001) is employed for model validation.

### 4.2.1 Problem Definition (Step 1)

The objective is to develop and validate gasification model using bubbling fluidized bed reactor in the Aspen Plus software.

### 4.2.2 Process and Product Specifications (Step 2)

Firstly for the process specification, the selected reactor is bubbling fluidized bed gasifier as the main reactor since the objective is to undergo gasification process using fluidized bed gasifier. For the raw material selection, pine sawdust is chosen and the relevant data from biomass database is extracted such as ultimate and proximate analysis as shown in Table 4.1. The targeted products in this case are the synthesis gas which is carbon monoxide, carbon dioxide, hydrogen and methane.

Table 4.1 Properties of beech chips

| **Proximate Analysis (wt % dry basis)** | |
|---|---|
| Moisture Content (wt %) | 25 |
| Volatile Matter | 80 |
| Fixed Carbon | 19.39 |
| Ash | 0.61 |
| **Ultimate Analysis (wt% dry basis)** | |
| C | 48.26 |
| H | 5.82 |
| O | 45.67 |
| N | 0.22 |
| S | 0.03 |

Source: Schuster et al. (2001)

### 4.2.3 Gasification Modeling (Step 3(a))

For modelling of fluidized bed gasification, Aspen Plus software has been applied for model development. Aspen Plus flowsheet and process flowchart to represent the fluidized bed gasification process are shown in Figures 4.1 and 4.2. Several number of Aspen Plus blocks were chosen and used to complete the overall gasification process. In order to represent the real bubbling fluidized bed gasifier, two main reactors which are RYIELD and RGIBBS were applied in order to simulate all the main process in bubbling fluidized bed gasification. Additionally, a MIXER and a number of SEPARATOR blocks were incorporated in the simulation model to complete the entire process. The whole gasification consists of three processes, namely pyrolysis, combustion (volatile reaction) and char gasification.

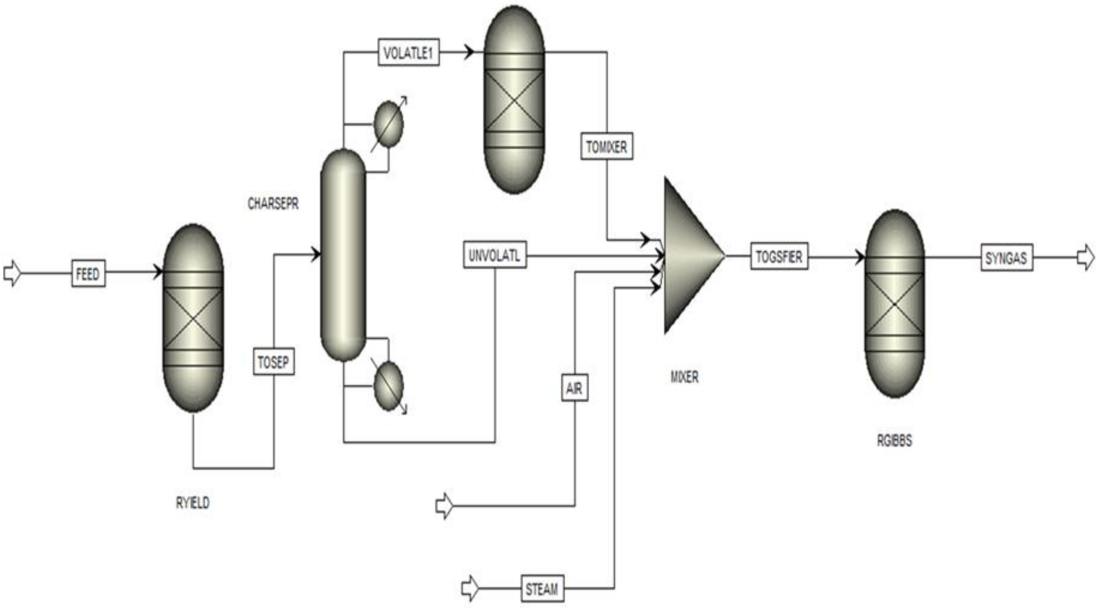

Figure 4.1 Fluidized bed gasification process flowsheet

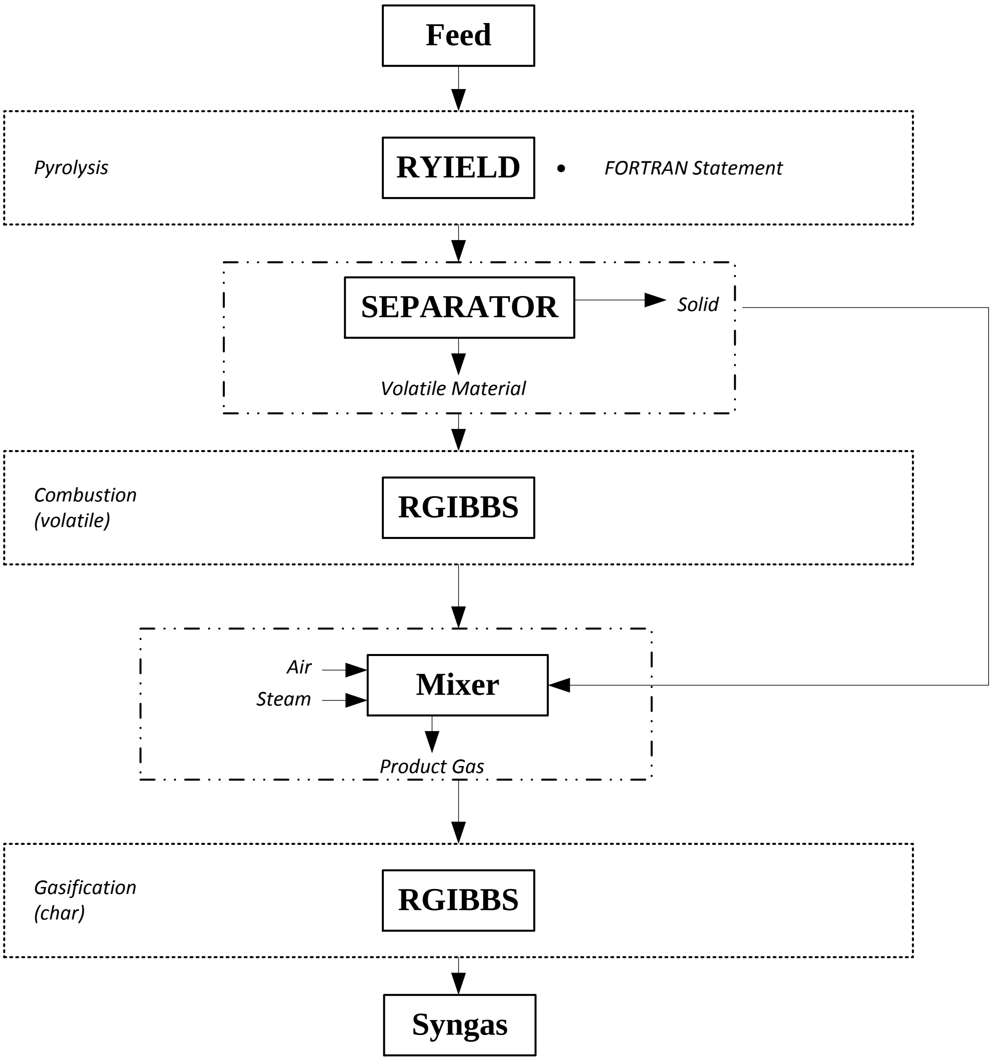

Figure 4.2 Fluidized bed gasification process flowchart

#### 4.2.3.1 Pyrolysis

The first stage of the gasification process is pyrolysis which is focusing on biomass decomposition stage. After the biomass enters the yield reactor, it is decomposed and undergoes pyrolysis process where the biomass is decomposed in the atom forms of carbon (C), hydrogen (H), oxygen (O), sulphur (S), nitrogen (N) and ash. These atoms were converted into synthesis gas components by specifying the yield distribution according to the ultimate analysis of the biomass. The RYIELD (block ID: RYIELD in Figure 4.1), an Aspen Plus yield reactor, was used to decompose the feed in the simulation. RYIELD is used when reaction stoichiometry and reaction kinetics are unknown or unimportant but the component yield distribution is known. In this step, beech chips which used for validation is converted into its constituent components which are $H_2$, $O_2$, C, sulphur (S), $N_2$ and ash by specifying the yield distribution according to the feed's ultimate analysis.

#### 4.2.3.2 Combustion

The next stage is combustion. In this stage the decomposed material from RYIELD which are volatile materials such carbon (C) and solid to combustion stage. Here, an Aspen Plus reactor, RGIBBS (block ID: VOLATLE in Figure 4.1), uses Gibbs free for energy minimization with phase splitting to calculate equilibrium. This reactor does not require specifying the reaction stoichiometry, but reactor temperature and pressure is known from experiment. RGIBBS is capable of calculating the chemical equilibrium between any number of conventional solid components and the fluid phases (Aspen Technology, 2004). In this study, RGIBBS was used for volatile combustion. In the Gibbs reactor, the volatile matter will undergo combustion process (reactions (3.4) and (3.5)) and the reaction is assumed to follow the Gibbs equilibrium. The pine sawdust mainly consists of C, $O_2$, $H_2$, $N_2$, S, moisture and ash. Here, the carbon (C) will partly compose the gas phase to take part in de-volatilization and the remaining part of C comprises the solid phase (char) and consequently results in char gasification. A SEPARATOR, a unit block in Aspen Plus was used before RGIBBS reactor to separate the volatile materials and solids from the decomposed components. The RGIBBS reactor performs the volatile reactions of separated volatile materials. The amount of volatile matter is specified in Aspen Plus based on the information of proximate analysis from Table 4.1.

#### 4.2.3.3 Gasification

For gasification the unit blocks that been used is RGIBBS (block ID: RGIBBS in Figure 4.1). Since the stoichiometry of all the reaction is unknown, RGBBS is used since the reactor temperature and pressure is known from experiment (Suwatthikul et al., 2017). The complete separated volatile matter is then fed into to the Gibbs reactor (RGIBBS). The agent of fluidizing such steam and air will be injected at one pinpoint which at mixer. An Aspen Plus block called MIXER was used to mix the entire volatile product from combustion and char with the gasification agent into the RGIBBS for gasification purpose. In RGIBBS, all the char will undergo char gasification process (reactions (3.6) until (3.12)). The product gas will be collected after the gasification for the future purpose.

After the flowsheet has been developed, it will undergo validation with previous literature. For validation purpose, the fluidized bed gasification process which use pine sawdust as feed is simulated in this step using the same operating conditions used in the works of Schuster et al (2001)as shown in Table 4.2.

Table 4.2 Operating conditions for gasification process

| Parameter | Operating Condition | Value |
|---|---|---|
| Fluidized bed reactor | Temperature (°C) | 650-1000 |
| | Pressure (bar) | 1 |
| Air | Temperature (°C) | 20 |
| | Flow rate ( kg/h) | 50 |
| Steam | Temperature (°C) | 400 |
| | Flow rate (kg/h) | 3.22 |
| Biomass feed | Flow rate (kg/hr) | 0.81 |

Source: Schuster et al. (2001)

Here, the predicted synthesis gas is compared with the literature (Schuster et al., 2001). The results obtained from the literature are focusing on the synthesis gas components which are carbon dioxide (Figure 4.3), carbon dioxide (Figure 4.4), methane (Figure 4.5) and hydrogen (Figure 4.6). Based on these figures, as the temperature is increased, more carbon and $CH_4$ are reacted which increase the amount of $H_2$ and CO. However, the $H_2$ yield reaches the highest values (56 %) at gasification temperature of 700 °C and reduces afterwards. This is because of the endothermic of water gas shift reaction that produces more CO and water. This explains why the CO is increasing and $CO_2$ is decreasing as the gasification temperature is increased.

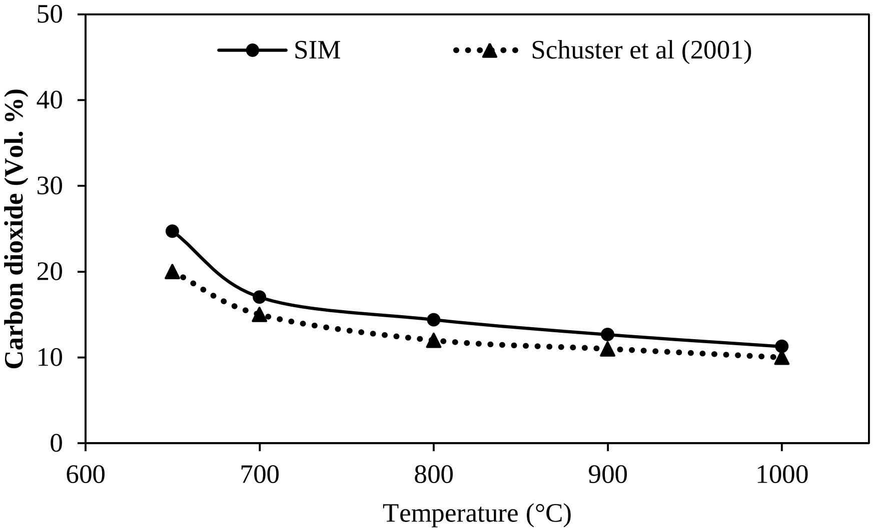

Figure 4.3 Comparison of carbon dioxide in fluidized bed reactor between simulation and predicted data

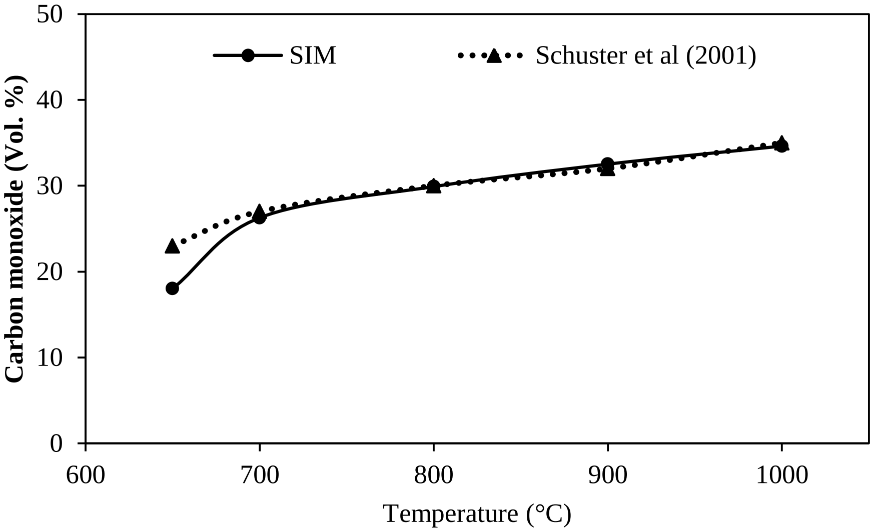

Figure 4.4 Comparison of carbon monoxide in fluidized bed reactor between simulation and predicted data

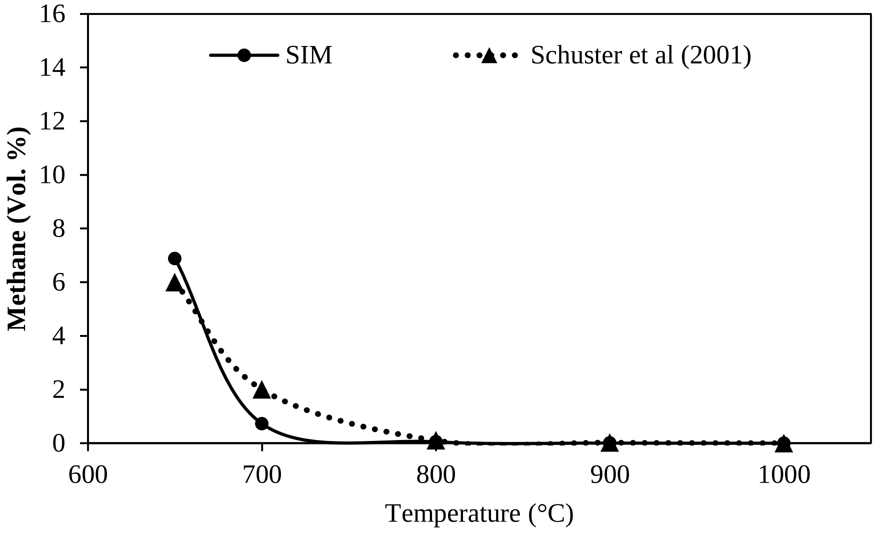

Figure 4.5 Comparison of methane in fluidized bed reactor between simulation and predicted data

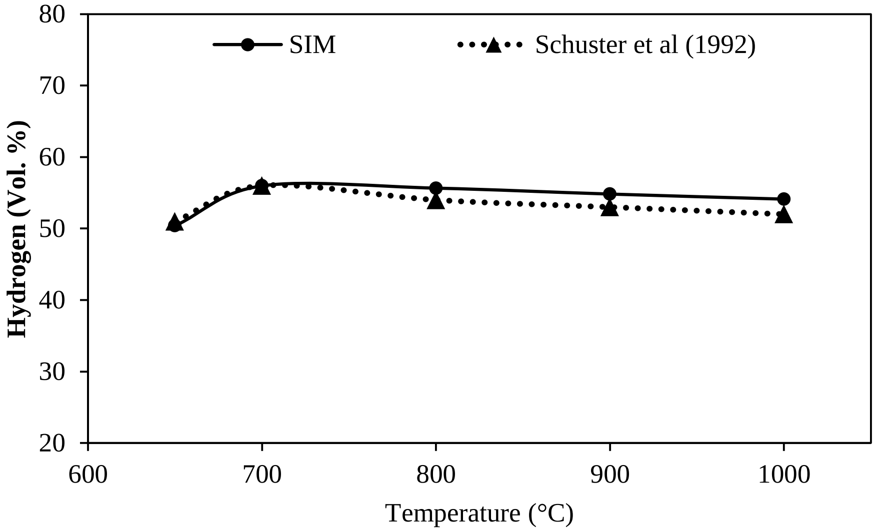

Figure 4.6 Comparison of hydrogen in fluidized bed reactor between simulation and predicted data

For model validation, the synthesis gas obtained in this simulation work is compared with the literature data. Based on the comparison, the trends for all synthesis gas produced from simulation are consistent with the synthesis gas obtained from Schuster et al (2001) as shown in Figure 4.3, Figure 4.4, Figure 4.5 and Figure 4.6 indicating a reliable fluidized bed model has been developed. In addition, the root mean square errors (RMSEs) are also calculated all range by using Equation (3.13) at gasification temperature from 650 °C to 1000 °C as shown in Table 4.3. Based on Table 4.3, the RMSEs obtained are relatively low which is lesser than 0.3 (Veerasamy et al., 2011) and generally in good agreement with the literature data indicating the developed model in this work is validated and indeed reliable to be used for gasification process.

Table 4.3 Performance comparison based on all range temperature of gasifier

| Components (%) | RMSE |
|---|---|
| $CO_2$ | 0.0233 |
| CO | 0.0342 |
| $CH_4$ | 0.1770 |
| $H_2$ | 0.0006 |

## 4.3 Case Study 2: Development of Fixed Bed Gasification Model

In this section, the workflow is used to develop a model for downdraft fixed bed gasification process. Similarly, the work from Moni and Sulaiman (2012) is adopted for model validation.

### 4.3.1 Problem Definition (Step 1)

The objective is to develop and validate gasification model using downdraft fixed bed reactor in the Aspen Plus software.

### 4.3.2 Process and Product Specifications (Step 2)

The selected reactor for process specification is downdraft fixed bed gasifier. The oil palm frond (OPF) is used as an input for gasification process and the data for proximate and ultimate analysis is extracted from the biomass database as shown in Table 4.4. The synthesis gas production is the product specification in this work.

Table 4.4 Properties of oil palm frond

| **Proximate Analysis (wt% dry basis)** | |
|---|---|
| Moisture Content | 12 |
| Volatile Matter | 51.3 |
| Fixed Carbon | 41 |
| Ash | 6.3 |
| **Ultimate Analysis (wt% dry basis)** | |
| C | 42.55 |
| H | 5.48 |
| O | 43.38 |
| N | 2.18 |
| S | 0.20 |

Source: Moni and Sulaiman (2012)

### 4.3.3 Gasification Modelling (Step 3(a))

For downdraft fixed bed gasification model, several stages of process which comprise the gasifier of downdraft fixed bed reactor which are drying of feed, pyrolysis and combustion and gasification. Aspen Plus software have been used for this model development. Since the real downdraft fixed bed gasifier consists of 4 stages of process, hence, several Aspen Plus blocks will be used to represent each stages. Three Aspen Plus blocks were used which are RSTOIC, RYIELD and RGIBBS to represent all the stages inside of the downdraft fixed bed gasifier. The FLASH SEPARATOR was added for completing the flowsheet of gasification model. The Aspen Plus flowsheet and process flowchart to represent the fluidized bed gasification process are shown in Figures 4.7 and 4.8.

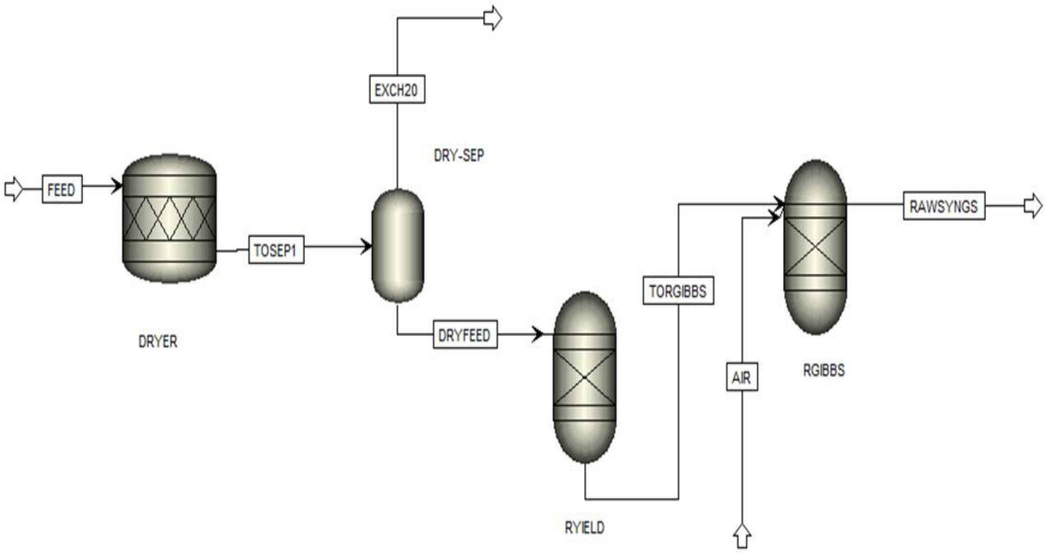

Figure 4.7 Flowsheet of fixed bed gasification

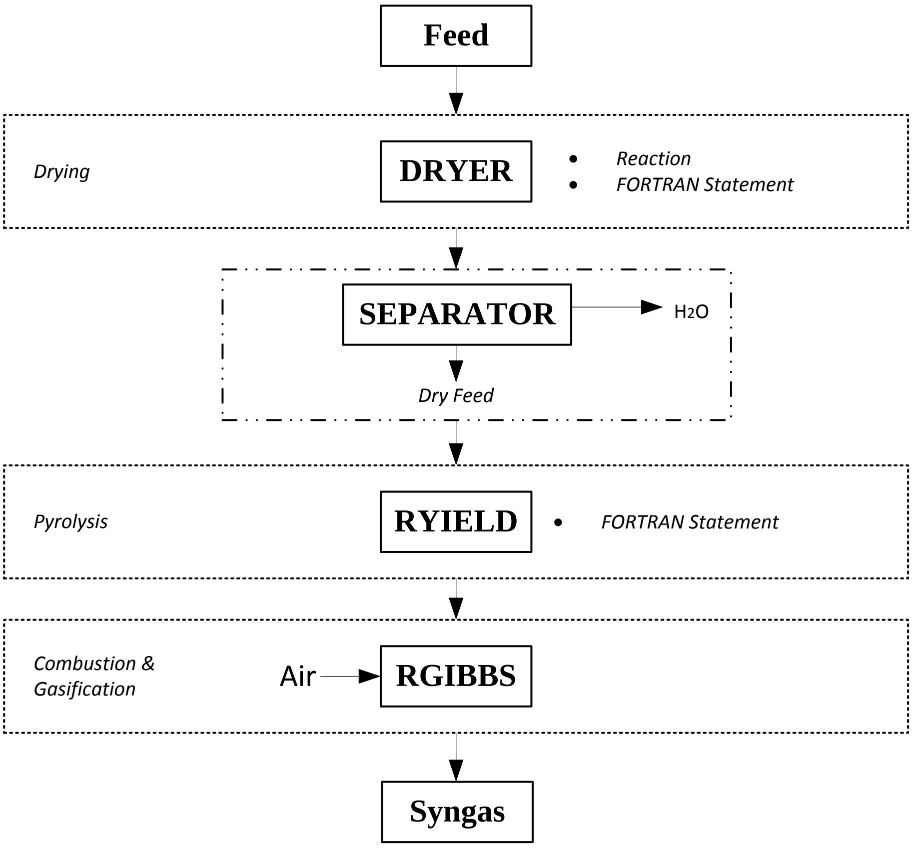

Figure 4.8 Flowchart of fixed bed gasification

### 4.3.3.1 Drying

The first stage of downdraft fixed bed gasifier is the drying of the feed in order to remove water content in the oil palm frond. The drying process is included in fixed bed reactor since the fixed bed consists of drying zone compared to fluidized bed reactor that have biomass perfect mixing with bed particle in fluidization medium. The RSTOIC reactor (block id: DRYER) is used to simulate the drying process of the feed. Here the FORTRAN reaction (Equation 4.1) which specifies in calculator block:

$$Biomass(wet) \rightarrow 0.0555084 H_2O \qquad 4.1$$

This FORTRAN statement is used in the RSTOIC reactor to transform some part of the inlet feed to water. In this step, the moisture content inside of the biomass is partially evaporated and then separated using a separator block, FLASH SEPARATOR (block ID: DRY-SEP) through split fractionation of the components. The evaporated moisture was removed from the process. The dried feedstock is placed into the next region for decomposition after being separated from the evaporated moisture.

#### 4.3.3.2 Pyrolysis

The next stage is pyrolysis where each biomass feedstock is decomposed into its elements. Aspen Plus yield reactor, RYIELD (block ID: RYIELD), was used to simulate the decomposition of the biomass feedstock. The yield reactor converts non-conventional feed into conventional components by using a FORTRAN statement. In this step, the oil palm fronds is converted into its components including carbon, $O_2$, $H_2$, sulphur and ash by specifying the yield distribution according to the biomass's ultimate analysis as shown in Table 4.4. The yield distribution of feed into its components was specified by a FORTRAN statement in the calculator block. The decomposed elements mixed with air at an Aspen MIXER block are ready for next process which is combustion and gasification.

#### 4.3.3.3 Combustion and Gasification

Since the biomass is one of the non-conventional component, RGIBBS was used because the Gibbs s reactor is a rigorous reactor for multiphase chemical equilibrium based on Gibbs free energy minimization (Begum et al., 2013). Therefore, before feeding the biomass into the RGIBBS block, it was decomposed into its elements (C, H, O, N and S) using the RYIELD reactor. The reactor calculates the syngas composition by minimizing the Gibbs free energy and assumes complete chemical equilibrium. The decomposed feed and air enter the RGIBBS block and will undergo combustion and gasification reactions (reactions (3.4) - (3.12)) in the RGIBBS reactor for producing the desired synthesis gas.

For validation of fixed bed gasifier, this model will be validated with the previous work which done from Moni and Sulaiman (2012). The same operating conditions used in the works of Moni and Sulaiman (2012) as shown in Table 4.5 will be applied in this model.

Table 4.5 Operating conditions for gasification process.

| Parameter | Operating Condition | Value |
|---|---|---|
| Fixed bed reactor | Temperature (°C) | 600-1000 |
| | Pressure (bar) | 1 |
| Air | Temperature (°C) | 700 |
| | Flow rate ( kg/h) | 0.18-0.2 |
| Biomass feed | Flow rate (kg/h) | 12 |

Source: Moni and Sulaiman (2012)

The simulation results obtained from fixed bed gasification process are shown in Figures 4.9 to 4.12. From Figure 4.9, the amount of $CO_2$ is decreased when the gasification temperature is increased. This is due to the domination of endothermic reaction of water gas shift reaction which consumed more $CO_2$ and $H_2$ which produces more CO and water. This explained why the amount of CO is increased and $H_2$ is decreased. The decreasing of methane is due to methanation process which produces more CO.

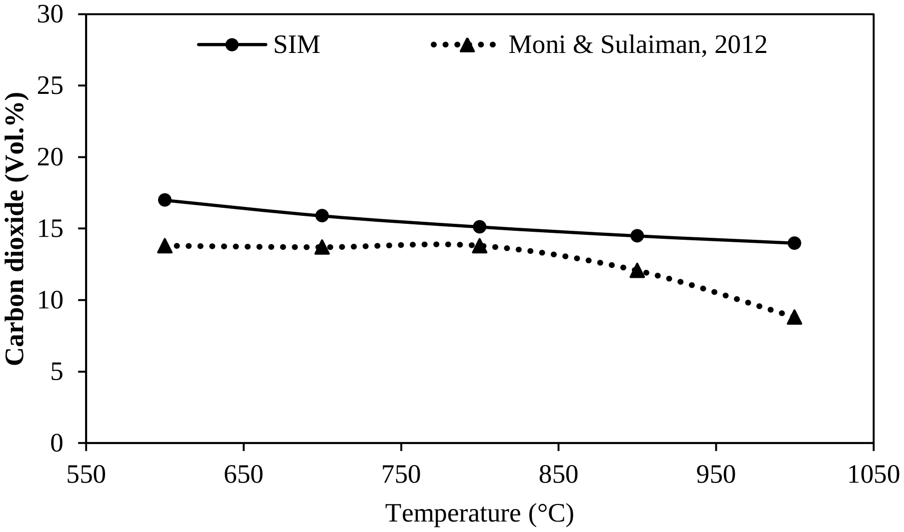

Figure 4.9 Comparison of carbon dioxide in fixed bed reactor between simulation and predicted data

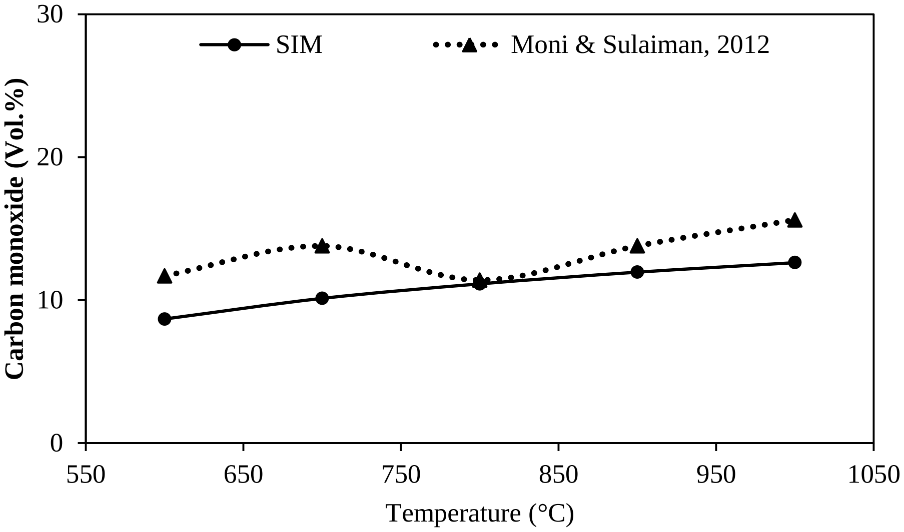

Figure 4.10 Comparison of carbon monoxide in fixed bed reactor between simulation and predicted data

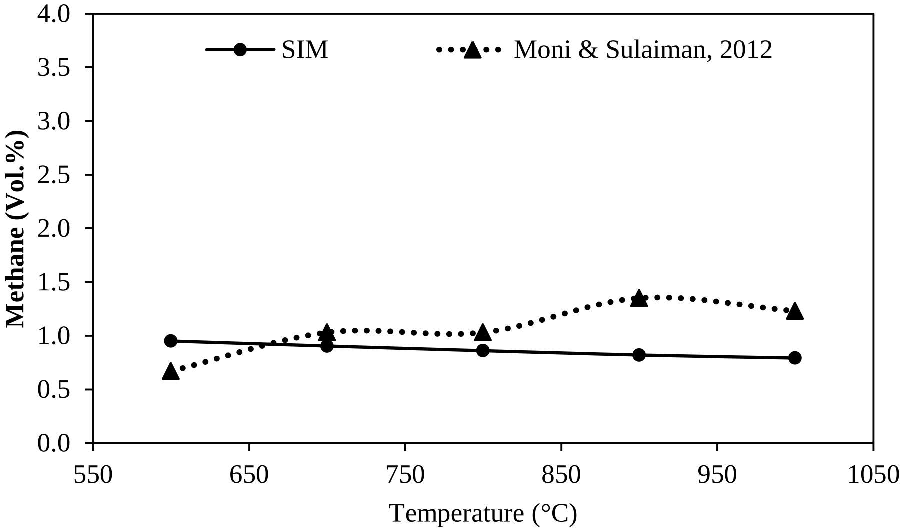

Figure 4.11 Comparison of methane in fixed bed reactor between simulation and predicted data

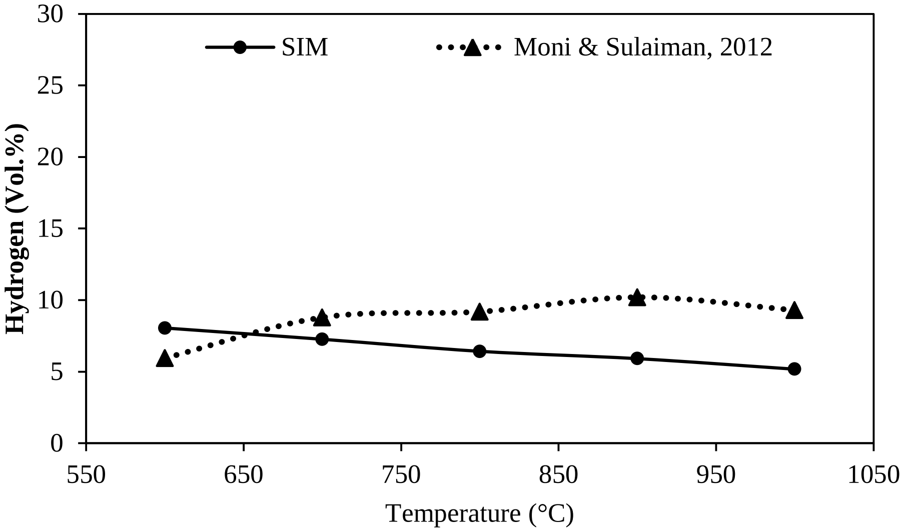

Figure 4.12 Comparison of hydrogen in fixed bed reactor between simualtion and predicted data

Based on the comparison, all the synthesis gas predicted from the simulation shows a good agreement with literature data indicating the developed model is indeed reliable. In addition, RMSE are calculated at all range of gasification temperature from 600 °C to 1000 °C as shown in Table 4.6. Based on Table 4.6, the RMSE obtained is lesser than 0.3 for all synthesis gas indicating the predicted synthesis is very close with literature data (Veerasamy et al., 2011). In overall, the model provides a good prediction of synthesis gas and subsequently be used for representing the gasification process.

Table 4.6 Performance comparison based on all range temperature of downdraft fixed bed gasifier

| **Components (%)** | **RMSE** |
|---|---|
| $CO_2$ | 0.0650 |
| CO | 0.1870 |
| $CH_4$ | 0.1918 |
| $H_2$ | 0.2525 |

## 4.4 Case Study 3: Performance Comparison Based On Different Gasifiers

In this section, the performance of downdraft fixed bed and bubbling fluidized bed gasification models are evaluated in terms of hydrogen production using different palm oil wastes. Here, the same gasification models from case studies 1 and 2 are employed for simulation works. The biomass selected for both gasification models is oil palm frond (OPF), empty fruit bunch (EFB), palm mesocarp fibre (PMF) and palm kernel shell (PKS). The ultimate and proximate analysis taken from biomass database for all palm oil wastes are shown in Table 4.7.

Table 4.7 Ultimate and proximate analysis for palm oil wastes

| **Parameters** | **Biomass** | | | |
|---|---|---|---|---|
| | Raw OPF | Raw EFB | Raw PMF | Raw PKS |
| | **Proximate analysis (wt. % wet basis)** | | | |
| Moisture content | 15.95 | 15.77 | 10.88 | 11.87 |
| Volatile matter | 66.17 | 67.01 | 69.04 | 70.02 |
| Fixed carbon | 15.01 | 13.37 | 14.42 | 12.07 |
| Ash | 2.87 | 3.85 | 5.66 | 6.04 |
| | **Ultimate analysis (wt.% wet basis)** | | | |
| C | 43.94 | 43.53 | 45.20 | 47.79 |
| H | 6.94 | 7.20 | 5.94 | 5.95 |
| N | 3.52 | 1.73 | 1.12 | 1.77 |
| S | 0.72 | 0.46 | 0.11 | 0.06 |
| O | 44.88 | 47.09 | 47.63 | 44.43 |
| HHV (MJ/kg) | 17.75 | 15.49 | 16.94 | 16.15 |

Source: Wahid et al. (2017)

### 4.4.1 Sensitivity Analysis (Step 4)

In the previous case studies 1 and 2, downdraft fixed bed and bubbling fluidized bed gasification models are successfully developed and validated against literature data. Therefore, sensitivity analysis (Step 4) is carried out in this section using palm oil wastes where the effects of gasification temperature, air to biomass ratio and steam to biomass ratio (applicable for fluidized bed model only) are investigated.

#### 4.4.1.1 Effects of Gasification Temperature

The sensitivity analysis of the gasification temperature is performed where the gasification temperature is varied between 600 °C to 1000 °C and the synthesis gas composition obtained were analysed. The air to biomass ratio was fixed on 0.2 in this analysis. Figures 4.13 to 4.16 show the synthesis gas composition based on the sensitivity analysis of gasification temperature for fluidized and fixed bed gasifiers.

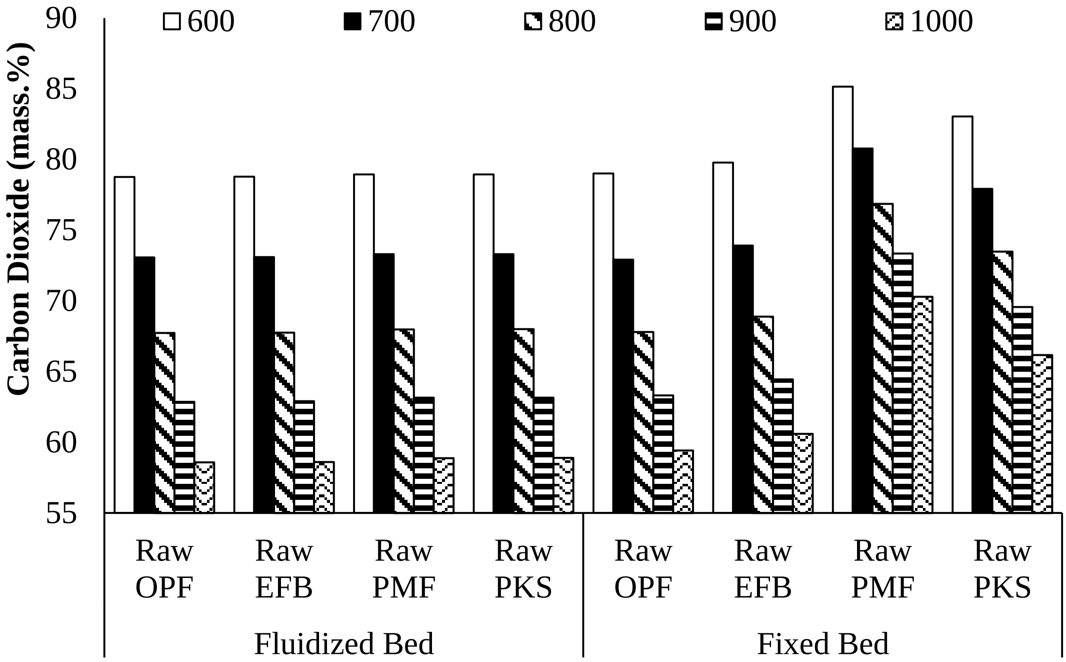

Figure 4.13 Effects of gasification temperature on carbon dioxide production in fluidized and fixed bed gasifiers

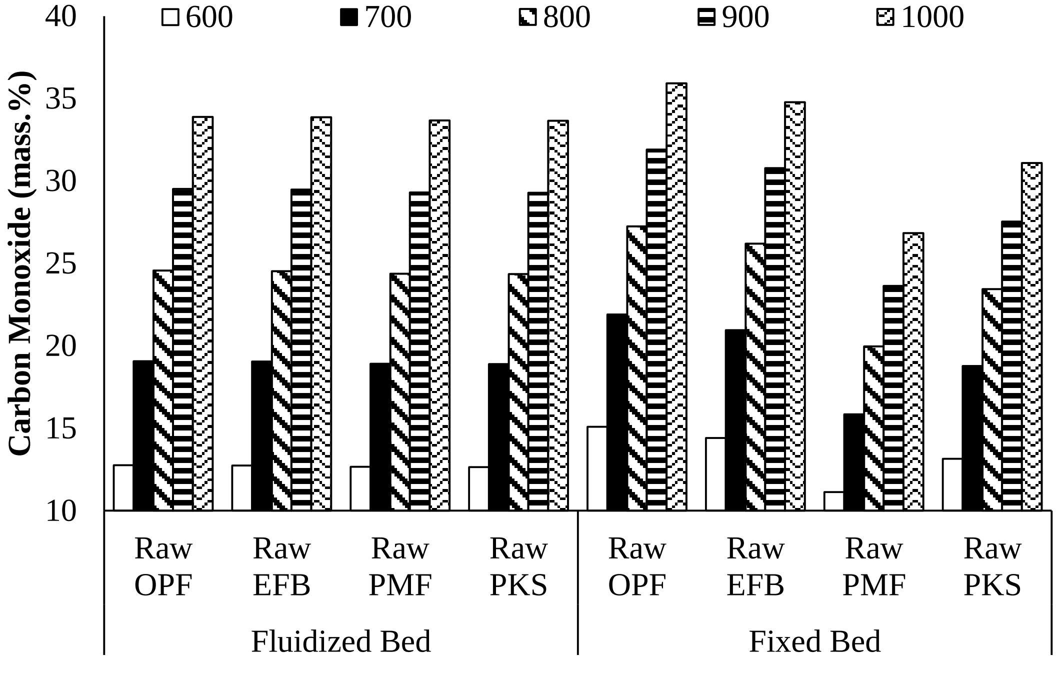

Figure 4.14 Effects of gasification temperature on carbon monoxide production in fluidized and fixed bed gasifiers

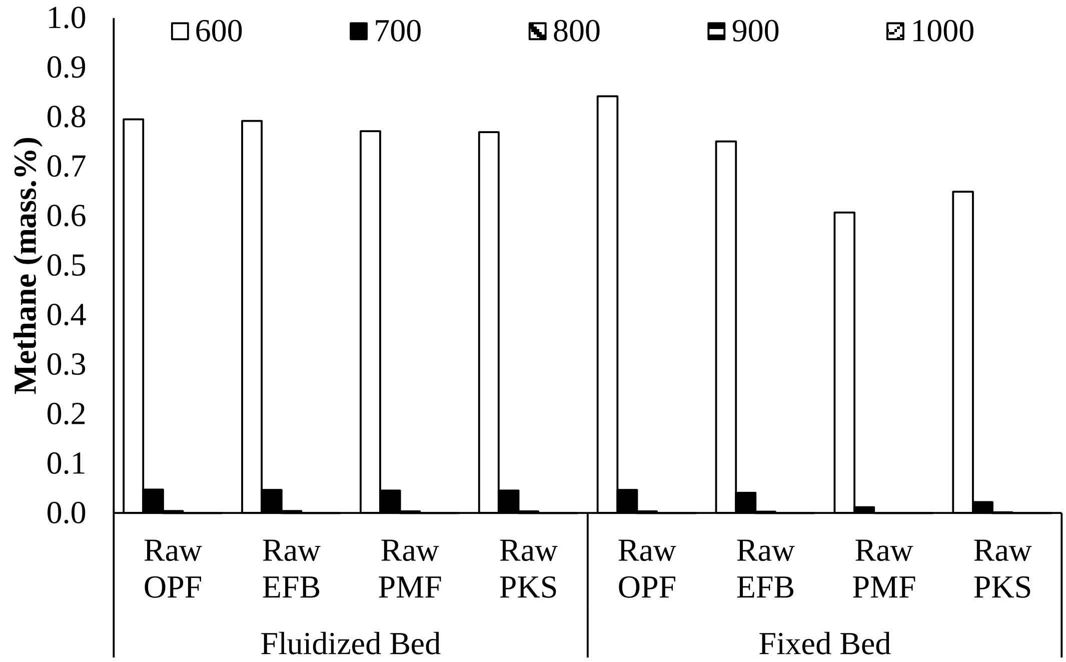

Figure 4.15 Effects of gasification temperature on methane production in fluidized and fixed bed gasifiers

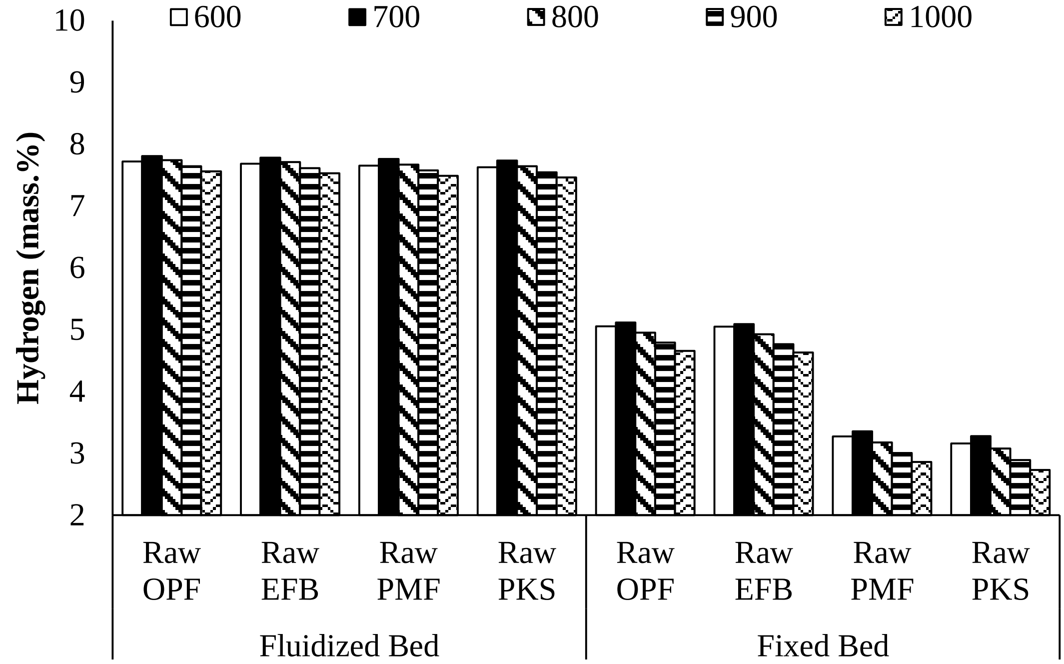

Figure 4.16 Effects of gasification temperature on hydrogen production in fluidized and fixed bed gasifiers

As the temperature increases, the CO gas produced (Figure 4.14) is increased but the $CO_2$ (Figure 4.13) and the $CH_4$ gases (Figure 4.15) produced are decreased for all palm oil wastes. According to the Le Châtelier's principle, if a dynamic equilibrium is disturbed by changing the operating condition, the equilibrium will be shifted in order to counteract the changes made. The increasing of the temperature in the system will disturb the equilibrium state of all the chemical reaction. The equilibrium chemical reactions then experiences a sudden change as the temperature is increased which cause the equilibrium shifts in the opposite direction to offset the changes (Wahid et al., 2016). The increasing temperature will shifts the equilibrium of endothermic reactions (3.7) and (3.8) in the direction of the product formation (CO and $H_2$), while the equilibrium of exothermic reactions (3.9) and (3.10) is moved in the direction of the reactants (mainly $H_2$).

The amount of hydrogen gas (Figure 4.16) shows a slight increase as the gasifier temperature is increased from 600 °C and reaches its peak at 700 °C for both gasifier. This is caused by conversion of steam-methane methanation reaction ($CH_4 + H_2O \leftrightarrow CO + 4H_2$) (Yunus et al., 2010). However, after 700 °C, the amount of $H_2$ is decreased which has been caused by domination reaction of endothermic reaction of Bourdouard reaction ($C + CO_2 \leftrightarrow 2CO$) and water gas shift reaction ($CO_2 + H_2 \leftrightarrow CO + H_2O$) which cause the increasing of CO and decreasing of $CO_2$ (Mahishi and Goswami, 2007). In addition some of the hydrogen is also converted into methane ($C + 2H_2 \rightarrow CH_4$) in methanation reaction which explains the low amount of hydrogen gas produced (Aly, 2013).

As for gasifier comparison, the hydrogen gas produced by bubbling fluidized bed for all palm oil wastes shows more percentages compare to downdraft fixed bed reactor. For example, for raw OPF at temperature 700 °C, fluidized bed produces 7.81 % hydrogen gas which is higher compared to 5.12 % of hydrogen gas using fixed bed. This is due to the presence of steam flow inside of the fluidized bed gasification which triggers the water gas shift reaction in order to increase the tendency of hydrogen production. In addition, the fluidized bed reactor provides excellent biomass mixing compare to fixed bed reactor. The solid fuel particles from biomass are brought into contact with a restricted supply of oxygen by feeding them into oxygen starved fluidized bed. The fuel particles are quickly heated to the bed temperature and undergo rapid drying and pyrolysis (Basu, 2006). This specification trigger the process inside of the gasification to have high tendency to gain high amount of heating value and this also improved the mass and heat transfer from biomass leading to the more hydrogen production. In terms of Aspen Plus modelling, bubbling fluidized bed model provide combustion of volatile product which include carbon, hydrogen, and oxygen as volatile components and solid carbon and ash as non-volatile product. With presence of char formation after the reaction, more high carbon source solid is available which provide more hydrogen production if the gasification process occurred. Unlike downdraft fixed bed model, the model consist only one flow of process and did not consist volatile reaction like bubbling fluidized bed model (Fatoni et al., 2014).

For biomass comparison, raw OPF provides the highest hydrogen production compare to another palm oil wastes which are 7.81 % from using fluidized bed gasifier and 5.12 % from using fixed bed gasifier respectively. This is because raw OPF contains lower amount of volatile matter which is 66.17 % of weight percentage compare to other palm oil wastes. Usually biomass with lower volatile matter content will become more reactive and therefore can be converted more easily into synthesis gas and producing less char. The produced char is more porous and reacts relatively fast. For this reason, biomass with high volatile matter content will have higher tendency to gasify more easily for producing hydrogen gas (Basu, 2006). From sensitivity analysis for gasification temperature, the best temperature for operating the gasification process is at 700 °C because more hydrogen is produced at this temperature.

#### 4.4.1.2 Effects of Air to Biomass Ratio

Figures 4.17 to 4.20 show the synthesis gas production based on different values of ABR. The effect of air to biomass ratio (ABR) is performed by varying the ABR from 0.2 to 1. Meanwhile the gasification temperature and steam to biomass ratio were fixed at 700 °C and 1.0. From Figure 4.17, Figure 4.18, Figure 4.19 and Figure 4.20, when the ABR is increased, the $CO_2$ production shows the increasing trend but the decreasing trends of carbon monoxide, methane and hydrogen are observed. From Figure 4.17, the increasing value of ABR mainly causes the increasing amount of $CO_2$ due to the endothermic reaction of combustion reaction ($C + O_2 \rightarrow CO_2$). The decreasing amount of CO as shown in Figure 4.18 is due to homogenous reaction of CO combustion ($CO + 0.5O_2 \rightarrow CO_2$) which also contributes in increasing amount of $CO_2$ where the oxygen gas (gasifying agent) supplied to the gasifier enhances the combustion process and subsequently the production of $CO_2$ is increased. More oxygen supply to the reactor will ultimately increase the ABR ratio which promotes the oxidation reaction and thus lowering the amount of CO content but increasing the $CO_2$ content.

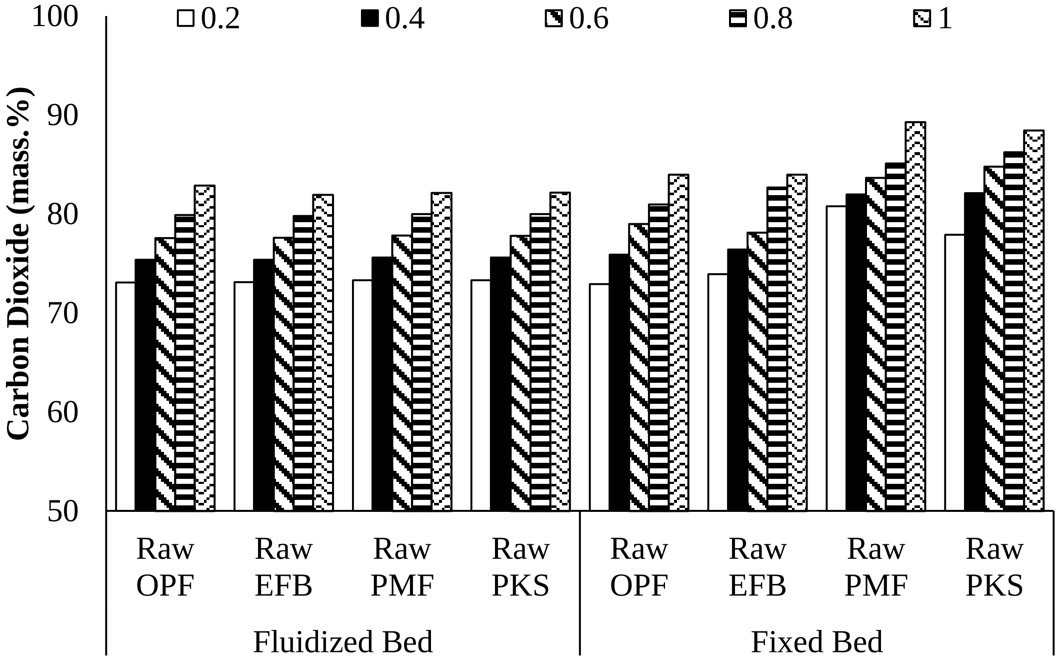

Figure 4.17 Effects of air to biomass ratio on carbon dioxide production in fluidized and fixed bed gasifiers

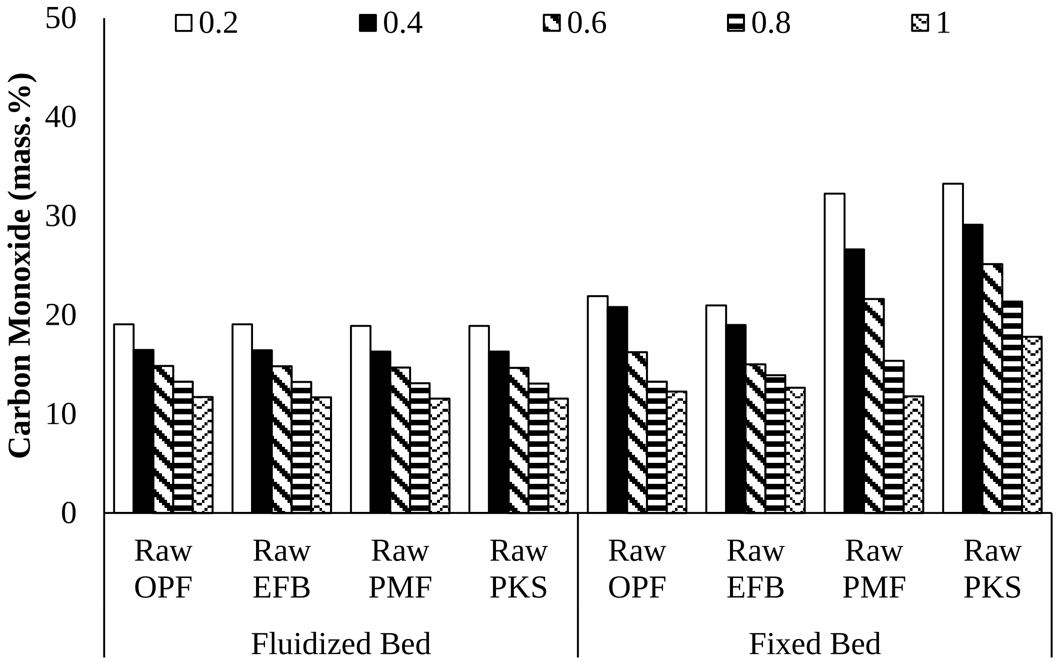

Figure 4.18 Effects of air to biomass ratio on carbon monoxide production in fluidized and fixed bed gasifiers

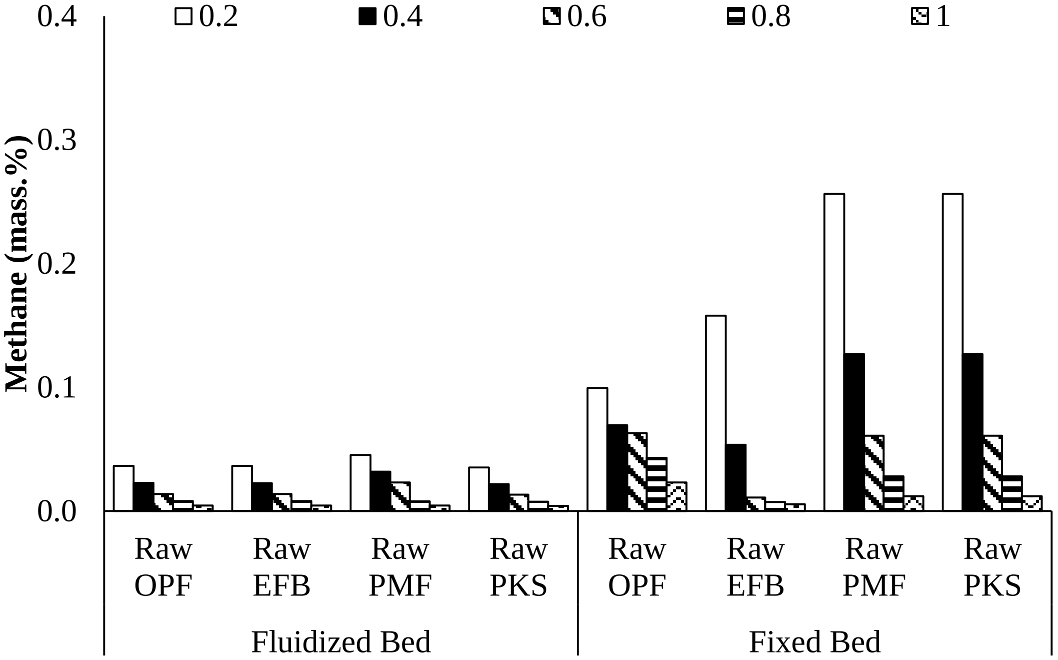

Figure 4.19 Effects of air to biomass ratio on methane production in fluidized and fixed bed gasifiers

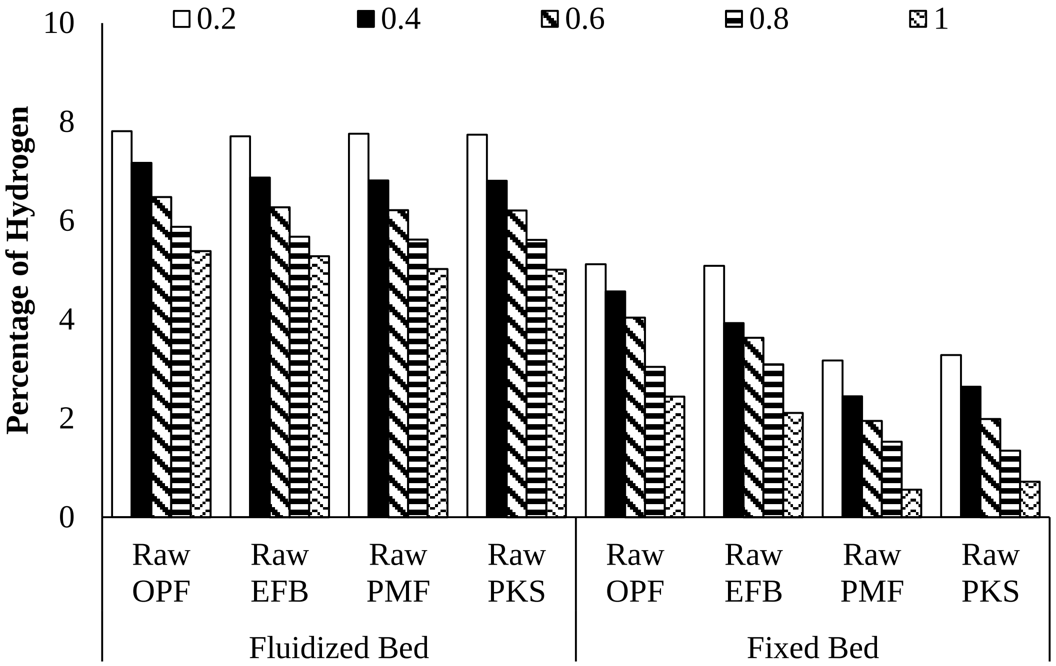

Figure 4.20 Effects of air to biomass ratio on hydrogen production in fluidized and fixed bed gasifiers

Besides, the amounts of $H_2$ (Figure 4.20) also decrease as the oxidation of hydrogen occurred to become water ($H_2 + 0.5O_2 \leftrightarrow H_2O$). Hence the amount of $H_2O$ will increase as the value of ABR is increased. Based on the simulation results, it shows that the fixed bed gasifier provide less $H_2$ compare to the fluidized bed gasifier. This is due to the fact that fixed bed gasifier provides high combustion compare to fluidized bed gasifier. High combustion means that the tendency of combustion process which occurred at high air equivalent ratio which supplies more air into the gasifier and improves char burning to produce $CO_2$ instead of combustible gases such as CO, $H_2$ and $CH_4$ (Kumar and Vivekanandan, 2014). Hence, less $H_2$ and more $CO_2$ will be produced by fixed bed gasifier compared to fluidized bed gasifier. For example, for raw OPF at ABR of 0.2, fixed bed gasifier produces only 6.37 % of hydrogen gas which is lower than 7.47 % of hydrogen gas produced from fluidized bed. Therefore fluidized bed is more compatible in producing hydrogen gas compared to fixed bed gasifier in terms of air biomass ratio. For ABR, the best operating condition for gasification is 0.2 where at this value; high amount of hydrogen gas will be produced.

#### 4.4.1.3 Effects of Steam to Biomass Ratio

The effects of steam to biomass ratio (SBR) on the production of synthesis gas for all feedstock are shown in Figures 4.21 to 4.24. Here, the other operating conditions are fixed at gasification temperature of 700 °C and 0.2 of air to biomass ratio.

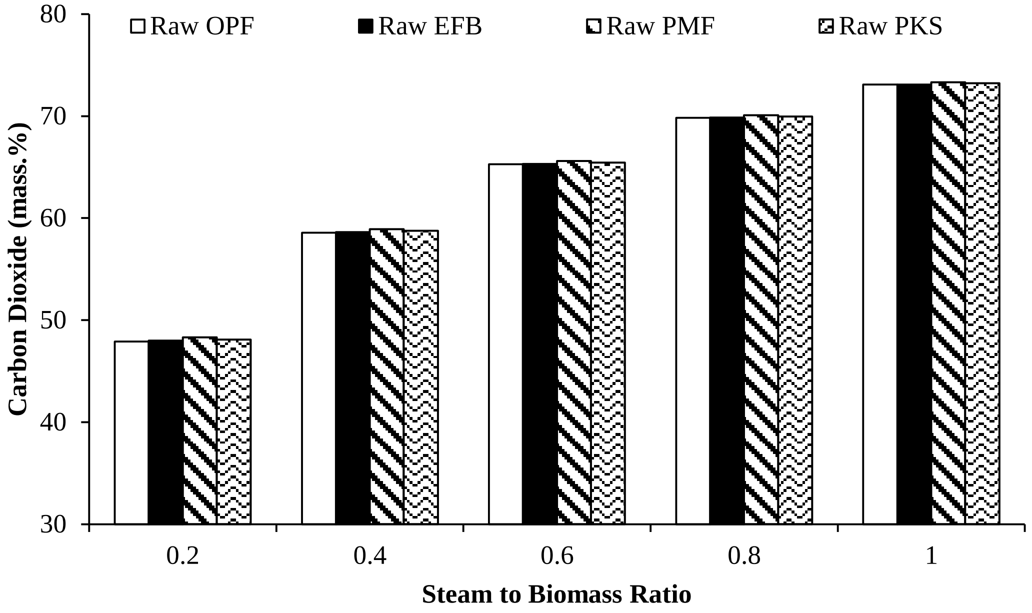

Figure 4.21 Effects of steam to biomass ratio on carbon dioxide production in fluidized bed gasifier

In this sensitivity analysis of SBR ratio, it has been observed that when content of steam in the converting agent is increased, the production of $H_2$ in Figure 4.24 and $CO_2$ in Figure 4.21 are also increased. This is due to the fact that if more steam fed to the gasification process then water-gas shift reaction ($CO + H_2O \leftrightarrow CO_2 + H_2$) and methane steam reforming reaction ($CH_4 + 2H_2O \leftrightarrow CO_2 + 4H_2$) becomes dominant and thus the $H_2$ and $CO_2$ concentrations are increased gradually but at the same time the amounts of CO in Figure 4.22 and $CH_4$ in Figure 4.23 concentrations are steadily decreased.

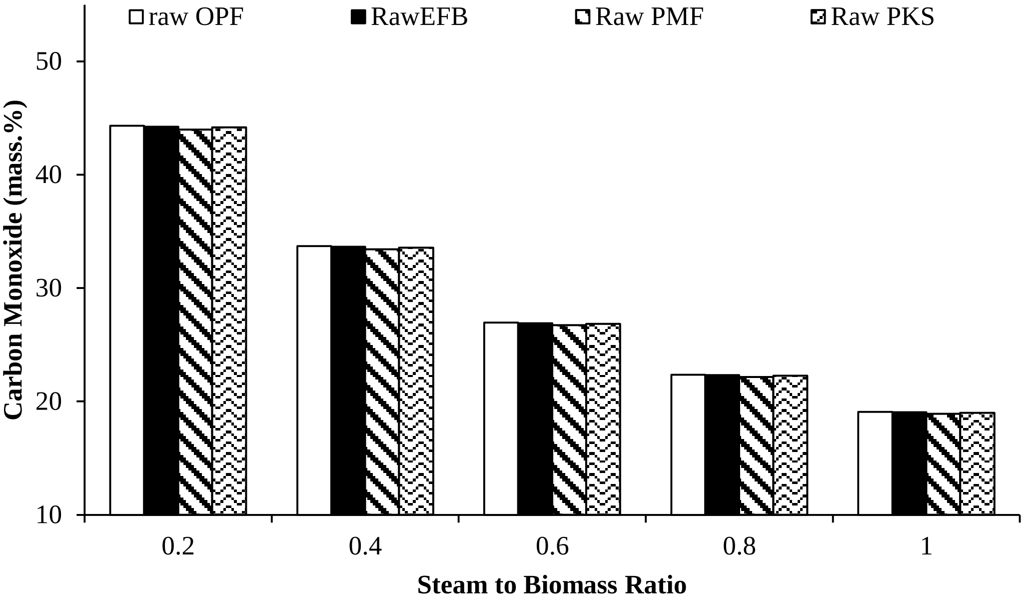

Figure 4.22 Effects of steam to biomass ratio on carbon monoxide production in fluidized bed gasifier

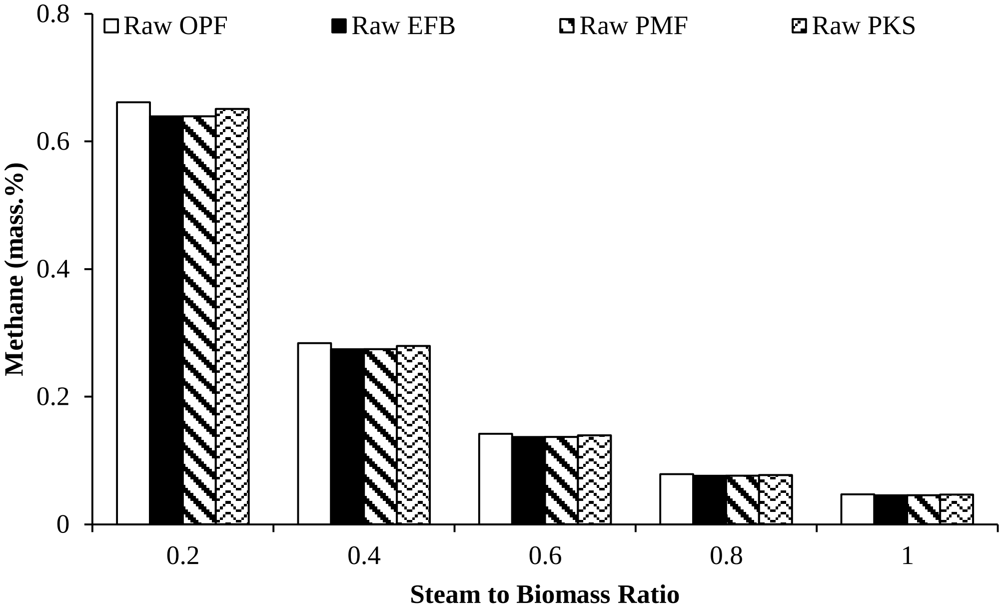

Figure 4.23 Effects of steam to biomass ratio on methane production in fluidized bed gasifier

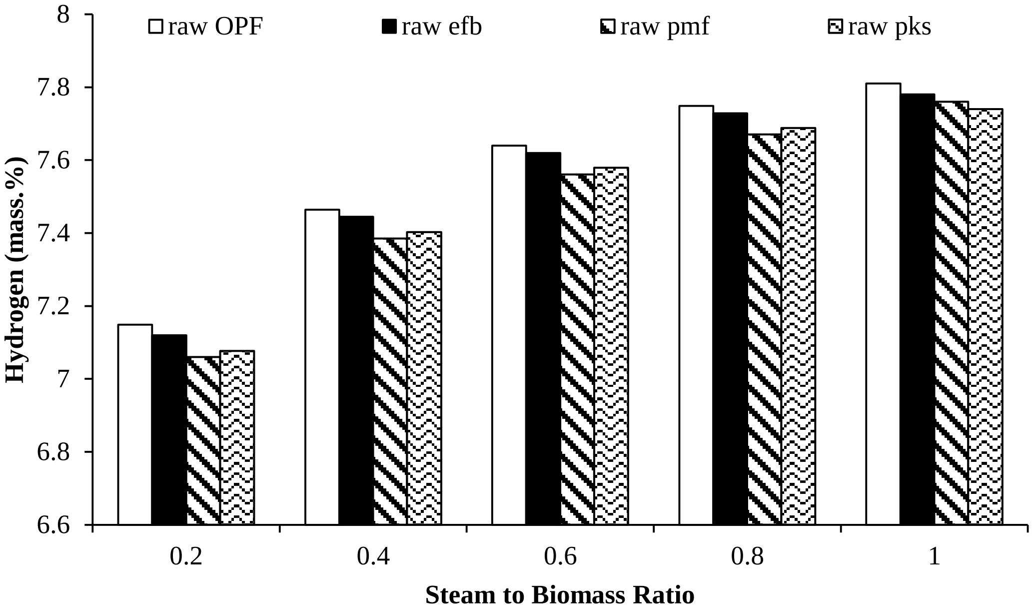

Figure 4.24 Effects of steam to biomass ratio on hydrogen production in fluidized bed gasifier

Due to water-gas shift reaction, more $CO_2$ and $H_2$ gases will be formed since the steam will react with CO to produce $H_2$ gas and $CO_2$ gas (Salami, 2012). The raw OPF provides the highest amount of $H_2$ gas produced around 7.82 % at SBR ratio of 1 compare to the other raw palm oil wastes which indicates that raw OPF provides high tendency to produce high amount of $H_2$ gas compare to other palm oil wastes.

## 4.5 Case Study 4: Effects of Torrefaction on the $H_2$ Production in Biomass Gasification Process

In case study 3, it shows that raw OPF produces the highest hydrogen gas compare to the other palm oil wastes for both gasifiers. In this section, the effects of biomass torrefaction on the hydrogen production is tested and evaluated. Here the OPF is torrefied at two different temperatures (270 °C and 300 °C) at 30 minutes of residence time are used as input for gasification process and the hydrogen gas obtained is evaluated and compare with raw OPF. The ultimate and proximate analyses for raw OPF and torrefied OPF are shown in Table 4.8.

Table 4.8 Ultimate and proximate analysis for all biomasses

| Parameters | Biomass | | |
|---|---|---|---|
| | Raw OPF | Tor OPF 270 °C | Tor OPF 300°C |
| **Proximate analysis (wt. %)** | | | |
| Moisture content | 15.95 | 6.78 | 4.81 |
| Volatile matter | 66.17 | 56.15 | 45.54 |
| Fixed carbon | 15.01 | 32.44 | 44.88 |
| Ash | 2.87 | 4.62 | 4.76 |
| **Ultimate analysis (wt.% dry basis)** | | | |
| C | 43.94 | 48.33 | 55.72 |
| H | 6.94 | 6.50 | 5.96 |
| N | 3.52 | 4.14 | 4.32 |
| S | 0.72 | 0.26 | 0.22 |
| O | 44.88 | 40.78 | 33.78 |
| HHV (MJ/kg) | 17.75 | 19.82 | 23.79 |

Source: Wahid et al. (2017)

### 4.5.1 Performance and Sensitivity Analysis (Step 5)

Bubbling fluidized bed and downdraft fixed bed gasification models are simulated again using torrefied OPF at 270 °C and 300 °C. Similarly the effect of gasification temperature, air to biomass ratio and steam to biomass ratio (for fluidized bed only) are carried out under sensitivity analysis.

#### 4.5.1.1 Effects of Gasification Temperature

Figures 4.25 to 4.28 show the synthesis gas composition obtained for both gasifiers based on the sensitivity analysis of gasification temperature between 600 °C to 1000 °C. The ABR in this case is fixed in 0.2. From Figure 4.28, both of the gasifiers provide the same results which are the biomass feedstock of oil palm fronds at torrefied temperature of 300 °C provide the highest hydrogen production compare to other OPF at 700 °C of gasifier temperature which are 7.85 % of hydrogen gas for fluidized bed and 5.65 % of hydrogen gas for fixed bed respectively. This is due to fact that higher amount of carbon content in ultimate analysis in both torrefied OPF at 270 °C and 300 °C compare to raw OPF as shown in Table 4.8. Basically, the carbon content involves in partial combustion (reactions 3.4 and 3.5), Boudouard reaction (reaction 3.7) and steam-reforming with carbon in solid state (reaction 3.8) to form CO and $H_2$ gases (Tapasvi et al., 2015).

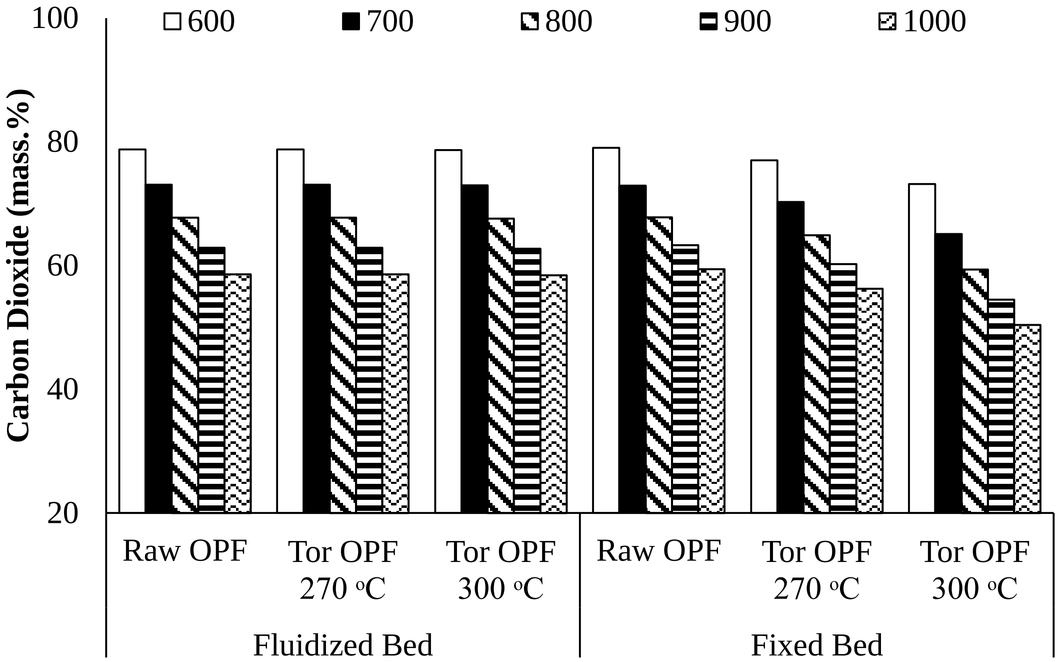

Figure 4.25 Effects of gasification temperature on carbon dioxide production using raw and torrefied OPF

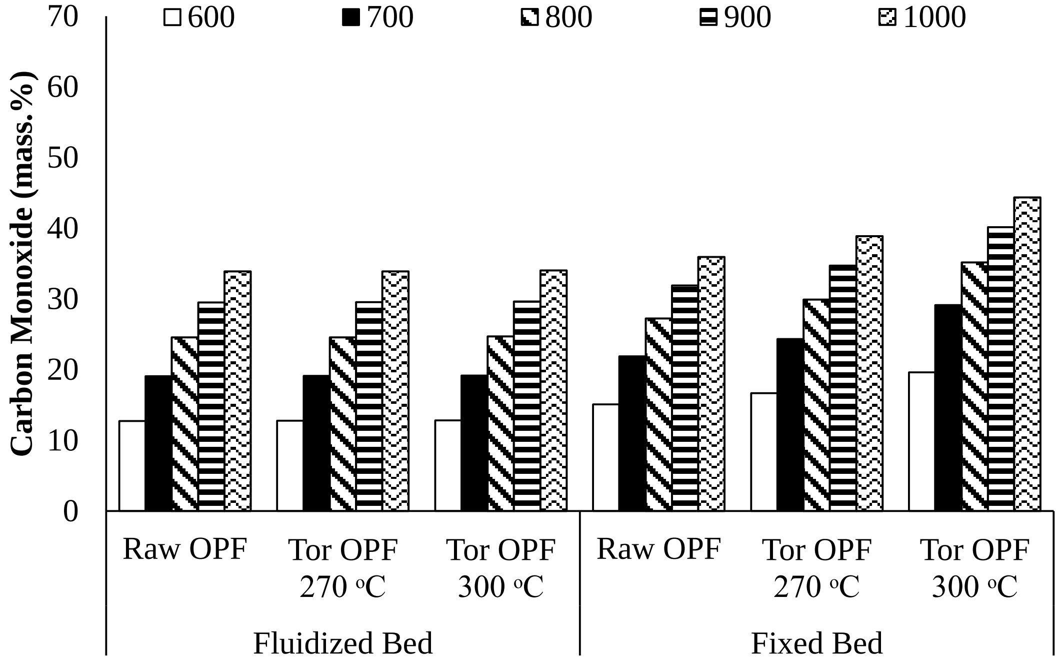

Figure 4.26 Effects of gasification temperature on carbon monoxide production using raw and torrefied OPF

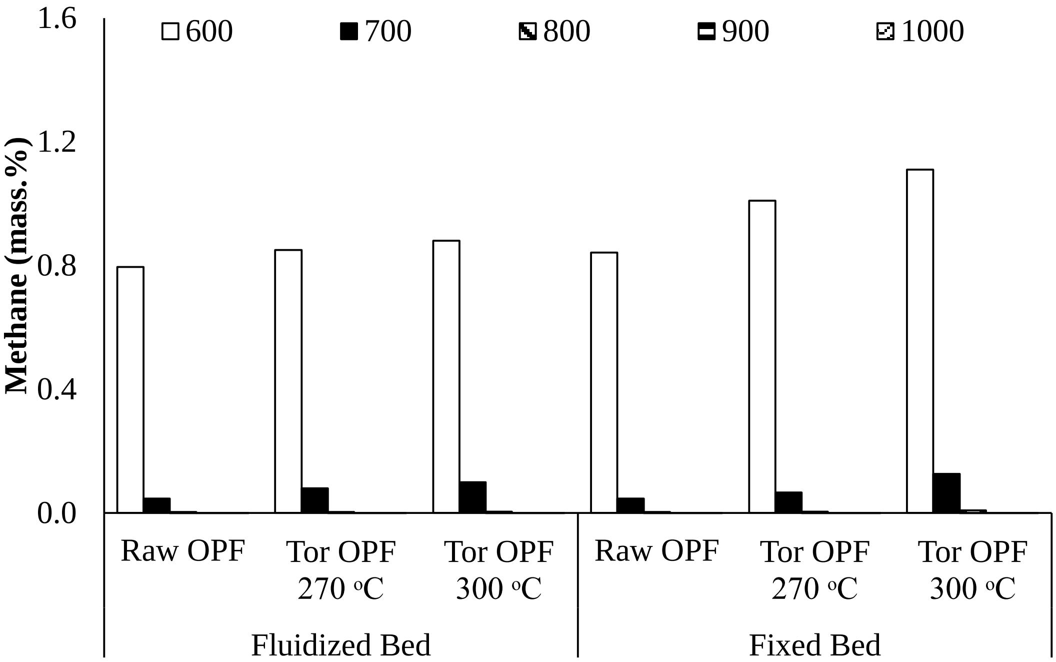

Figure 4.27 Effects of gasification temperature on methane production using raw and torrefied OPF

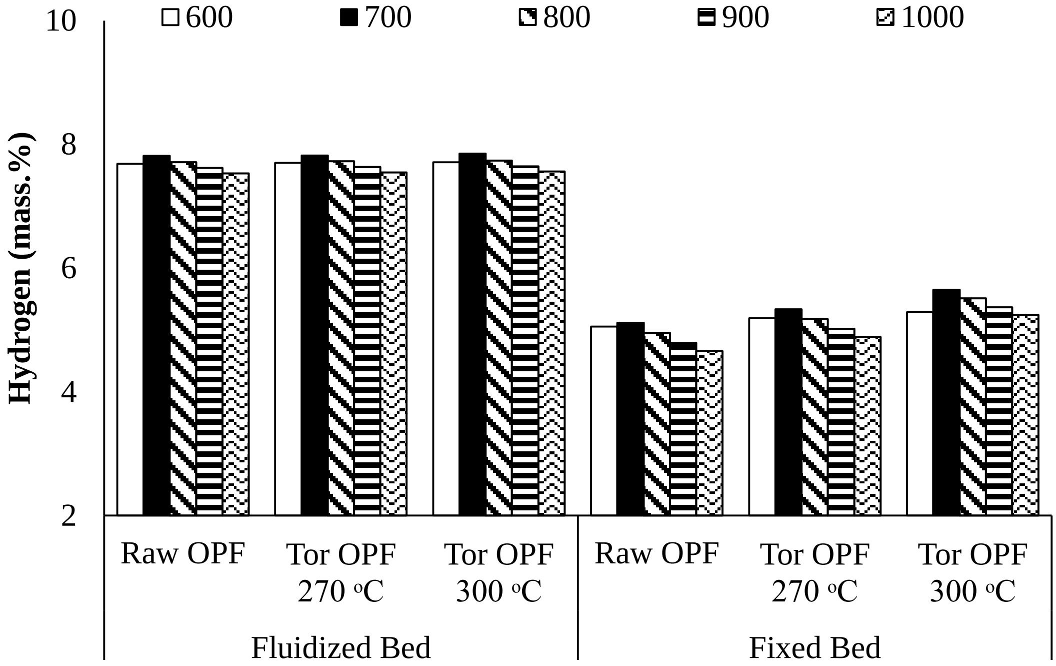

Figure 4.28 Effects of gasification temperature on hydrogen production using raw and torrefied OPF

Besides, the decrement of volatile matter also contributes directly on output synthesis gas production in both gasifiers. The volatile matter content is decreased from 66.17 % for raw OPF down to 64.86 % and 45.54 % for the torrefied OPF at 270 °C and 300 °C as shown in Table 4.8. The biomass which has lower volatile matter usually have high tendency to produce more hydrogen gas (Muslim et al., 2017). Moreover, the amount of synthesis gas produced also affected by the amount of fixed carbon in the biomass. The higher percentage of fixed carbon will definitely increase the calorific value and improve the quality of biomass. In gasification, the higher amount of fixed carbon will enhance the reaction of carbon combustion, Boudouard reaction, water gas shift reaction and methanation reaction during the gasification which contributing to more hydrogen gas production. The increasing temperature will increase the amount of CO and $H_2$ (until gasification temperature of 700 °C) for both gasifier which caused by the shifting of endothermic reaction inside of both gasifier as explained in Case 3. Hence, in this gasification temperature analysis, the torrefied OPF provides higher amount of hydrogen gas production compare to raw OPF.

### 4.5.1.2 Effects of Air to Biomass Ratio

Figures 4.29 to 4.32 show the synthesis gas production based on different values of ABR for fluidized and fixed bed gasifiers. The effects of air to biomass ratio (ABR) are performed by varying the ABR values from 0.2 to 1 which fixed gasification temperature at 700 °C.

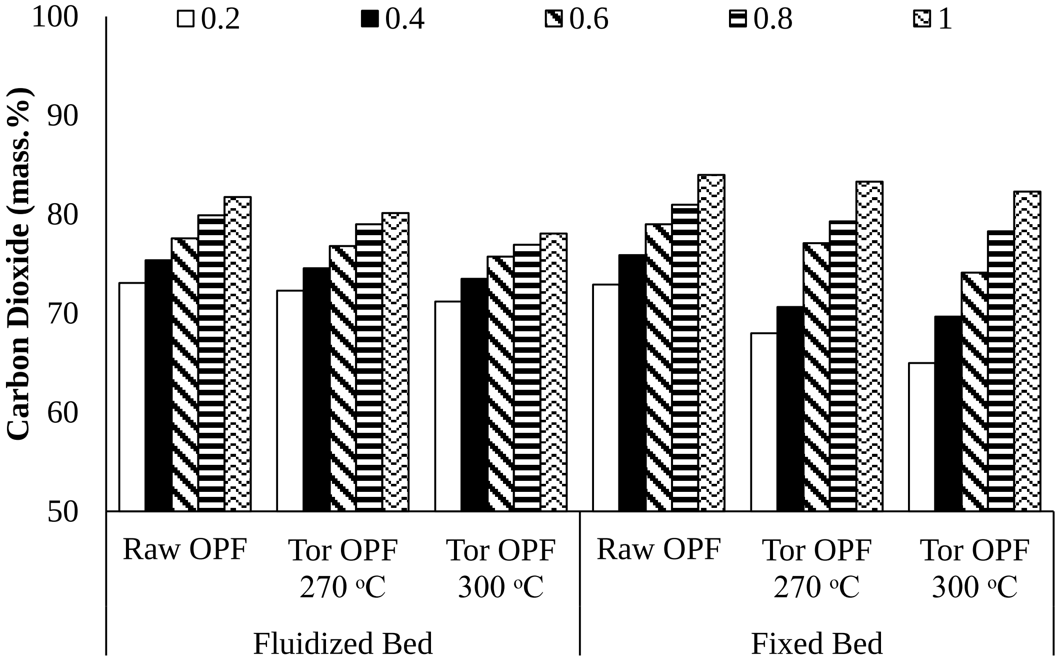

Figure 4.29 Effects of air to biomass ratio on carbon dioxide production using raw and torrefied OPF

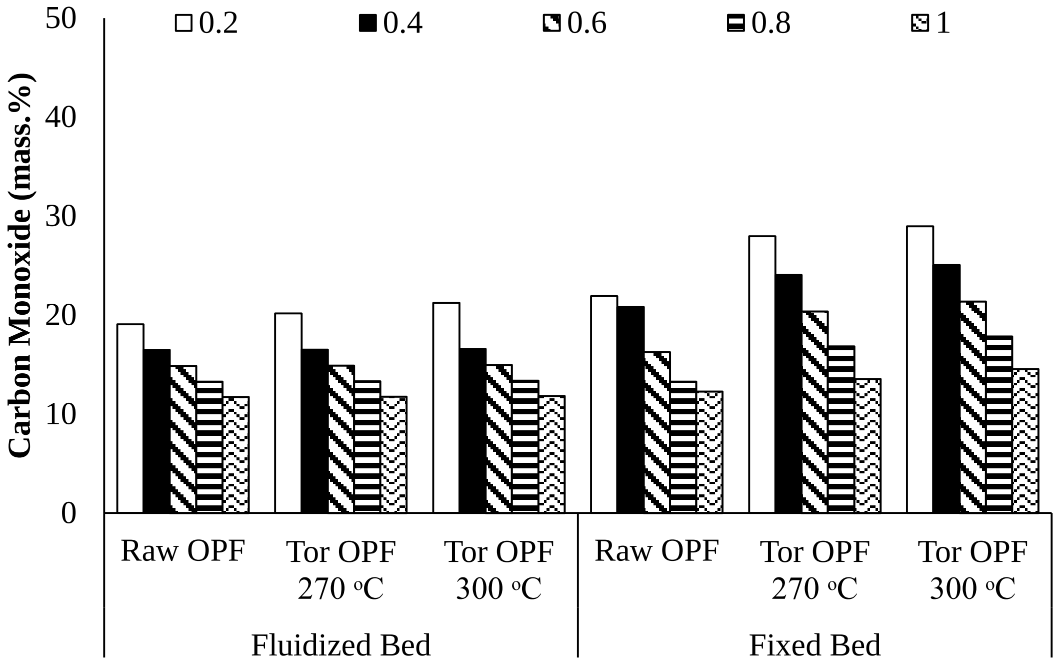

Figure 4.30 Effects of air to biomass ratio on carbon monoxide production using raw and torrefied OPF

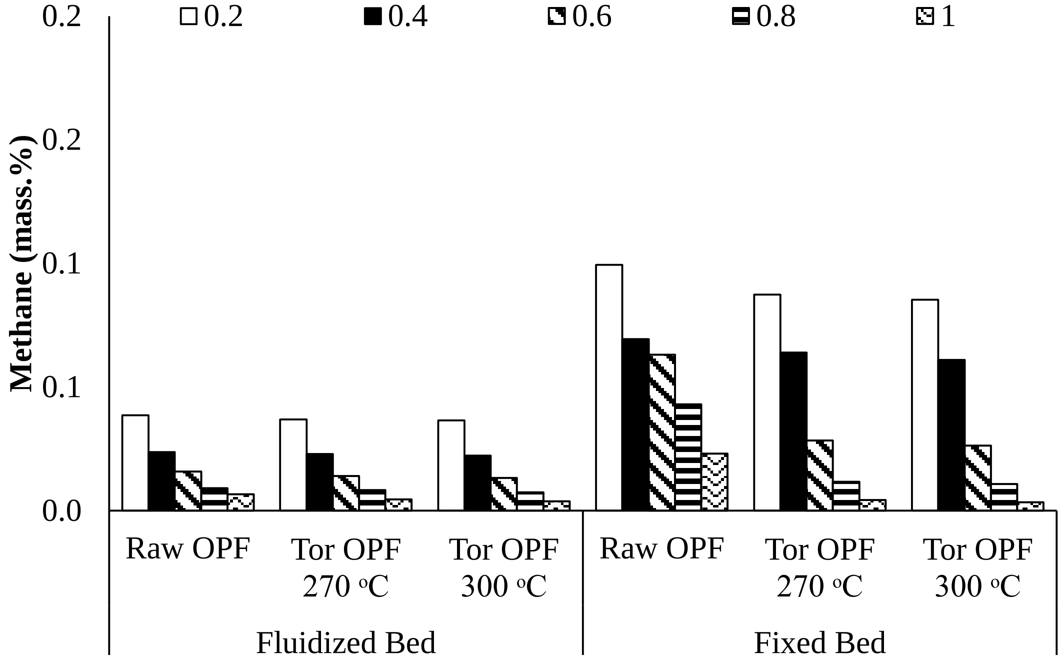

Figure 4.31 Effects of air to biomass ratio on methane production using raw and torrefied OPF

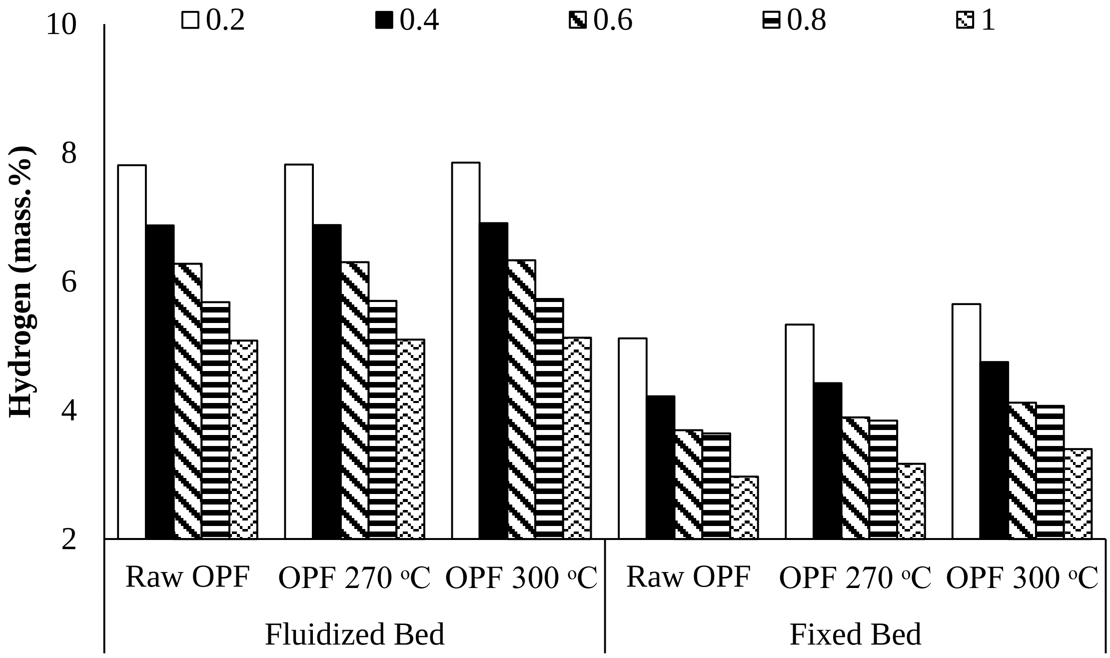

Figure 4.32 Effects of air to biomass ratio on hydrogen production using raw and torrefied OPF

The increasing of ABR means that more air is supplied into the gasifier during the gasification process. By increasing the amount of air supplied into both reactors, the output synthesis gas are affected which more carbon dioxide are produced and more carbon monoxide, methane and hydrogen are reacted. Both gasifier show that the torrefied OPF at 300 °C provides higher CO (Figure 4.30) and $H_2$ (Figure 4.32) and less $CO_2$ (Figure 4.29) compare to the raw OPF and torrefied OPF at 270 °C. This is due to the fact that the torrefied OPF at 300 °C contains the lowest amount of oxygen content (33.78 %) compare to the raw OPF and torrefied OPF at 270 °C (each 44.88 % and 40.78 % respectively) as shown in Table 4.8. The lowest amount of oxygen content will make the torrefied OPF at 300 °C provide the lowest amount of oxygen to carbon ratio (O/C) which is 0.606 compared to raw OPF and torrefied OPF at 270 °C (each 1.021 and 0.920 respectively). The hydrogen generated depends upon O/C ratios. Biomass with lower O/C will provide more hydrogen yield which also contribute to higher high heating value (HHV) (George et al., 2016). Higher HHV value indicates that the biomass have better conversion to produce more synthesis gas and thus ultimately increases the carbon conversion rate.

In addition, the endothermic reaction occurs in both gasifier which are combustion reaction with the presence of oxygen from air will increase the amount of $CO_2$ gas (Kuo et al., 2014). The amount of methane is decreasing (Figure 4.31) in both gasifier because of the steam-methane reforming occurred meanwhile the hydrogen is decreasing because of domination of oxidation in hydrogen reaction occurred since more air is provided into the gasifier. For gasifier comparison, at 0.2 of ABR with raw OPF, fluidized bed (7.67 %) provides higher amount of hydrogen gas compare to fixed bed (6.37 %) since the additional presence of steam flow in fluidized bed that boost the production of hydrogen gas.

#### 4.5.1.3 Effects of Steam to Biomass Ratio

The effects of steam to biomass ratio (SBR) on the production of synthesis gas for all feedstock in fluidized bed gasifier are shown in Figures 4.33 to 4.36. In this analysis, the gasification temperature and ABR used is 700 °C and 0.2 with the SBR ratio is varied from 0.2 to 1.

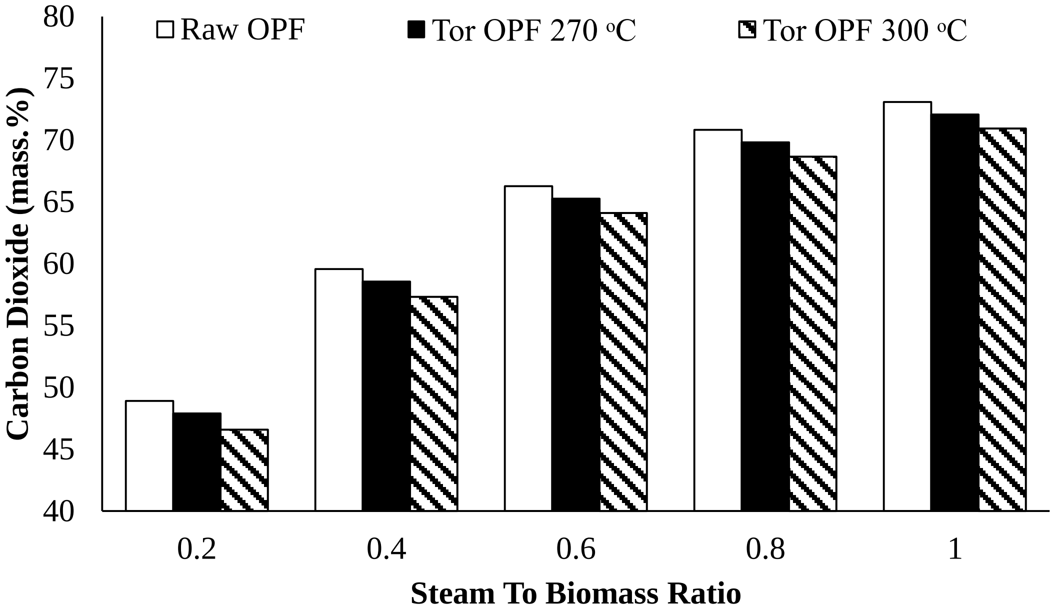

Figure 4.33 Effects of steam to biomass ratio on carbon dioxide production in fluidized bed gasifier

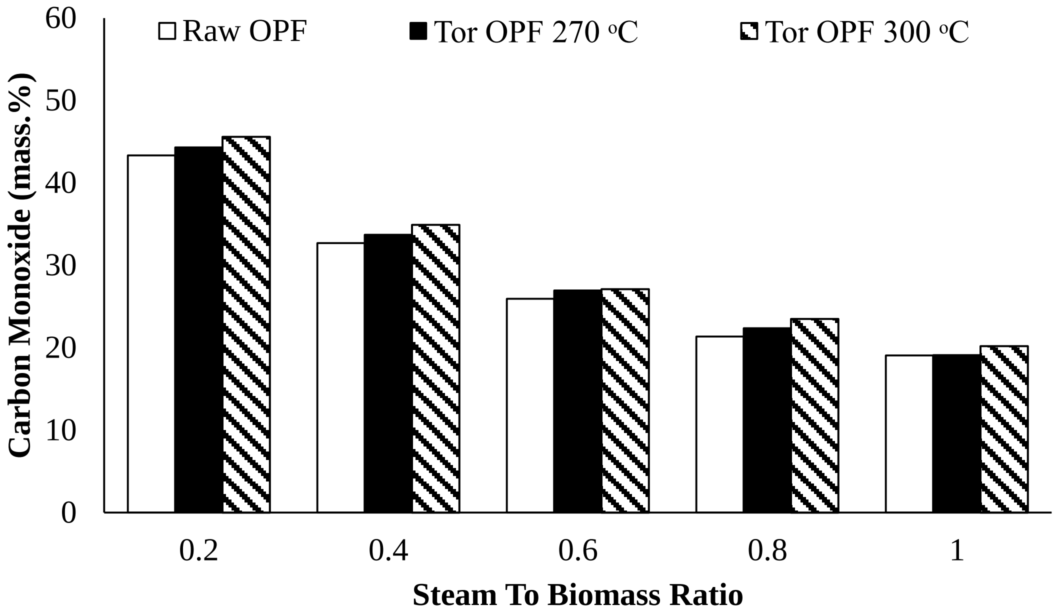

Figure 4.34 Effects of steam to biomass ratio on carbon monoxide production in fluidized bed gasifier

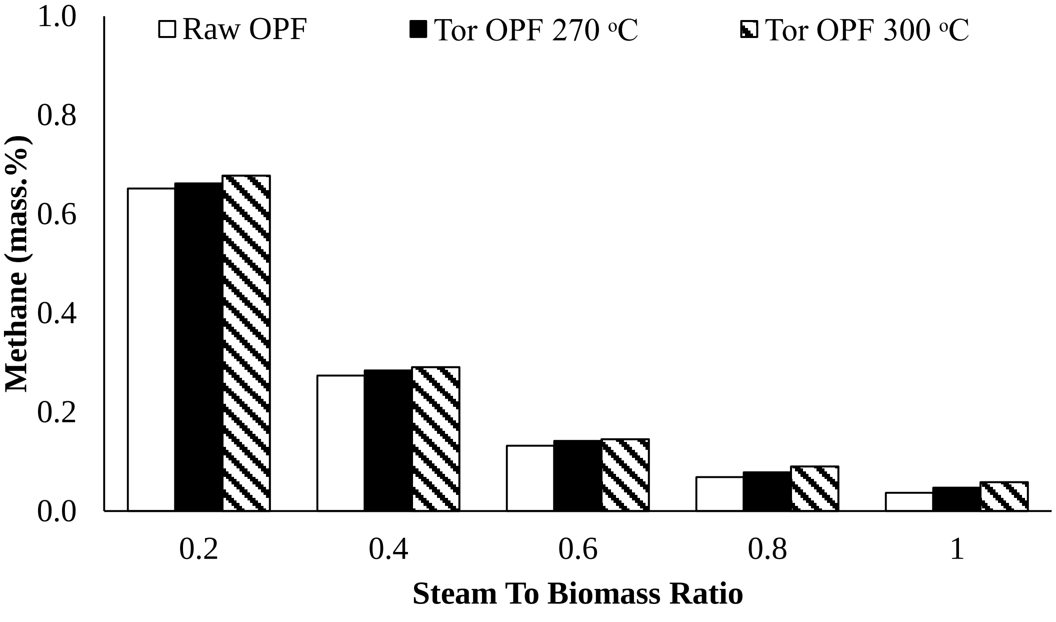

Figure 4.35 Effects of steam to biomass ratio on methane production in fluidized bed gasifier

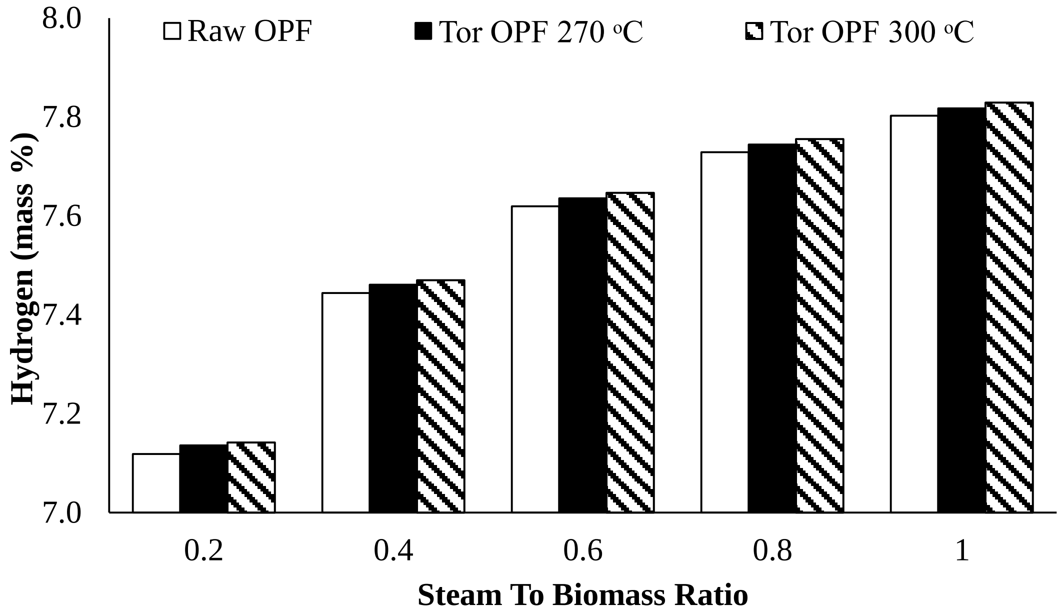

Figure 4.36 Effects of steam to biomass ratio on hydrogen production in fluidized bed gasifier

From all profiles, torrefied OPF at 300 °C provides the higher amount of hydrogen gas production compare to the other feedstock where approximately 7.83 % in hydrogen percentage which produced at SBR ratio of 1.0. In this sensitivity analysis of SBR ratio, it has been observed that the amount of $CO_2$ (Figure 4.33) and $H_2$ (Figure 4.36) are increased when the content of steam in the converting agent is increased. This is because the increasing amount of steam input providing more oxygen to undergo gasification reaction inside of the gasifier. The reactions such as water gas-shift and methane reforming reaction will basically more active with the presence more oxygen from air to produce more hydrogen and carbon dioxide gases. The conversion of CO with water will produce more $CO_2$ and $H_2$ gases. This is the main reason why the amount of $CO_2$ and $H_2$ gases amount are increased with increasing amount of SBR. This also explained the reason CO gas amount is decreasing with increasing amount of SBR. It is important to note that the torrefied OPF is more reactive which provides more synthesis gas production. Torrefied OPF at 300 °C contain high amount of carbon content (55.72 %) compare to torrefied OPF at 270 °C (48.33 %) and raw OPF (43.94 %) as shown in Table 4.8. The higher carbon content will enhance the carbon conversion rate which will produce more $H_2$ gas. In other words, more carbon will trigger steam reforming reaction (reaction 3.8) to produce more hydrogen gas. With the presence of steam, steam to carbon ratio for torrefied OPF at 300 °C will be higher which explains more synthesis gas will be produced compare to raw OPF and torrefied OPF at 270 °C. This is one of the reasons why the torrefied OPF provides more $H_2$ gas compare to raw OPF as shown in Figure 4.36.

#### 4.5.1.4 Effects of Temperature on Lower Heating Value (LHV) and Cold Gas Efficiency (CGE)

Figures 4.37 and 4.38 show the effects of gasification temperature on LHV and CGE for both bubbling fluidized bed and downdraft fixed bed gasifiers. The LHV and CGE are very important since both are representing the efficiency of fuel conversion inside the gasifier. LHV is the amount of heat value released when the biomass is combusted and gasified. Meanwhile CGE is defined as ratio of the flow of energy in the gases and energy in biomass. The higher CGE shows the higher biomass conversion inside the gasifier.

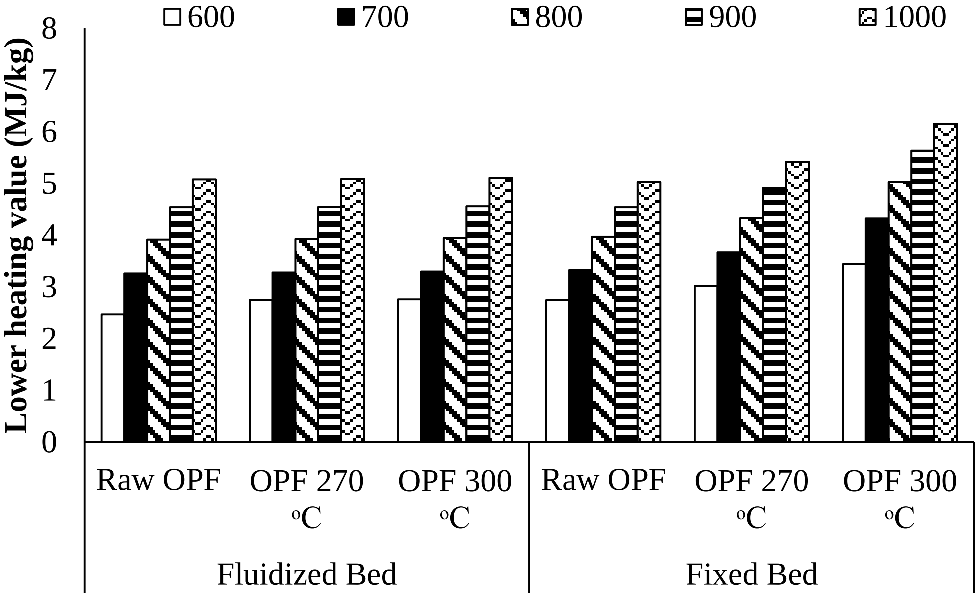

Figure 4.37 Effects of gasification temperature on lower heating value in fluidized bed and fixed bed gasifiers

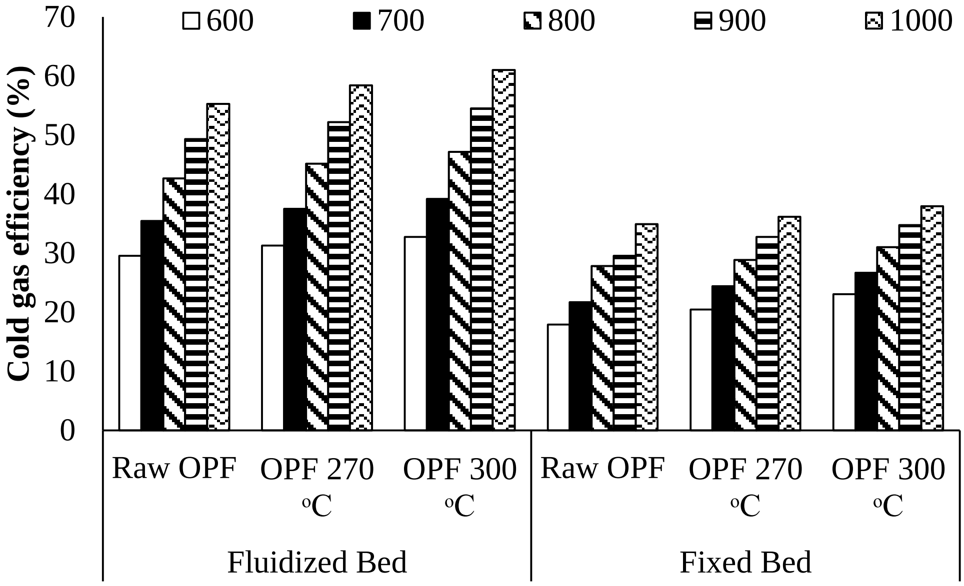

Figure 4.38 Effects of temperature on cold gas efficiency in fluidized bed and fixed bed gasifiers

Based on Figure 4.37, the increasing of gasification temperature will increase the amount of LHV for both gasifier. Here the ABR and SBR is fixed at 0.1 and 1.0. The higher LHV obtained for fluidized bed is 5.21 MJ/kg and for fixed bed is 6.16 MJ/kg when using torrefied OPF at 300 °C as input. The value of LHV changes due to the variation in the gas composition of the gas product (Inayat et al., 2016). This is because fixed bed provide higher amount of CO compared to fluidized bed (Figure 4.26) which provide more LHV value when Equation 3.22 is applied for LHV calculation. Based on Figure 4.36, the increasing temperature also shows the increasing amount of CGE (Yu et al., 2016). Based on Figure 4.37 and Figure 4.38, the torrefied OPF at 270 °C and 300 °C provides the higher LHV and CGE compare to raw OPF. One of the factors that affect the value of LHV and CGE is the total moisture content. The torrefied OPF at 270 °C and 300 °C has lower moisture content (6.78 % and 4.81 %) compare to raw OPF (15.95 %) which causes the quality of synthesis gas is increased (Dudynski et al., 2015). According to Quaak et al. (1999), a biomass often contains some moisture content which is released during heating process. This means that some of heat liberated during thermochemical reactions is absorbed by process of evaporation. For that reason heating value is influenced by its moisture content. High moisture content in a biomass will reduce not only the heating value of biomass itself but reduced the heating value of product gas. The presence of high moisture content inside raw OPF contributes to the lower LHV of the biomass compare to torrefied OPF. Moreover, the torrefied OPF at the higher gasification temperature provides more net calorific value and gas efficiency compare to raw OPF. As shown in Equation (3.23), the LHV of biomass is depending on the HHV of feedstock and its ultimate analysis. Table 4.8 shows the HHV for torrefied OPF at 270 °C and 300 °C (19.82 MJ/kg and 23.79 MJ/kg) is higher than raw OPF (17.75 MJ/kg). This contributes to the higher LHV of torrefied OPF compare to the raw OPF. Meanwhile the increase in HHV for torrefied OPF indicates better conversion of solid biomass to synthesis gas production and thus ultimately increases the carbon conversion rate. Since CGE is related to LHV of the biomass, hence, the torrefied OPF provides the higher efficiency compare to raw OPF which in the ranges of 50-60 % for fluidized bed and 30-40 % for fixed bed. For gasifier comparison, the fluidized bed provides higher amount of CGE than fixed bed gasifier. It means that the biomass have higher conversion inside of fluidized bed compare to fixed bed. It is because the effect of gas velocity and bed diameter cause the perfect mixing of the biomass which increase the biomass conversion rate which ultimately increasing the CGE (Jia et al., 2017). Besides, the presence of air and steam flow inside of fluidized bed also contributing to the higher efficiency for hydrogen gas production compare to fixed bed gasifier.

#### 4.5.1.5 Effects of Air to Biomass Ratio on Lower Heating Value (LHV) and Cold Gas Efficiency (CGE)

The influences of the air to biomass ratio on lower heating value and cold gas efficiency of raw and torrefied OPF at 270 °C and 300 °C are shown in Figures 4.39 and 4.40. The gasifier temperature and SBR is fixed at 700 °C and 1.0. Based on Figure 4.39, the increasing of air to biomass ratio will decrease the amount of LHV. This can be explained by the fact that as the ABR value increases, exothermic carbon combustion reactions, ($C + O_2 \rightarrow CO_2$) and ($C + 0.5O_2 \rightarrow CO$) are favoured, which will provides more heat to the decomposition and gasification sections. However, the heating value of synthesis gas will become lower due to further oxidation reaction ($C + O_2 \rightarrow CO_2$), which leads to more $CO_2$ gas production but less combustible gases. As a result, it is very important to choose a proper ABR at a certain gasifier temperature to get higher heat conversion efficiency.

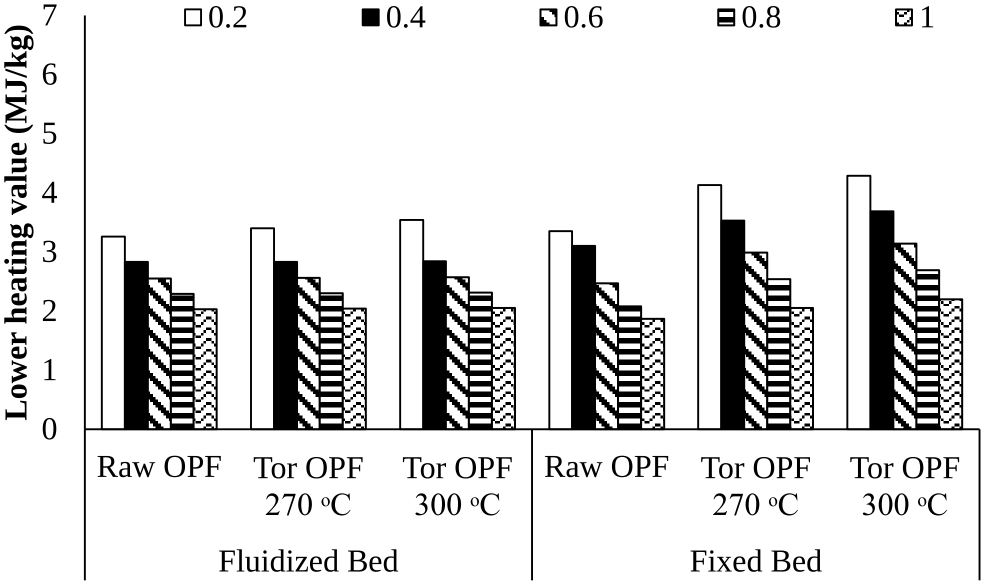

Figure 4.39 Effects of air to biomass ratio on lower heating value in fluidized bed and fixed bed gasifiers

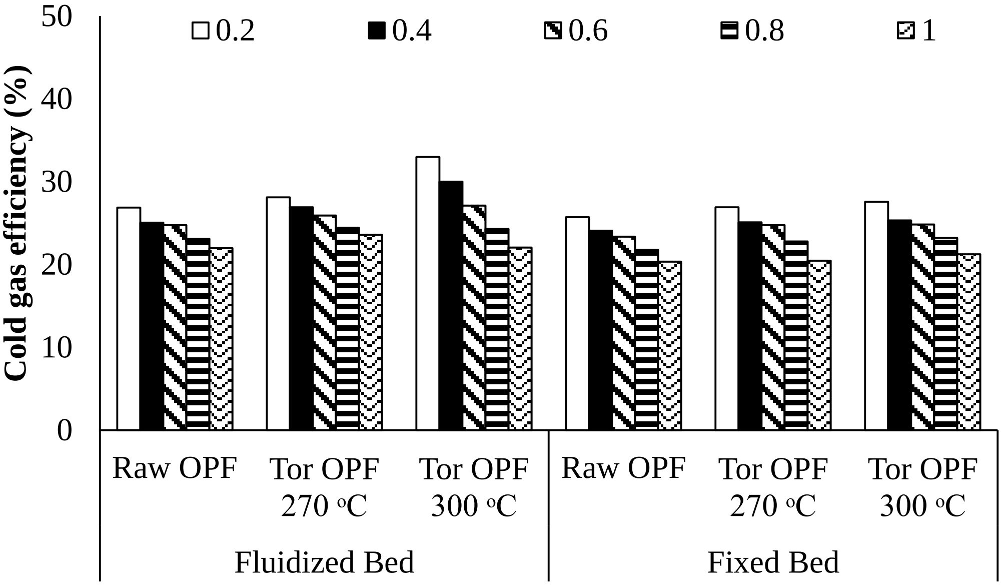

Figure 4.40 Effects of air to biomass ratio on cold gas efficiency in fluidized bed and fixed bed gasifiers

The consumption of combustion gas also cause the higher ABR occurred which result in lower gasification temperatures or deterioration of heating values of synthesis gas

(Yang et al., 2006). Meanwhile, at low ABR, the torrefied OPF at 300 °C provides higher LHV value (3.54 MJ/kg for fluidized bed and 4.29 MJ/kg for fixed bed) compared to raw and torrefied OPF at 270 °C. It mainly caused by the torrefied OPF at 300 °C have the lowest oxygen to carbon ratio compared to raw and torrefied OPF at 270 °C which more hydrogen will be produced since the torrefied OPF at 300 °C provide the highest amount of carbon content and the lowest amount of oxygen content compared to another biomass. Since the value of CGE is related to LHV value, hence, the amount of CGE is decreasing with increment of ABR since the LHV decreasing with increment of ABR. The highest CGE for fluidized bed is 32.98 % and 27.57 % for fixed bed which gain at ABR of 0.2. Hence, in order to achieve the highest amount of LHV and CGE, it is recommended to operate the gasification with lower amount of ABR for both gasifier.

#### 4.5.1.6 Effects of Steam to Biomass Ratio on Lower Heating Value (LHV) and Cold Gas Efficiency (CGE)

Figures 4.41 to 4.42 show the changes of synthesis gas composition based on variation in steam to biomass ratio (mass basis) for all OPF in fluidized bed gasifier. The temperature for the gasifier is 700 °C and the ABR is 0.1. All of the biomass feedstock which are raw OPF, torrefied OPF at 270 °C and 300 °C shows similar decreasing trends of LHV (Figure 4.41) and CGE (Figure 4.42) when the SBR is increased. When the SBR is increased, the steam injection could adjust the $H_2$/CO ratio of synthesis gas by the combination of the water-gas reaction (Equation 3.8) and water gas shift reaction (Equation 3.10) (Niu et al., 2013). By increasing the amount of steam, the water gas shift reaction will be shifted into the right which explains the increasing of $H_2$ and $CO_2$ concentrations and decrease the amounts of CO concentration. The increasing in $H_2$ gas is outweighed by the drop in CO and $CH_4$ gases. In addition, when the SBR ratio is increased, this indicates the increase of steam flow rate to the gasification system. Here the steam is mixing with the biomass and this contributes to the increase of the total $H_2O$ inside the gasification process. As consequence, when Equation 3.23 is used, the amount of LHV will be reduced as shown in Figure 4.41 due to the rise of moisture content amount. Ultimately, the CGE of gasification process will be reduced when Equation 3.24 is used as shown in Figure 4.42 since the CGE calculation is relying on the amount of LHV value. Hence, the operation at higher SBR is not advisable considering the detrimental effect on LHV (Doherty, 2014). For SBR analysis, the highest LHV are 6.63 MJ/kg and CGE are 63.40 %.

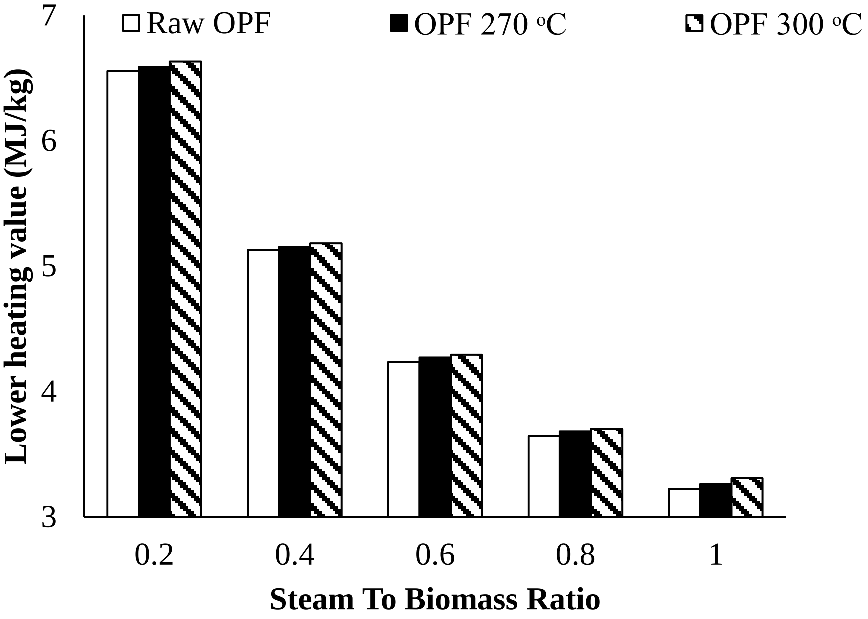

Figure 4.41 Effects of steam to biomass ratio on lower heating value in fluidized bed gasifier

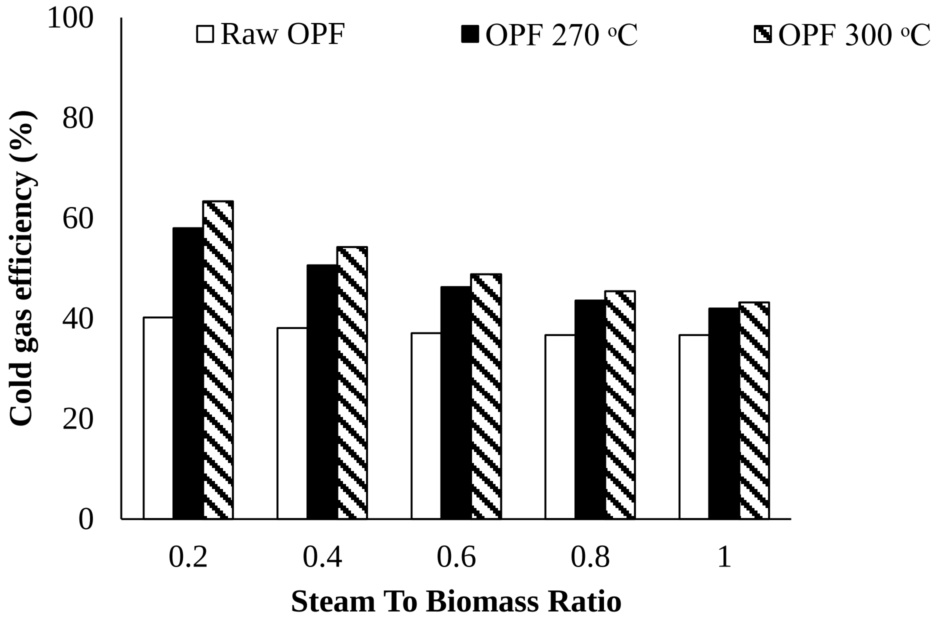

Figure 4.42 Effect of steam to biomass ratio on cold gas efficiency in fluidized bed gasifier

## 4.6 Case Study 5: Integration of Biomass Gasification Model and PEMFC for Power Production

The application of this model-based workflow is highlighted through the integrated biomass gasification and PEMFC for power production.

### 4.6.1 Problem Definition (Step 1)

The objective is to integrate biomass gasification model with PEMFC model for producing the desired power.

### 4.6.2 Process and Product Specifications (Step 2)

For process specification, the selected reactors are fluidized bed and fixed bed gasifiers with purification using CO-PROX reactor as additional reactors. This CO-PROX is added in order to purify the hydrogen gas which serves as an input for PEMFC. The same inputs used in case study 4 are employed. For PEMFC, the input material is the pure hydrogen that comes from CO-PROX reactor. The targeted products in this case are the hydrogen gas and power (kW).

### 4.6.3 Gasification Modelling (Step 3 (a))

For this step, the validated model from case studies 1 and 2 are used again for synthesis gas production purpose. However, in this case, water gas shift reactor and CO-PROX reactor are added for both gasifier models as shown in Figures 4.43 and 4.44. In hydrogen purification stage, the synthesis gas will go to the HTS (high-temperature water gas shift reactor) and LTS (low temperature water gas shift reactor). In the HTS and LTS reactors, the water gas shift reaction between CO and steam occurs as shown in Equation 3.22. The HTS is operated at temperature of 300 °C and the LTS is operated at temperature of 200 °C. Both of these reactors (HTS, LTS) are using RSTOIC since the reaction and CO conversion are known. After HTS, the exit CO concentration is expected to be in the range of 2 % to 4 % and 1 % for LTS. The CO-selective oxidation reaction (Equation 3.24) takes place in the preferential oxidation reactor, represented by the unit PROX. This reactor is operated at temperature of 150 °C. At this stage, the remaining CO in the $H_2$ feed is reduced to an acceptable level for PEMFC applications (lesser than 10 ppm).

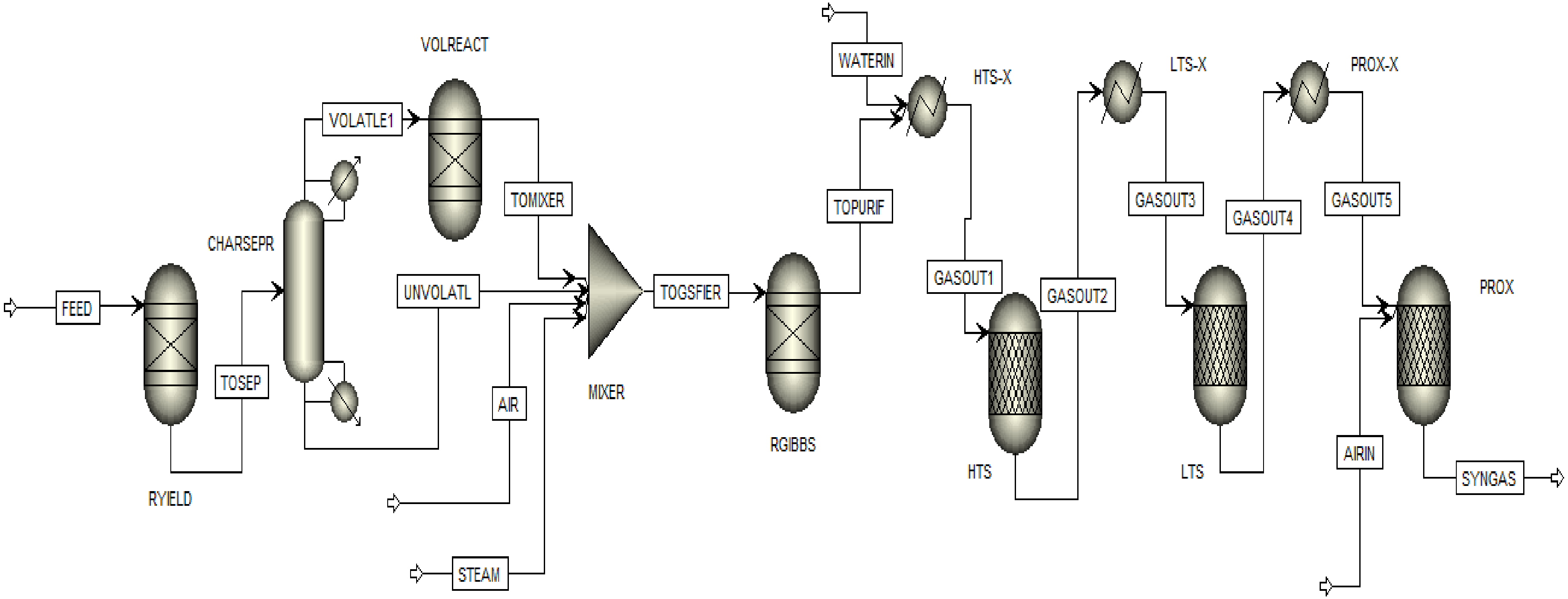

Figure 4.43 Flowsheet of fluidized bed gasification with CO-PROX

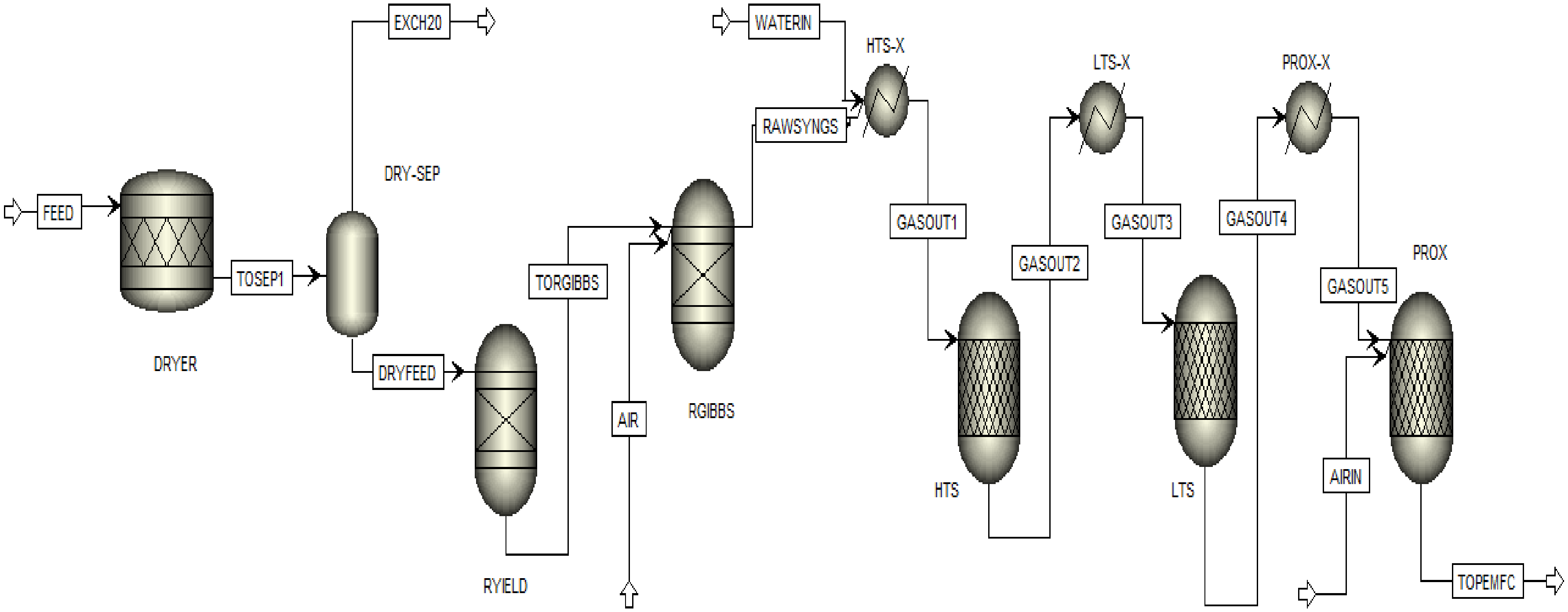

Figure 4.44 Flowsheet of fixed bed gasification with CO-PROX

### 4.6.4 PEMFC Modeling (Step 3(b))

After Step 3(a), Step 3(b) PEMFC modelling will be applied since the objective is to produce the desired power after gasification. In this step, the mathematical model as shown in Equations (3.17) to (3.21) was applied in order to calculate the activation loss at the anode ($\eta$a), the activation loss at the cathode($\eta$c), and ohmic loss ($\eta$ohmic). In this work the experimental data from Yan et al. (2006) is employed for model validation. The operating conditions used are as follows: the operating temperature is at 80 °C, the pressure is 4 atm, the air and hydrogen ($H_2$) stoichiometry is 2 and 1.2 respectively and both the anode and cathode humidity is at 100 %. Meanwhile the number of cell used is 25 (Yan et al., 2006).

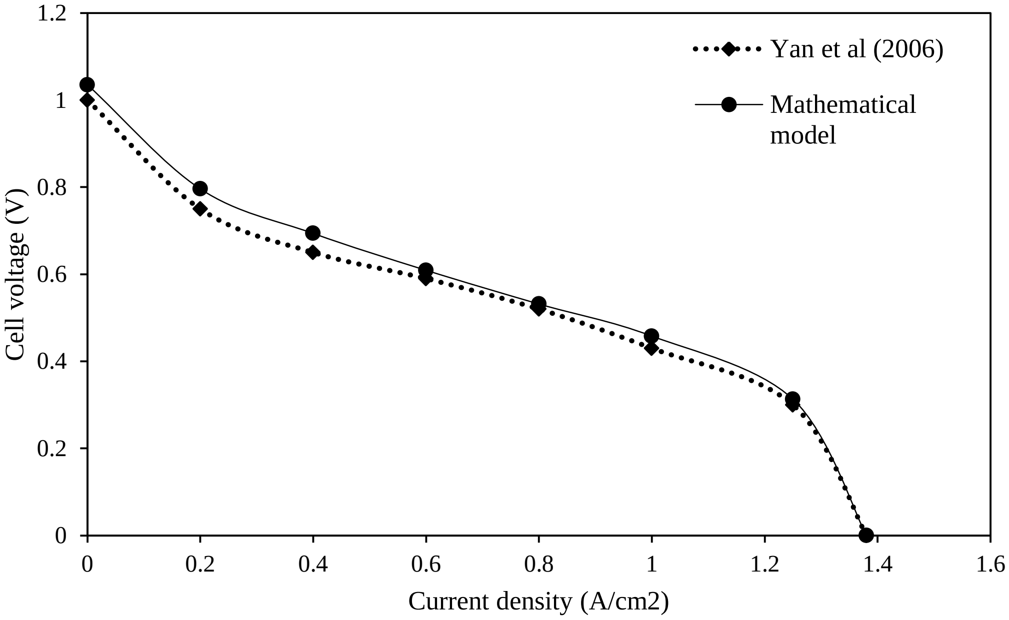

Figure 4.45 Comparison of cell potential between mathematical model and predicted data

The PEMFC model is calculated by using mathematical model as shown in Equations (3.17) to (3.21) and input from Table 3.2. The result obtained is shown in Figure 4.45. Based on Figure 4.45, the maximum cell voltage that the PEMFC can achieve is 1.02 V when there is no current flow present. However, as the cell current becomes high in the fuel cell, the electrochemical reaction rate on the electrodes surface is higher. This contributes to the slower mass transfer rate of the electrons and ions which cause the kinetic reaction on the surfaces of electrodes is slow. As consequence the activation loss is dropped on the surface of the electrodes in cell voltage (Hao et al., 2016). Based on Figure 4.45, the polarization curve obtained using PEMFC model have a good agreement with the experimental data and have a low RMSE around 0.00024 which is below 0.3 (Veerasamy et al., 2011). Thus it is concluded the developed PEMFC model is validated and can be used for power production purpose. The next step is Step 3(c) for integrating biomass gasification and PEMFC.

### 4.6.5 Integrated Biomass Gasification and PEMFC modeling (Step 3(c))

For integrated biomass gasification and PEMFC, both validated gasification and PEMFC model from Step 3 (a) and Step 3(b) will be simulated together simultaneously. Here the gasification model will be simulated in Aspen Plus software and the output of the simulation will be used back as an input in PEMFC modelling. Since the amount of carbon monoxide is corrosive to PEMFC layer and the amount is needed to reduce to 10 ppm then the integrated biomass system and PEMFC will undergo hydrogen purification and CO removal to reduce the CO amount. The synthesis gas from gasification will go through purification step and then will enter as input of the PEMFC.

### 4.6.6 Sensitivity Analysis (Step 4)

After the model from Step 3 have been developed, the next step is Step 4 which involving the sensitivity analysis. Here, the analysis will be focusing on two parameter which are: 1) the optimum output syngas produced from the gasifier and PROX using raw and torrefied biomass in bubbling fluidized bed and downdraft fixed bed gasifier, 2) the power production that produced from the PEMFC.

#### 4.6.6.1 Percentage of output syngas of gasifier and PROX

Table 4.9 shows the amount of product gas composition in terms of percentages at the outlets of the gasifier and a preferential oxidation reactor (PROX) is included in the fixed bed and fluidized bed gasifiers. The product gases from all biomass gasifier contains high percentage of CO which are range from 19.07 % to 19.18 % from the fluidized bed gasifier and 21.91% to 33.89 % for fixed bed using all biomasses which exceeding the allowable limit of 1 % for PEMFC application. According to Moretti et al. (2007), the PEMFC performance degrades when CO is present in the synthesis gas and thus contributing to the CO poisoning. The CO has a strong tendency to be adsorbed onto catalyst surface on the PEMFC and blocking the active catalyst sites which are required for hydrogen oxidation reaction. Since this problem happened, the product gas should undergo catalytic preferential oxidation of CO (CO-PROX) flow through high temperature shift reactor (HTS) and lower temperature shift reactor (LTS) and lastly preferential oxidation reactor (PROX) (Grashoff et al., 1983). As shown in Table 4.9, the amounts $CO_2$ and $H_2$ gases are then increased while the amount of CO is decreased when all of these gases went through HTS and LTS for all biomasses. The torrefied OPF at 300 °C provides the highest amount of CO and $H_2$ gases for output synthesis gas from the gasifier compare to other biomasses since the presence of carbon element inside torrefied OPF at 300 °C is the highest compare to others. As shown in Figure 4.43 and 4.44, the output synthesis gas for both reactors will go to the HTS and LTS reactor. Here, the conversion of the CO achieved approximately 96 % to 98 %. This is due to the water gas shift reaction (Equation 3.10) occurs in both reactors (Lima et al., 2012). The synthesis gas is then fed to the PROX reactor where the $O_2$ and CO gases underwent partial oxidation which produces $CO_2$ as shown in Equation 3.23. Here the CO concentration is reduced to be lesser than 10 ppm and the total hydrogen amount is increased for both reactors. In terms of hydrogen flow, the simulation result shows the increasing amount of pure hydrogen produced from the catalytic purification. As shown in Table 4.9, for fluidized bed gasification, the hydrogen gas is increased from 7.85 % to 8.22 % for the torrefied OPF at 300 °C, 7.82 % to 8.19 % for torrefied OPF at 270 °C and 7.81 % to 8.17 % for raw OPF. Meanwhile for fixed bed reactor, the hydrogen gas is increased from 5.65 % to 6.52 % for the torrefied OPF at 300 °C, 5.33 % to 5.81 % for torrefied OPF at 270 °C and 5.12 % to 5.59 % for raw OPF. The torrefied OPF at 300 °C provides the highest purify hydrogen compare to other biomass which is 8.22 % for fluidized bed and 6.52 % for fixed bed reactor. All hydrogen gas is increased in terms of percentage after undergoes purification. Fluidized bed shows the highest production because it uses steam ($H_2O$) as a gasifying agent which not only adds more hydrogen source into the gasifier but also shifts the reaction between carbon and steam to produce more $H_2$ gas. Besides, the amount of CO gas for both gasifier is also reduced to be lesser than 1 % after the purification as shown in Table 4.9. This indicates that, the output synthesis gas can be used for PEMFC since the amount of CO is complying with the requirement of PEMFC membrane. Moreover, it can be concluded that the fluidized bed is the most effective gasifier compare to fixed bed gasifier for gasification process since its produce more hydrogen gas even after PROX reactor has been implemented to both reactors during the gasification-purification process. All this purify hydrogen will used back for determination of power production in PEMFC.

Table 4.9 Percentages of output synthesis gas of gasifier and PROX

| **Reactor** | **Syngas** | **Percentage of output synthesis gas (%)** | | | | | |
|---|---|---|---|---|---|---|---|
| | | Gasifier | | | PROX | | |
| | | Raw OPF | Tor OPF 270 °C | Tor OPF 300 °C | Raw OPF | Tor OPF 270 °C | Tor OPF 300 °C |
| Fixed Bed | $CO_2$ | 72.92 | 70.28 | 65.03 | 95.32 | 94.01 | 93.37 |
| | CO | 21.91 | 24.32 | 33.89 | 0.00 | 0.00 | 0.00 |
| | $CH_4$ | 0.05 | 0.07 | 0.19 | 0.02 | 0.03 | 0.11 |
| | $H_2$ | 5.12 | 5.33 | 5.65 | 5.59 | 5.81 | 6.52 |
| Fluidized Bed | $CO_2$ | 73.08 | 73.07 | 72.87 | 91.79 | 91.77 | 91.74 |
| | CO | 19.07 | 19.11 | 19.18 | 0.00 | 0.00 | 0.00 |
| | $CH_4$ | 0.05 | 0.08 | 0.10 | 0.04 | 0.04 | 0.04 |
| | $H_2$ | 7.81 | 7.82 | 7.85 | 8.17 | 8.19 | 8.22 |

#### 4.6.6.2 Performance of the PEMFC integrated system

All pure hydrogen from purification process is used as input for PEMFC. Here, the total power produced is calculated by using Equation 3.24. Meanwhile, the efficiency of the PEMFC will be determined by calculating the electrical efficiency (Equation 3.25), thermal efficiency (Equation 3.26), overall efficiency (Equation 3.27) and stack efficiency (Equation 3.28). Table 4.10 shows all the performance of the integrated gasification with PEMFC model in terms of power produced. This system involves the recovery of waste thermal energy back into the system as a useful thermal power. The performance of this integrated system is defined by its ability to convert the chemical energy contained in biomass into electrical and thermal power. Both the electrical efficiency and the thermal efficiency are directly related to the amount of $H_2$ gas flowing into fuel cell stack. The increasing amount of hydrogen gas produced will cause the decreasing amount of thermal efficiency. It mainly because of less biomass is fed into afterburner to generate heat and power (Muslim et al., 2015). In the other words, when more hydrogen gas is required, more biomass will be converted into power. In terms of power, the torrefied OPF at 300 °C provides the higher power which is 5.74 kW and 6.65 kW for fixed bed and fluidized bed gasifiers respectively. The amount of power produced is relevant since the maximum power capacity that produced by palm oil waste in laboratory scale is 6.674 kW (Mahlia et al., 2001).

The amount of pure hydrogen gas used as input is the main player for producing the desired power. The increasing amount of hydrogen gas used will contributes to the higher amount of power (kW) obtained. The torrefied OPF at 300 °C provides the higher electrical efficiency around 48.27 % and 55.88 % for fixed bed and fluidized bed gasifiers respectively. It shows that torrefied OPF at 300 °C have the higher ability to convert energy in biomass into electrical power. The increasing of electrical efficiency will increase the amount of power produced because a greater amount of energy in biomass is converted into electricity to meet the power demand (Chutichai et al., 2013). In other words, the thermal efficiency is affected by a change in power production which the amount will be decreased because less biomass is combusted. In addition, although increasing power production may imply that more unreacted $H_2$ flows into afterburner and then be oxidized, the thermal energy released owing to the anode off gas combustion is still low and does not have a strong effect on thermal efficiency. The increasing of electrical efficiency will affect the overall efficiency since the total efficiency is depending on the total amount electrical and thermal efficiency (Equation 3.28). According to Gimba et al. (2015), the maximum fuel cell efficiencies typically in the range from 60 to 80 % and all the overall efficiency from the result are within the range. For stack efficiency, with increasing the amount of hydrogen gas, more current density will be used to produce more power, which will increase the stack efficiency of the PEMFC (Pourmovahed, 2005). In general, the torrefied OPF at 300 °C provides the higher power production (kW), overall efficiency and stack efficiency compare to torrefied OPF 270 °C, and raw OPF.

Table 4.10 Performance of the integrated gasification with PEMFC model

| **Reactor** | **Biomass** | **Hydrogen percentage** | **I (A/CM2)** | **$E_{Cell}$ (V)** | **Power (kW)** | **Electrical (%)** | **Thermal (%)** | **Overall (%)** | **Stack efficiency (%)** |
|---|---|---|---|---|---|---|---|---|---|
| Fixed bed | Raw OPF | 5.59 | 0.42 | 0.68 | 5.15 | 43.32 | 23.05 | 66.37 | 26.26 |
| | Tor OPF 270 °C | 5.81 | 0.44 | 0.67 | 5.30 | 44.53 | 22.60 | 67.13 | 26.68 |
| | Tor OPF 300 °C | 6.52 | 0.49 | 0.65 | 5.74 | 48.27 | 21.20 | 69.47 | 27.74 |
| Fluidized bed | Raw OPF | 8.17 | 0.61 | 0.62 | 6.63 | 55.71 | 18.42 | 74.13 | 34.88 |
| | Tor OPF 270 °C | 8.19 | 0.62 | 0.61 | 6.63 | 55.76 | 18.40 | 74.16 | 34.84 |
| | Tor OPF 300 °C | 8.22 | 0.63 | 0.60 | 6.65 | 55.88 | 18.35 | 74.24 | 34.98 |

## 4.7 Concluding Remark

In this chapter, the applications of the systematic integration biomass gasification and PEMFC have been highlighted through different case studies. Firstly, it involves model development of downdraft fixed bed and bubbling fluidized bed gasifiers. These two models have been developed in Aspen Plus and then validated againts published literature. The validated models then have been tested using different types of palm oil wastes as the input such as oil palm fronds (OPF), empty fruit bunch (EFB), palm kernel shell (PKS) and palm mesocarp fibre (PMF). Based on the simulation results analysis, the raw OPF produces the highest amount of hydrogen produced of 7.81 % for fluidized bed and 5.12 % for fixed bed gasifier compare to raw PKS, PMF and EFB. Since the raw OPF provides the highest hydrogen production, it has been selected for torrefaction effects case study. The torrefied OPF at two different torrefaction temperatures which are at 270 °C and 300 °C were used as feed for gasification and integrated gasification with PEMFC. For sensitivity analysis, it was found that the gasifier should be operated at high temperature and low ABR. In this case, the torrefied OPF at 300 °C produces around 7.85 % (fluidized bed) and 5.65 % (fixed bed) of hydrogen gas at gasification temperature of 700 °C and ABR at 0.2. Using the same operating condition with SBR set at 1 for fluidized bed gasifier, the the torrefied OPF at 300 °C produces around 7.83 % of hydrogen gas. The analysis of LHV and CGE is also conducted. For gasification temperature, the highest LHV obtained are 5.21 MJ/kg (fluidized bed) and 6.16 MJ/kg (fixed bed) and CGE are 61.01 % (fluidized) and 37.98 % (fixed). Meanwhile for ABR, the highest LHV obtained are 3.54 MJ/kg (fluidized bed) and 4.29 MJ/kg (fixed bed) and CGE are 32.98 % (fluidized) and 27.57 % (fixed). For SBR, the highest LHV are 6.63 MJ/kg and CGE are 63.40 %. The effects of purification is also included in this work where the hydrogen gas produced by torrefied OPF at 300 °C shows an increment up to 8.22 % for fluidized bed and 6.52 % for fixed bed reactor and at the same time the amount of CO is decreased until lesser than 10 ppm. Overall, the torrefied OPF at 300 °C provides the highest amount of power production (kW), overall efficiency and stack efficiency. In the case of fluidized bed gasifier, the torrefied OPF at 300 °C produces 6.65 kW for power, 55.88 % for electrical efficiency 74.24% for overall efficiency and 34.98 % for stack efficiency. Meanwhile for fixed bed gasifier, the power produced is 5.74 kW, 48.27 % for electrical efficiency 69.47% for overall efficiency and 27.74 % for stack efficiency.

# CHAPTER 5

# CONCLUSIONS

## 5.1 Conclusions

In this work, the systematic integrated biomass gasification and PEMFC model-based workflow have been successfully developed which can be used to generate the gasification model as a stand-alone model and/or to integrate biomass gasification with PEMFC for power production. Four main steps have been introduced in the workflow which consists of problem definition, process and product specification, gasification model and PEMFC model, and sensitivity analysis. The biomass database has been developed for collecting the necessary data for biomass in terms of proximate and ultimate analysis. From this workflow, the study related to gasification and PEMFC modelling, synthesis gas composition, effects of torrefaction as pre-treatment, hydrogen purification and power production can be achieved by using this workflow. In this work, the workflow has been applied for developing bubbling fluidized bed and downdraft fixed bed gasifiers in order to study the gasification process. Both models have been validated with previous experimental literature data and can be used for gasification purpose.

Both of validated models have been used to study performance of biomass gasification using different types of palm oil wastes namely OPF, PKS, EFB and PMF. Here, raw OPF produces the highest amount hydrogen production which is 7.81 % for fluidized bed and 5.12 % for fixed bed gasifier compare to raw PMF, raw PKS and raw EFB. The increasing of gasification temperature and steam to biomass ratio (SBR) also contributes the increment of hydrogen production meanwhile the increasing of air to biomass ratio (ABR) shows the opposite trends. The fluidized bed gasifier provides more hydrogen production compare to fixed bed gasifier indicating that fluidized bed have higher efficiency to produce hydrogen compare to fixed bed. The effects of torrefaction as a pre-treatment method on the biomass have been investigated. Two types of OPF have been selected which consists of torrefied OPF at 270 °C and torrefied OPF at 300 °C. Here, the torrefied OPF at 300 °C shows an improvement in terms of amount of hydrogen generated compare to raw OPF and torrefied OPF at 270 °C. Based on sensitivity analysis, torrefied OPF at 300 °C as an input for gasification process, the simulation results show the fluidized bed obtain 7.85 % and fixed bed achieve 5.65 % of hydrogen gas at gasification temperature of 700 °C and ABR at 0.2. For SBR in the fluidized bed gasifier, the best condition for gasification operation is at SBR ratio of 1 for producing the highest amount of hydrogen gas around 7.82 %. For lower heating value (LHV) and cold gas efficiency (CGE), the increasing gasification temperature and SBR is the main factors for the increment amounts of LHV and CGE. The torrefied OPF at 300 °C shows an improvement in LHV and CGE in terms of increasing temperature and SBR compare to raw OPF and torrefied OPF at 270 °C. For gasification temperature, the highest LHV are 5.21 MJ/kg (fluidized bed) and 6.16 MJ/kg (fixed bed) and CGE are 61.01 % (fluidized bed) and 37.98 % (fixed bed) respectively. Meanwhile for ABR, the highest LHV obtained are 3.54 MJ/kg (fluidized bed) and 4.29 MJ/kg (fixed bed) and CGE are 32.98 % (fluidized) and 27.57 % (fixed). For SBR, the highest LHV are 6.63 MJ/kg and CGE are 63.40 %. All these values are obtained when using torrefied OPF at 300 °C as the input and these values obtained are higher compare to the values obtained when using raw OPF and torrefied OPF at 270 °C.

For integrated biomass gasification and PEMFC, the synthesis gas underwent the purification of hydrogen stages. Based on the purification stages, there are improvements in terms of hydrogen gas amount in the outlet of the PROX reactor. At the same time, the amount of carbon monoxide gas is successfully decreased to be lesser than 1 % which is met the allowable limit for PEMFC. For PEMFC, the torrefied OPF at 300 °C provides more power production, higher electrical and overall efficiency and higher stack efficiency compare to raw OPF and torrefied OPF at 270 °C. For fluidized bed, the torrefied OPF at 300 °C produces 6.65 kW for power, 55.88 % for electrical efficiency 74.24 % for overall efficiency and 34.98 % for stack efficiency. Meanwhile for fixed bed using torrefied OPF at 300 °C, the power produced is 5.74 kW, 48.27 % for electrical efficiency 69.47 % for overall efficiency and 27.74 % for stack efficiency. It shows that fluidized bed gasifier is more prominent and efficiency for power production compare to fixed bed gasifier. In overall, the integrated gasification and PEMFC is able to be used as tools for power production and efficiency indicator and torrefaction as pre-treatment method is a useful for upgrading the hydrogen and power production. In conlusion, the entire objective that has been targeted already successfully achieved in the end of this research.

## 5.2 Recommendations

There are several recommendations that can be used for future work:

a) **Entrained flow reactor:** This research is focusing on the fluidized and fixed bed reactor. There is one more reactor that can be utilized in the future work which is the entrained flow reactor. The comparison in performance between entrained flow reactor with fluidized bed and fixed bed can be performed in the future.

**b)** **Co-gasification:** The co-gasification can be come as additional scopes for future works. Since this work is only focusing on utilizing palm oil wastes as an input for gasification process, the coal can be introduced as additional input or blending with palm oil wastes for gasification in order to achieve the desired hydrogen gas.

c) **Municipal solid waste:** This research is just focusing on oil palm waste biomass waste. Hence, another waste material such as municipal solid waste can be recommended as one of the additional scopes in the future work in order to study the feasibility of the integrated biomass gasification and PEMFC system.

# REFERENCES

Adams, D. (2013). *Sustainability of biomass for co-firing*.

Aghamohammadi, N., Reginald, S. S., Shamiri, A., Zinatizadeh, A. A., Wong, L. P., and Sulaiman, N. M. B. N. (2016). An investigation of sustainable power generation from oil palm biomass: A case study in Sarawak. *Sustainability (Switzerland)*, 8(5), 1–19.

Aly, M. R. (2013). Pelagia Research Library. *Der Chemica Sinica*, 4(4), 68–72.

Apergis, N., and Danuletiu, D. C. (2014). Renewable energy and economic growth: Evidence from the sign of panel long-run causality. *International Journal of Energy Economics and Policy*, 4(4), 578–587.

Arena, U. (2012). Process and technological aspects of municipal solid waste gasification. A review. *Waste Management*, 32(4), 625–639.

Arnavat, M. P. (2011). *Performance modelling and validation of biomass gasifiers for trigeneration plants*. Universitat Rovira I Virgili.

Asafu-Adjaye, J., Byrne, D., and Alvarez, M. (2016). Economic growth, fossil fuel and non-fossil consumption: A pooled mean group analysis using proxies for capital. *Energy Economics*, 60, 345–356.

Aspen Technology, I. (2004). *Getting Started Modeling Processes with Solids*. USA.

Aspen Technology Inc. (2010). Thermodynamic property models. In *Aspen Physical Property System - Physical Property Models* (pp. 12–184). USA.

Balan, C., Dey, D., Eker, S.-A., and Peter, M. (2004). Coal integrated gasification fuel cell system study final report. *Power*.

Barelli, L., Bidini, G., Gallorini, F., and Servili, S. (2008). Hydrogen production through sorption-enhanced steam methane reforming and membrane technology: A review. *Energy*, 33(4), 554–570.

Bartels, M., Lin, W., Nijenhuis, J., Kapteijn, F., and van Ommen, J. R. (2008). Agglomeration in fluidized beds at high temperatures: Mechanisms, detection and prevention. *Progress in Energy and Combustion Science*, 34(5), 633–666.

Basu, P. (2013). *Combustion and gasification in fluidized beds* (Vol. 53). Taylor & Francis Group.

Basualdo, M. S., Feroldi, D., and Outbib, R. (2012). PEM fuel cells with bio-ethanol processor systems: a multidisciplinary study of modelling, simulation, fault diagnosis and advanced control. *Green Energy and Technology*, 87.

Batidzirai, B., Mignot, A. P. R., Schakel, W. B., Junginger, H. M., and Faaij, A. P. C. (2013). Biomass torrefaction technology: Techno-economic status and future prospects. *Energy*, 62, 196–214.

Begum, S., Rasul, M. G., Akbar, D., and Ramzan, N. (2013). Performance analysis of an integrated fixed bed gasifier model for different biomass feedstocks. *Energies*, 6(12), 6508–6524.

Bhatia, K. K., and Wang, C. Y. (2004). Transient carbon monoxide poisoning of a polymer electrolyte fuel cell operating on diluted hydrogen feed. *Electrochimica Acta*, 49(14), 2333–2341.

Chen, W. H., Chen, C. J., Hung, C. I., Shen, C. H., and Hsu, H. W. (2013). A comparison of gasification phenomena among raw biomass, torrefied biomass and coal in an entrained-flow reactor. *Applied Energy*, 112, 421–430.

Chui, E. H., Majeski, A. J., Lu, D. Y., Hughes, R., Gao, H., McCalden, D. J., and Anthony, E. J. (2009). Simulation of entrained flow coal gasification. *Energy Procedia*, 1(1), 503–509.

Chutichai, B., and Arpornwichanop, A. (2015). Performance improvement of biomass gasification and PEMFC integrated system-design consideration for achieving high overall energy efficiency and power-to-heat ratio variation. *Chemical Engineering Transactions*, 43, 1501–1506.

Chutichai, B., Authayanun, S., Assabumrungrat, S., and Arpornwichanop, A. (2013). Performance analysis of an integrated biomass gasification and PEMFC (proton exchange membrane fuel cell) system: Hydrogen and power generation. *Energy*, 55, 98–106.

Demirbas, A. (2004). Combustion characteristics of different biomass fuels. *Progress in Energy and Combustion Science*, 30(2), 219–230.

Doherty, W. (2014). *Modelling of Biomass Gasification Integrated with a Solid Oxide Fuel Cell System*.

Dudynski, M., Van Dyk, J. C., Kwiatkowski, K., and Sosnowska, M. (2015). Biomass gasification: Influence of torrefaction on syngas production and tar formation. *Fuel Processing Technology*, 131, 203–212.

Eden, M. R. (2012). *Introduction to ASPEN PLUS Simulation*.

Eysenbach, G. (2008). Module 4: Fuel Cell Engine Technology. *Journal of Medical Internet Research*, 10(3), 22.

Faaij, A. P. (2004). Biomass combustion. *Encyclopedia of Energy*, I: 175–191.

Fantini, M. (2010). *Biorefineries. Green Energy and Technology* (Vol. 36).

Fatoni, R., Gajjar, S., Gupta, S., Handa, S., and Elkamel, A. (2014). Modeling biomass gasification in a fluidized bed reactor. In *International Conference on Industrial Engineering and Operations Management,* 1047–1056.

Fermeglia, M., Cudicio, A., Desimon, G., Longo, G., and Pricl, S. (2005). Process simulation for molten carbonate fuel cells. *Fuel Cells*, 5(1), 66–79.

Fontes, B. E., Ab, C., Nilsson, E., and Generics, C. (2012). Modeling the fuel cell, 2–5.

Fulton, L. (2004). *Reducing oil consumption in transport: Combining three approaches* (No. 1–24). Paris.

Garcia, R., Pizarro, C., Lavin, A. G., and Bueno, J. L. (2013). Biomass proximate analysis using thermogravimetry. *Bioresource Technology*, 139: 1–4.

George, J., Arun, P., and Muraleedharan, C. (2016). Stoichiometric equilibrium model based assessment of hydrogen generation through biomass gasification. *Procedia Technology*, 25, 982–989.

Gimba, I. D., Abdulkareem, A. S., Jimoh, A., and Afolabi, A. S. (2015). Theoretical energy and exergy analyses of proton exchange membrane fuel cell by computer simulation. *Journal of Applied Chemistry*, 23, 123-128.

Gomez-Barea, A., and Leckner, B. (2010). Modeling of biomass gasification in fluidized bed. *Progress in Energy and Combustion Science*, 36(4): 444–509.

Gordillo, G., Annamalai, K., and Carlin, N. (2009). Adiabatic fixed-bed gasification of coal, dairy biomass, and feedlot biomass using an air-steam mixture as an oxidizing agent. *Renewable Energy*, 34(12), 2789–2797.

Grashoff, B. G. J., Pilkington, C. E., and Corti, C. W. (1983). The purification of hydrogen, (4), 157–169.

Gulzow, E. (1996). Alkaline fuel cells: A critical view. *Journal of Power Sources*, 61(1–2), 99–104.

Gulzow, E., Schulze, M., and Steinhilber, G. (2002). Investigation of the degradation of different nickel anode types for alkaline fuel cells (AFCs). *Journal of Power Sources*, 106(1–2), 126–135.

Haile, S. M. (2003). Fuel cell materials and components. *Acta Materialia*, 51(19): 5981–6000.

Han, J., Liang, Y., Hu, J., Qin, L., Street, J., Lu, Y., and Yu, F. (2017). Modeling downdraft biomass gasification process by restricting chemical reaction equilibrium with Aspen Plus. *Energy Conversion and Management*, 153, 641–648.

Hao, D., Shen, J., Hou, Y., Zhou, Y., and Wang, H. (2016). An improved empirical fuel cell polarization curve model based on review analysis. *International Journal of Chemical Engineering*.

Holmes, M. (2010). Hydrogen separation membranes. *Technical Brief*, (May): 4.

Hulteberg, P. C., Brandin, J. G. M., Silversand, F. A., and Lundberg, M. (2005). Preferential oxidation of carbon monoxide on mounted and unmounted noble-metal catalysts in hydrogen-rich streams. *International Journal of Hydrogen Energy*, 30(11), 1235–1242.

IEA. 2017. Global Energy and CO2 Status Report (2017). *Global Energy and CO2 Status Report 2017*, (March).

Inayat, A., Ahmad, M. ., Mutalib, M. I. ., Yusup, S., and Khan, Z. (2016). Parametric study on the heating values of product gas via steam gasification of palm waste using CaO as sorbent material, (December): 654–658.

Ishida, H. (2013). Casual relationship between fossil fuel consumption and economic growth in Japan: A multivariate approach. *International Journal of Energy Economics and Policy*, 3(2), 127–136.

Jayathilake, R., and Rudra, S. (2017). Numerical and experimental investigation of equivalence ratio (ER) and feedstock particle size on birchwood gasification. *Energies*, 10(8), 1232.

Jia, Z., Zhang, C., Cai, D., Blair, E., Qian, W., and Wei, F. (2017). The analysis of hot spots in large scale fluidized bed reactors. *RSC Advances*, 7(33), 20186–20191.

Johansson, E. (2013). *Process integration study of biomass-to- methanol ( via gasification ) and methanol-to- olefins ( MTO ) processes in an existing steam cracker plant*. Chalmers University of Technology Abstract.

Jones, J. M., Lea-Langton, A. R., Ma, L., Pourkashanian, M., and Williams, A. (2014). Pollutants generated by the combustion of solid biomass fuels (pp. 9–25). Springer.

Kamarudin, S. K., Daud, W. R. W., Som, A. M., Mohammad, A. W., Takriff, S., and Masdar, M. S. (2004). The conceptual design of a PEMFC system via simulation. *Chemical Engineering Journal*, 103(1–3), 99–113.

Kaushal, P., and Tyagi, R. (2017). Advanced simulation of biomass gasification in a fluidized bed reactor using Aspen Plus. *Renewable Energy*, 101, 629–636.

Khan, Z., Yusup, S., Ahmad, M. M., Chok, V. S., Uemura, Y., and Sabil, K. M. (2010). Review on hydrogen production technologies in Malaysia. *International Journal of*

*Engineering and Technology*, 10(02), 85–92.

Kivisaari, T. (2001). *System studies of fuel cell power plants*. *Fuel Cell*.

Kohnke, H., Sauer, G., Schudt, S., Gmbh, G., Coyle, E., and Kennedy, D. (2005). Water and KOH transport in an alkaline fuel cell.

Kumar, M. S., and Vivekanandan, S. (2014). Effect of design and operating parameters on the gasification process of biomass in a downdraft fixed bed: An experimental study. *International Journal of Hydrogen Energy*, 39(11): 5625–5633.

Kuo, P. C., Wu, W., and Chen, W. H. (2014). Gasification performances of raw and torrefied biomass in a downdraft fixed bed gasifier using thermodynamic analysis. *Fuel*, 117, 1231–1241.

Lawrence, D. L. (2010). *Purification of Hydrogen from a Thermo-chemical Process using a Single-Column Pressure Swing Adsorption System with Compound Written for presentation at the 2010 ASABE Annual International Meeting Sponsored by ASABE* (Vol. 0300). Pennsylvania.

Lee, S. (2007). Gasification of Coal. In *Handbook of Alternative Fuel Technologies* (pp. 25–79). Taylor & Francis Group.

Li, X. T., Grace, J. R., Lim, C. J., Watkinson, A. P., Chen, H. P., and Kim, J. R. (2004). Biomass gasification in a circulating fluidized bed. *Biomass and Bioenergy*, 26(2), 171–193.

Lima, D. F. B., Zanella, F. A., Lenzi, M. K., and Ndiaye, P. M. (2012). Modeling and simulation of water gas shift reactor: An industrial case. *Cdn.Intechopen.Com*.

Mahat, A. S. (2012). *The palm oil industry from the perspective of sustainable development: a case study of Malaysian palm oil industry*. Ritsumeikan Asia Pacific University Japan.

Mahishi, M. R., and Goswami, D. Y. (2007). Thermodynamic optimization of biomass gasifier for hydrogen production. *International Journal of Hydrogen Energy*, 32(16), 3831–3840.

Mahlia, T. M. I., Abdulmuin, M. Z., Alamsyah, T. M. I., and Mukhlishien, D. (2001). An alternative energy source from palm wastes industry for Malaysia and Indonesia, 42, 2109–2118.

Malaysia Palm Oil Palm Statistics (2018). Monthly Oil Palm Products Processed : 2018 ( Tonnes ). Retrieved from http://bepi.mpob.gov.my/index.php/en/statistics/sectoral-status/190-sectoral-status-2018/863-oil-palm-products-processed-2018.html

McKendry, P. (2002). Energy production from biomass (part 3): Gasification technologies. *Bioresource Technology*, 83(1), 55–63.

McPhail, S. J., Cigolotti, V., and Moreno, A. (2012). Fuel cells in the waste-to-energy chain. *Green Energy and Technology*, 45, 23–45.

Mert, S. O., Ozcelik, Z., Ozcelik, Y., and Dincer, I. (2011). Multi-objective optimization of a vehicular PEM fuel cell system. *Applied Thermal Engineering*, 31(13), 2171–2176.

Mikko, K. (2011). *Biomass gasification*.

Mikulandric, R., Bohning, D., Bohme, R., Helsen, L., Beckmann, M., and Loncar, D. (2016). Dynamic modelling of biomass gasification in a co-current fixed bed gasifier. *Energy Conversion and Management*, 125, 264–276.

Milne, T. A., Elam, C. C., and Evans, R. J. (2002). *Hydrogen from biomass: State of the art and research challenges*. *International Energy Agency Agreement on the Production and Utilization of Hydrogen*. USA.

Mirmoshtaghi, G. (2016). *Modeling and simulation bed gasifiers*. Malardalen University Press Dissertations.

Mishra, A., and Prasad, R. (2011). A review on preferential oxidation of carbon monoxide in hydrogen rich gases. *Bulletin of Chemical Reaction Engineering & Catalysis*, 6(1), 1–14.

Moka, V. K. (2012). *Estimation of calorific value of biomass from its elementary components by regression analysis*. National Institute Of Technology Rourkela.

Moni, M. N. ., and Sulaiman, S. A. (2012). Downdraft gasification of oil palm fronds : Effects of temperature and operating time. *Journal of Applied Sciences*, 24(12), 2574–2579.

Moretti, E., Lenarda, M., Storaro, L., Talon, A., Frattini, R., Polizzi, S., and Jiménez-López, A. (2007). Catalytic purification of hydrogen streams by PROX on Cu supported on an organized mesoporous ceria-modified alumina. *Applied Catalysis B: Environmental*, 72(1–2), 149–156.

MTI. (2007). *National energy policy report*. Singapore.

Muslim, M. B., Saleh, S., and Samad, N. A. F. (2017). Effects of purification on the hydrogen production in biomass gasification process. *Chemical Engineering Transactions*, 56, 1495–1500.

Muslim, M. B., Saleh, S., and Samad, N. A. F. (2017). Torrefied biomass gasification: A simulation study by using empty fruit bunch. *MATEC Web of Conferences*, 131.

Muslim, M. B., Wahid, F. R. A. A., Saleh, S., and Samad, N. A. F. A. (2015). Application of integrated biomass gasification and proton exchange membrane fuel cell for power production. In *Proceeding of 28th Symposium of Malaysian Chemical Engineers* (pp. 1–10). Putrajaya.

Nagel, F. P., Schildhauer, T. J., McCaughey, N., and Biollaz, S. M. A. (2009). Biomass-integrated gasification fuel cell systems - Part 2: Economic analysis. *International Journal of Hydrogen Energy*, 34(16), 6826–6844.

Ni, M., Leung, D. Y. C., Leung, M. K. H., and Sumathy, K. (2006). An overview of hydrogen production from biomass. *Fuel Processing Technology*, 87(5): 461–472.

Nikoo, M. B., and Mahinpey, N. (2008). Simulation of biomass gasification in fluidized bed reactor using Aspen Plus. *Biomass and Bioenergy*, 32(12), 1245–1254.

Niu, M., Huang, Y., Jin, B., and Wang, X. (2013). Simulation of syngas production from municipal solid waste gasification in a bubbling fluidized bed using Aspen Plus. *Industrial & Engineering Chemistry Research*, 52(42), 14768–14775.

Ohta, T. (2009). Alkaline Fuel Cells. In *Energy Carriers And Conversion Systems With Emphasis On Hydrogen* (Vol. II, p. 320). EOLSS Publications.

Ozturk, I. (2010). A literature survey on energy-growth nexus. *Energy Policy*, 38(1), 340–349.

Paengjuntuek, W., Boonmak, J., and Mungkalasiri, J. (2015). *Energy Efficiency Analysis in an Integrated Biomass Gasification Fuel Cell System*. *Energy Procedia* (Vol. 79). Elsevier B.V.

Pala, L. P. R., Wang, Q., Kolb, G., and Hessel, V. (2017). Steam gasification of biomass with subsequent syngas adjustment using shift reaction for syngas production: An Aspen Plus model. *Renewable Energy*, 101, 484–492.

Park, E. D., Lee, D., and Lee, H. C. (2009). Recent progress in selective CO removal in a H2-rich stream. *Catalysis Today*, 139(4), 280–290.

Perez, J. F., Benjumea, P. N., and Melgar, A. (2015). Sensitivity analysis of a biomass gasification model in fixed bed downdraft reactors: Effect of model and process parameters on reaction front. *Biomass and Bioenergy*, 83, 403–421.

Pourmovahed, A. (2005). Performance of a PEM fuel cell system. In *Proceedings of the 2005 American Society for Engineering Education Annual Conference & Exposition*. Michigan: American Society for Engineering Education.

Prins, M. J., Ptasinski, K. J., and Janssen, F. J. J. G. (2006). More efficient biomass gasification via torrefaction. *Energy*, 31(15), 3458–3470.

Puig-Arnavat, M., Bruno, J. C., and Coronas, A. (2010). Review and analysis of biomass gasification models. *Renewable and Sustainable Energy Reviews*, 14(9), 2841–2851.

Quaak, P., Knoef, H., and Stassen, H. (1999). Energy from biomass: A review of combustion and gasification technologies. *World Bank Technical Paper*, 422, 1–78.

Quintana, N., Van Der Kooy, F., Van De Rhee, M. D., Voshol, G. P., and Verpoorte, R. (2011). Renewable energy from Cyanobacteria: Energy production optimization by metabolic pathway engineering. *Applied Microbiology and Biotechnology*, 91(3), 471–490.

Rabbani, R. A., and Rokni, M. (2012). Dynamic simulation of a proton exchange membrane fuel cell system for automotive applications. *Proceedings of SEEP2012*, 311–316.

Ragland, K. W., Aerts, D. J., and Baker, A. J. (1991). Properties of wood for combustion analysis. *Bioresource Technology*, 37(2), 161–168.

Rajashekara, K. (2000). Propulsion system strategies for fuel cell vehicles. *Sae Technical Paper Series*, (724).

Remick, R., and Wheeler, D. (2010). *Molten carbonate and phosphoric acid stationary fuel cells: Overview and gap analysis molten carbonate and phosphoric acid stationary fuel cells: Overview and gap analysis*. *National Renewable Energy Laboratory*. USA.

Rexed, I. (2014). *Applications for molten carbonate fuel cells*. KTH Royal Institute of Technology.

Rupesh, S., Muraleedharan, C., and Arun, P. (2016). ASPEN plus modelling of air–steam gasification of biomass with sorbent enabled CO2 capture. *Resource-Efficient Technologies*, 2(2), 94–103.

Salami, N. (2012). *Gasification in Fluidized Bed : Effect of Using of the Air / Stream As Gasifying Agent on the Syngas Composition*. *Proceedings of the Conference on Energy from Biomass XIII*.

Sardella, M. (2013). *Energy analysis of a fuel cell system for commercial greenhouse applications*. KTH School of Industrial Engineering and Management.

Sarkar, J., and Bhattacharyya, S. (2012). Operating characteristics of transcritical CO2 heat pump for simultaneous water cooling and heating. *Archives of Thermodynamics*, 33(4), 23–40.

Sattler, G. (2000). Fuel cells going on-board. *Journal of Power Sources*, 86, 61–67.

Schmidt, D. D., and Gunderson, J. R. (2000). Opportunities for hydrogen: An analysis of the application of biomass gasification to farming operations using microturbines and fuel cells. In *Proceedings of the 2000 Hydrogen Program Review* (pp. 1–12).

Schonbrod, B., Marino, F., Baronetti, G., and Laborde, M. (2009). Catalytic performance of a copper-promoted CeO2 catalyst in the CO oxidation: Influence of the operating variables and kinetic study. *International Journal of Hydrogen Energy*, 34(9), 4021–4028.

Schudt, S., Kennedy, D., and Sauer, G. (2009). Engineering of a single alkaline fuel cell part II : Long-term operation in air. *Journal on Electrical Engineering*, 2(4).

Schuster, G., Loffler, G., Weigl, K., and Hofbauer, H. (2001). Biomass steam gasification--an extensive parametric modeling study. *Bioresource Technology*, 77(1), 71–79.

Shaari, N., and Kamarudin, S. K. (2015). Chitosan and alginate types of bio-membrane in fuel cell application: An overview. *Journal of Power Sources*, 289, 71–80.

Shahbaz, M., Yusup, S., Inayat, A., Patrick, D. O., Partama, A., Inayat, A., and Fadzil, A. (2016). Thermal Investigation of Palm Kernel Shell ( PKS ) with Coal Bottom Ash in Thermo Gravimetric Analyser ( TGA ) in Inert Atmosphere, 5(1), 1–5.

Shaohua, L., Deyong, C., Wenguang, Y., and Haigang, W. (2012). The effect of ER on biomass gasification in a fixed bed using Aspen Plus simulation. *World Automation Congress 2012*, 1–4.

Sharaf, O. Z., and Orhan, M. F. (2014). An overview of fuel cell technology: Fundamentals and applications. *Renewable and Sustainable Energy Reviews*, 32, 810–853.

Sheth, P. N., and Babu, B. V. (2009). Experimental studies on producer gas generation from wood waste in a downdraft biomass gasifier. *Bioresource Technology*, 100(12), 3127–3133.

Shuit, S. H., Tan, K. T., Lee, K. T., and Kamaruddin, A. H. (2009). Oil palm biomass as a sustainable energy source: A Malaysian case study. *Energy*, 34(9), 1225–1235.

Siedlecki, M., de Jong, W., and Verkooijen, A. H. M. (2011). Fluidized bed gasification as a mature and reliable technology for the production of bio-syngas and applied in the production of liquid transportation fuels-a review. *Energies*, 4(3), 389–434.

Sikarwar, V. S., Zhao, M., Clough, P., Yao, J., Zhong, X., Memon, M. Z., and Fennell,

P. S. (2016). An overview of advances in biomass gasification. *Energy & Environmental Science*, 9(10), 2939–2977.

Singhal, S. (2000). Advances in solid oxide fuel cell technology. *Solid State Ionics*, 135(1), 305–313.

Singhal, S. C. (2007). Solid oxide fuel cells. *The Electrochemical Society Interface*, 41–44.

Sordi, A., Lopes, D. G., and Neto, A. J. M. (2017). *Biomass gasification and fuel cell integration : The potential and eficiency*.

Steward, D., Penev, M., and Saur, G. (2010). Fuel cell power model startup guide system designs and case studies modeling electricity heat and hydrogen generation (November).

Susastriawan, A. A. P., Saptoadi, H., and Purnomo (2017). Small-scale downdraft gasifiers for biomass gasification: A review. *Renewable and Sustainable Energy Reviews*, 76, 989–1003.

Suwatthikul, A., Limprachaya, S., Kittisupakorn, P., and Mujtaba, I. M. (2017). Simulation of steam gasification in a fluidized bed reactor with energy self-sufficient condition. *Energies*, 10(3), 1–15.

Tagliabue, M., Farrusseng, D., Valencia, S., Aguado, S., Ravon, U., Rizzo, C., and Mirodatos, C. (2009). Natural gas treating by selective adsorption: Material science and chemical engineering interplay. *Chemical Engineering Journal*, 155(3): 553–566.

Takenaka, S., Shimizu, T., and Otsuka, K. (2004). Complete removal of carbon monoxide in hydrogen-rich gas stream through methanation over supported metal catalysts. *International Journal of Hydrogen Energy*, 29(10), 1065–1073.

Takizawa, K. (1988). *Molden Carbonate Fuel Cells* (Vol. II).

Tapasvi, D., Kempegowda, R. S., Tran, K. Q., Skreiberg, O., and Gronli, M. (2015). A simulation study on the torrefied biomass gasification. *Energy Conversion and Management*, 90, 446–457.

Tasma, D., Uzunanu, K., and Panait, T. (2007). The effect of excess air ratio on syngas produced by gasification of agricultural residues briquettes. *Carbon*, 29, 22–60.

Tripathy, R. (2013). *Production of Hydrogen Gas From Biomass Wastes Using Fluidized Bed Gasifier*. National Institute of Technology Rourkela-769008.

U.S. Department of Energy (2011). Comparison of fuel cell technologies. *Energy Efficiency & Renewable Energy*, (February): 3463.

Varela-Gandia, F. J., Berenguer-Murcia, A., Lozano-Castello, D., and Cazorla-Amoros, D. (2010). Hydrogen purification for PEM fuel cells using membranes prepared by ion-exchange of Na-LTA/carbon membranes. *Journal of Membrane Science*, 351(1–2), 123–130.

Veerasamy, R., Rajak, H., Jain, A., Sivadasan, S., Varghese, C. P., and Agrawal, R. K. (2011). Validation of QSAR Models - Strategies and Importance. *International Journal of Drug Design and Disocovery*, 2(3), 511–519.

Wahid, F. R. A. A., Harun, N. H. H. M., Rashid, S. R. M., Samad, N. A. F. A., and Saleh, S. (2017). Physicochemical property changes and volatile analysis for torrefactionn of oil palm frond. *Chemical Engineering Transactions*, 56, 199–204.

Wahid, F. R. A. A., Muslim, M. B., Saleh, S., and Abdul Samad, N. A. F. (2016). Integrated gasification and fuel cell framework: Biomass gasification case study. *ARPN Journal of Engineering and Applied Sciences*, 11(4), 2673–2680.

Warnecke, R. (2000). Gasification of biomass: Comparison of fixed bed and fluidized bed gasifier. *Biomass and Bioenergy*, 18(6), 489–497.

WOC. (2016). *World Energy Resources Bioenergy 2016*.

Xue, X. D., Cheng, K. W. E., and Sutanto, D. (2006). Unified mathematical modelling of steady-state and dynamic voltage-current characteristics for PEM fuel cells. *Electrochimica Acta*, 52(3), 1135–1144.

Yan, Q., Toghiani, H., and Causey, H. (2006). Steady state and dynamic performance of proton exchange membrane fuel cells (PEMFCs) under various operating conditions and load changes. *Journal of Power Sources*, 161(1), 492–502.

Yang, W., Ponzio, A., Lucas, C., and Blasiak, W. (2006). Performance analysis of a fixed-bed biomass gasifier using high-temperature air. *Fuel Processing Technology*, 87(3), 235–245.

Yu, H., Chen, G., Xu, Y., and Chen, D. (2016). Experimental study on the gasification characteristics of biomass with CO2/air in an entrained-flow gasifier. *BioResources*, 11(3), 6085–6096.

Yunus, M. K., Ahmad, M. ., Inayat, A., and Yusup, S. (2010). Simulation of enhanced biomass gasification for hydrogen production using iCON. *World Academy of Science,* 4(2), 753–760.

Zhu, W. Z., and Deevi, S. C. (2003). A review on the status of anode materials for solid oxide fuel cells. *Materials Science and Engineering A*, 362(1–2), 228–239.

# APPENDIX A
# LIST OF PUBLICATIONS

## A-1 Journals

Wahid, F.R.A., Muslim, M.B., Saleh, S., and Samad, N.A.F.A. 2016. Integrated gasification and fuel cell framework: Biomass gasification case study. ***ARPN Journal of Engineering and Applied Sciences***, 11(4): 2673–2680.

Muslim, M.B., Saleh, S., Samad, N.A.F.A. 2017. Effects of purification on the hydrogen production in biomass gasification process. ***Chemical Engineering Transaction***, 56: 1495–1500.

Muslim, M.B., Saleh, S., Samad, N.A.F.A. 2017. Torrefied biomass gasification: A simulation study by using empty fruit bunch. ***MATEC Web of Conferences***, 131: 1–6.

Muslim, M.B., Samad, N.A.F.A. 2017. Integrated biomass gasification and proton exchange membrane fuel cell for power production using oil palm fronds. ***Chemical Engineering Journal***. (Submitted).

Muslim, M.B., Saleh, S., Samad, N.A.F.A. 2017. Performance of hydrogen production using raw and torrefied oil palm frond in fluidized bed gasification process. ***International Journal of Chemical Engineering***. (Submitted).

## A-2 Conference/ Seminar Proceedings

Muslim, M.B., Saleh, S., Abdullah, T.A.T., Ahmad, A., Samad, N.A.F.A. 2015. Performance analysis of biomass gasification using fluidized bed gasifier. *Proceeding of 5th International Conference on Fuel Cell and Hydrogen Technology (ICFCHT),* 1–8.

Muslim, M.B., Wahid, F.R.A., Saleh, S., Samad, N.A.F.A. 2017. Application of integrated biomass gasification and proton exchange membrane fuel cell for power production. *Proceeding of 28th Symposium of Malaysian Chemical Engineers (SOMChE 2015).* 1–10.

Muslim, M.B., Saleh, S., Abdullah, T.A.T., Ahmad, A., Samad, N.A.F.A. 2016. Performance comparison on biomass gasification reactor for hydrogen production. *Proceeding of 7th International Symposium on Design, Operation and Control of Chemical Processes (PSE ASIA 2016),* 1–6.

Muslim, M.B., Saleh, S., Samad, N.A.F.A. 2016. Comparison of hydrogen production using raw and torrefied oil palm frond in fluidized bed gasification process. *Proceeding of International Conference of Chemical Engineering & Industrial Biotechnology (ICCEIB 2016)*, 1–9.

# APPENDIX B

## B-1 FORTRAN Subroutine

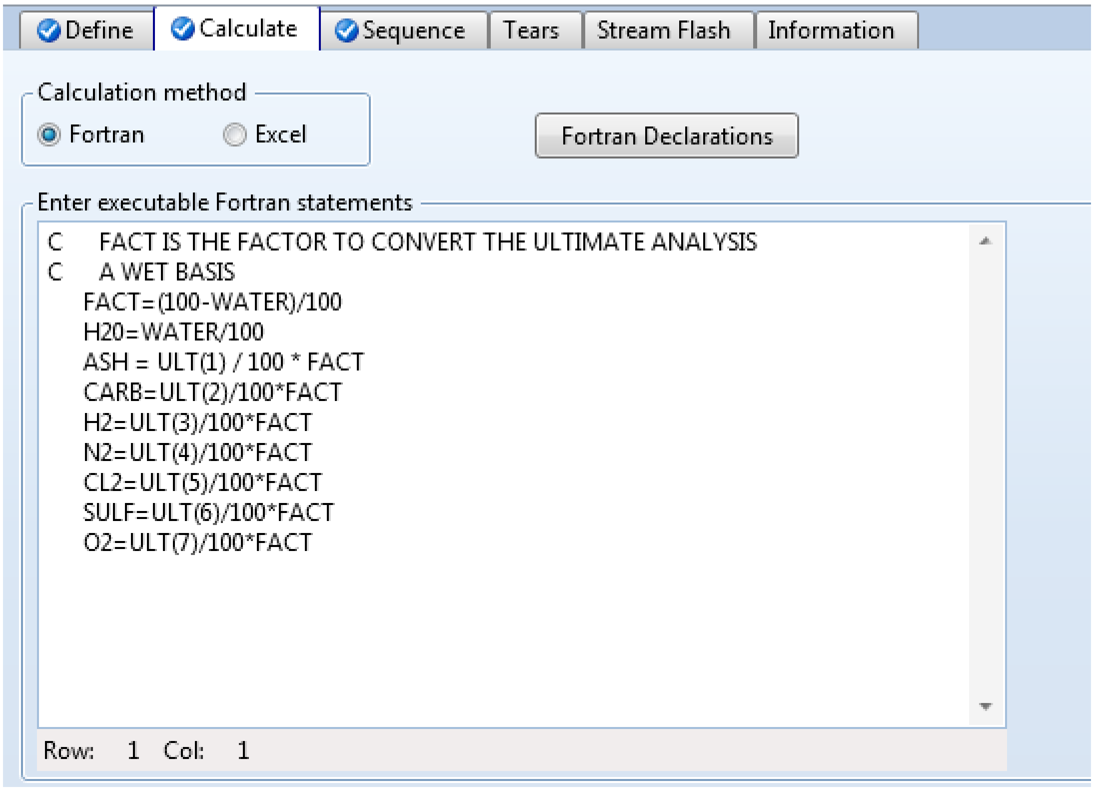

```
C     FACT IS THE FACTOR TO CONVERT THE ULTIMATE ANALYSIS
C     A WET BASIS
      FACT=(100-WATER)/100
      H20=WATER/100
      ASH = ULT(1) / 100 * FACT
      CARB=ULT(2)/100*FACT
      H2=ULT(3)/100*FACT
      N2=ULT(4)/100*FACT
      CL2=ULT(5)/100*FACT
      SULF=ULT(6)/100*FACT
      O2=ULT(7)/100*FACT
```